APPLICABILITY OF A TWO DIMENSIONAL, DIGITALLY INTEGRATING, SILICON VIDICON SYSTEM IN THE DETECTION OF NATURAL RESOURCES

by

GREGORY BYRON PAVLIN

B.S., Ohio University

1972

SUBMITTED IN PARTIAL FULFILLMENT

OF THE REQUIREMENTS FOR THE

DEGREE OF MASTER OF SCIENCE

at the

MASSACHUSETTS INSTITUTE OF TECHNOLOGY

September, 1973

Signature of Author.....
Department of Earth and Planetary Science,
August 13, 1973

Certified by..
.....
Thesis Supervisor

Accepted by.....
Chairman, Departmental Committee
on Graduate Students

APPLICABILITY OF A TWO DIMENSIONAL, DIGITALLY INTEGRATING, SILICON VIDICON SYSTEM IN THE DETECTION OF NATURAL RESOURCES

By

Gregory Byron Pavlin

Submitted to the
Department of Earth and Planetary Sciences
August, 1973
in partial fulfillment of the requirements for the
degree of Master of Science

ABSTRACT

The feasibility of using a two-dimensional, digitally integrating silicon vidicon system (McCord and Westphal, 1972) to differentiate terrestrial rock structure and mineralization was explored.

The potential usefulness of the vidicon system for the detection of natural resources is based on its ability to photometrically detect the spectral signature of terrestrial minerals in the spectral range 400.0 to 1100.0 nanometers and produce two-dimensional imagery. Interpretation of the imagery is based on developing libraries of recorded reflection spectra of geologic materials and the semiquantitative explanation of spectral features by Crystal Field Theory.

The instrumentation was tested for its ability to: differentiate minerals; resolve detailed mineralized rock structure; enhance imagery of rock structure and/or mineralized features using computer software techniques; identify mineralogy without prior ground truth; distinguish altered from unaltered rock units associated with porphyry copper deposits; perform as a practical geophysical tool in the field.

It is concluded that the vidicon system is a potentially powerful geophysical tool that should be applied to geological problems by using remote-sensing techniques. However, its potential use will be realized only if the recommendations that developed from this study are acted upon.

Thesis Supervisor: Thomas B. McCord

Title: Professor of Planetary Physics

DEDICATION

This work is dedicated in appreciation of my parents, Mr. Carl T. Pavlin Sr. and Mrs. Glennie L. Pavlin (née, Clark), for their role in molding me into the person that I am.

ACKNOWLEDGEMENTS

To thank the many people who have assisted me in the planning, experimentation, and processing of the data for the purposes of helping me produce a relevant thesis is an obligation that will take more than two pages of acknowledgements to satisfy. To express my thanks through an acknowledgement page, is a cold means of expression; however, the following people's acknowledgement seems to be institutionally and financially the correct means of thanks at this time.

I am especially grateful to Bill Ezell of MITPAL who assisted me in all experimentation-- which at times was very dull work; and conversely, at times the work was very intense and exhausting. Lenny Vanderhave was an invaluable assistant in the rerun of the last experiment; his trouble shooting capabilities permitted the winning of respectable data.

Paul Kinnucan was my coach in the manipulation of the data with the LNS Computer. My gratitude is due Carlie Pieters, Lawrence Bass, and Jean Harrison for their advice, data processing, and picture processing respectively.

In addition to the advice and good will of my thesis advisor Dr. Thomas B. McCord, I was also fortunate to snare the advice of Dr. T. McGetchin, Dr. R. Burns, Dr. H. Fairbairn, Dr. R. Huguenin, Dr. J. Southard, and Dr. R. Naylor. The latter people are responsible for keeping me on the right track when I left those tracks which were considered to be the best route in producing a relevant thesis. Special thanks should be conferred on Tom McCord for his advice and concern for the problems that accompany graduate students.

To some readers, the following may seem to be nit-picking thanks; however, I consider it important to thank those unusual people who helped me with some logistical problems; that is, getting the right equipment to the right place at the right time. My gratitude is due some personnel of the M.I.T. Central Utilities Plant: George F. Gibney, George S. Reid, John Stowe, and Harold Browning. They assisted in the acquisition of electric generators, typewriters, tables and the time to work on my thesis (while I was working to pay for my thesis).

In yet a different category, George Panoussis assisted me in a marathon geologic expedition through New England to determine a feasible site for a vidicon experiment. Miss Suzanne Sayer generously discussed and enumerated the mineralogy of an outcrop that was used in this study. The outcrop was the subject of Miss Sayer's thesis which discusses the outcrop in terms of genesis, absolute age and geochemical aspects.

There were others like Alan Goldberg and Bill Mixon who took time to advise and assist in the various aspects of preparation for an experiment; they are mentioned here to emphasize the degree of help I had in performing this study. This lengthy and detailed acknowledgement was presented to illustrate how dependent a graduate student has to be in developing his thesis. I am not apologizing for the dependence upon these people, because in each case, I would have missed something during my stay at M.I.T. if I had not met them.

INTRODUCTION

Geology is a science of observation that employs the visible portion of the electromagnetic spectrum. A field geologist's purpose is to determine lithology on the basis of mineralogy, petrology, structure, time relationships and genesis. Understanding the geochemistry, depositional chronology, and spatial relationships(both surface and subsurface), permits the geologist to predict the location of potential mineable mineral concentrations. Geophysics is an earth science that employs physics to expand the criteria of a geologist's predictions beyond that of mere surficial observations.

This report describes a study of the feasibility of using an integrating vidicon system as a geophysical tool for the remote detection of terrestrial natural resources. Prior to this study, the vidicon system was used to map the compositional features of some planets. This report also records the procedures by which an instrument is tested for its usefulness in geophysical exploration; consequently, the format of this manuscript will follow the order of experimentation rather closely.

Following a brief review of the instrumentation, a presentation of theory is given to prepare the reader for the discussion of the experiment's results. The experiments were designed test the instrumentation's ability to: differentiate mineralogy; resolve detailed mineralized rock structure; enhance imagery of rock structure and/or mineralized features using computer software techniques; identify mineralogy without prior ground truth; distinguish altered versus unaltered rock units associated with porphyry copper deposits; perform as a practical geophysical

tool in the field. After reviewing conclusions concerning the experimentation, this presentation terminates with a discussion of recommendations for refining this prototype instrument into a hardened, remote-sensing tool for geophysical exploration.

TABLE OF CONTENTS

TABLE OF CONTENTS(continued)

TABLE OF FIGURES

TABLE OF CONTENTS(continued)

TABLE OF TABLES

INSTRUMENTATION

The evaluated instrument is a two-dimensional, digitally integrating, silicon vidicon system. This system's importance is founded on its proven ability to detect and provide two-dimensional imagery for the spectral range of 400.0 Nm to 1100.0 Nm(Nm-nanometer)(McCord and Westphal, 1972). This ability permits the operator to extend his observations of a subject from the visible to the near-infrared portion of the electromagnetic spectrum.

The general mechanics of the vidicon system are as follows: visible and near-infrared radiation from a target is focused by an optical system on to the detector of the vidicon tube; the incident photon energy is converted to electrons which are integrated at each picture element for the given exposure time; the resultant record of intensity is transcribed on to a magnetic tape. The data tape may then be manipulated by using several functions of the computer library to obtain: printout of intensities (0 to 255 scale); SC4020 pictures and plots; polaroid film imagery. Computer library functions that enhance different aspects of the imagery(if used properly) do exist (Kunin, 1972).

The optics of the vidicon system were designed with moderate cost and simplicity in mind. The lens is a converted 80 mm Xerox lens with a focal length of 13.5 cm and a diaphragm that adjusts the f-stop from f-2 to f-8. This was ideal for laboratory studies that required a field of view of 8 to 30 cm; however it proved to be inadequate for field work requiring large fields of view(tens of meters). This lens also exhibited defocusing

when light with longer wavelengths (800.0 Nm to 1100.0 Nm) was used to examine various subjects.

Besides the optics, the vidicon system includes: a manual filter wheel which holds preselected interference filters for the particular experiment; electric shutter; vidicon tube contained within a coldbox cooled by solid CO_2; electronics rack with vidicon monitor and controls; oscilloscope; cable; and magnetic tape recorder. The system is described in detail by McCord and Westphal(1972) and Kunin(1972). The software used in the data processing is thoroughly explained by Kunin (1972). The additional instrumentation used to perform this study's various experiments are described in the respective experiment's discussion section.

THEORY

The scientific principles which support the usefulness of the vidicon system for geophysical applications incorporate geometrical optics, quantum mechanics, structural geology, geochemistry, petrology, mineralogy and geomorphology. If the spectral character of light incident upon and reflected from a material is known, then the observed spectral differences may be accounted for by applying quantum mechanical models(crystal field theory). Spectral differences incorporate absorption bands and the bands respective characteristics: eg. width, position in the spectrum, etc. By the interpretation of these spectral differences, the mineralogy and lithology of rock material may be identified. The vidicon system is capable of detecting the spectral signatures of minerals. The latter feature, complemented by applying spectral interpretation theory to the vidicon imagery, infers that the vidicon system would be potentially useful in the compositional mapping of mineralized terrestrial structure. The following discussion of the theoretical aspects of the vidicon system will permit an appreciation of the system's usefulness.

Incident light upon a nonopaque dielectric material is both specularly and diffusely reflected. Specular reflection occurs at the first interface between light transmitting media and is described by Fresnel's equations(Born and Wolf, 1970). Diffuse reflection occurs when incident light is transmitted through the target medium and diffusely radiated away from the target upon being reflected from an adjacent particle of the target material(Fowles,1968; Pieters, 1972). Photons of the dif-

fusely reflected component have experienced selective absorption by the transmitting medium. Such absorption is explained quantitatively by quantum mechanics and qualitatively by crystal field theory (Burns, 1970). It is the diffusely reflected component that primarily accounts for the spectral signature of minerals (Hunt and Salisbury, 1970; Burns, 1970).

To avoid redundancy, a discussion of specular reflection in terms of Fresnel's equations is omitted; however, a thorough discussion of this subject may be found in Born and Wolf(1970), Jenkins and White(1957), etc. So that the discussions of experiments may be understandable, the remainder of this section will discuss the concepts of diffuse reflection and crystal field theory.

To reiterate, the diffuse component of reflection from a dielectric material arises from the reflection of light from a crystalline material's surficial particles after the light has been previously transmitted by adjacent particles. During the transmission, the electromagnetic wave experiences absorption to a degree dependent upon the associated photon energies. The absorption results from interaction of the photons with the electronic structure of the crystalline medium. Photon absorption is a function of the mean optical path length that the light travelled through the absorbing medium. Size of the particulate material, the porosity of the material, and the phase of the irradiance effect the mean optical path length(Pieters, 1972).

Crystal field theory is a semiquantitative theory that employs quantum mechanics, electrostatics, and physical mineral-

ogy concepts to explain the absorption bands of both the transmission and reflection spectra of minerals containing either transition or lanthanide elements (Burns, 1970; Gaffey, 1973). This theory serves to explain the spectral reflectance absorption bands of various minerals and permits the determination of an unknown mineral's chemistry through the application of the theory to spectral interpretation(Burns,1970; Adams and Filice,1967; McCord and Adams, 1970).

Transition elements are characterized by the partly filling of their 'd' and 'f' shells (Quagliano, 1963). The elements of the first transition series are: Sc, Ti, V, Cr, Mn, Fe, Co, Ni, Cu and the adjacent series ions of K, Ca, Zn, Ga, and Ge. Each of these element's ions, when located in an isolated state, has its 'd' orbitals at an equal energy state and are "degenerate" (Burns, 1970; Gaffey, 1973). When these ions within a crystalline material interact electrostatically in the crystal field, the transition element's orbitals are distorted from their degenerate state. This distortion is due to the electrostatic forces imposed by the coordination (cations surrounded by anions) of those ions in the crystal. The distortion of the orbitals forces the transition element electrons to seek nondegenerate energy levels (Gaffey, 1973; Burns, 1970; Pieters, 1972). The redistribution of energy may result from the coordination of ions or ligands (dipolar group with an assigned charge)(Burns, 1970). The change in the orbital's energy levels, or the energy differential, corresponds directly to the energy of the photons absorbed by the mineral. The absorbed photon energy permits the

electrons to make the transition from the degenerate to the nondegenerate states (Castellan, 1971; Pieters, 1972; Gaffey, 1973). Figures G-1, G-2, G-3 illustrate the discussed concepts; ie: effects of crystal coordination on the orbitals' energy states; variation of energy levels as a function of the coordination site symmetries. The magnitude of the energy differential and the respective energy of the absorbed photon is a function of the crystal coordination state(Mason and Berry, 1968), the transition ion itself, and the distances between the adjacent interacting ions. These effects are enhanced by more differentiation of energy levels when the symmetry of the crystal site is distorted (Burns, 1970).

Absorption bands are also caused by charge transfer. Charge transfer occurs when electrons migrate between neighboring ions - anions, cations, ligands. This process is attributed to photochemical oxidation-reduction of a mineral by photons of the ultraviolet and visible regions of the electromagnetic spectrum. Cinnabar and other sulphides illustrate this process (See Figure G-6, Cinnabar)(Burns,1970; Hunt and Salisbury, 1970).

The diffuse reflection spectral absorption bands, produced by the selective absorption of photons by the mineral, are variable in width. This feature corresponds to the thermal vibrations of the crystal lattice where the mean of the band correlates to the mean cation-anion distances(Burns, 1970).

The previous discussion accounts for absorption bands in the reflection spectrum of dielectric material; however there are other effects that alter the spectral features. These effects

of particle size, illumination angle (angle between the light source, target, and detector), packing of particulate material and compositional mixing of particles have been investigated by Adams and Filice(1967) and Gaffey(1973). These effects will be reviewed to assist in the interpretation of reflectivity spectra. Spectra interpretation is applicable to the vidicon system's ability to map, differentiate, and identify terrestrial minerals.

The albedo of a particulate material is a function of the particle size and the rock type(Adams and Filice, 1967). Generally(there are exceptions) the albedo increases as the particle size decreases. This is because the ability of a particle to transmit light and contribute to the diffuse reflection component increases with the decrease in particle size (Gaffey, 1973).

Packing a particulate material results in a slight increase of albedo in the visible spectral range and a decrease in the infrared portion of the spectrum. Adams and Filice(1967) concluded that the effects of packing had a negligible effect in the interpretation of reflectivity spectra.

The work of Adams and Filice(1967) examined the relationship of albedo to the angle of illumination(light source to target to detector angle). Ratios of the reflected intensities in the red portion of the spectrum to the blue portion show an increase in albedo as the illumination angle increases to thirty degrees. The intensity ratios decrease for illumination angles greater than thirty degrees. This effect may be relevant to laboratory studies and some practical applications; eg., in remote detection of geologic materials illuminated by direct sunlight--

there may be an optimum illumination angle that may assist in the survey(complicated by shadow problems).

Gaffey (1973) gives an excellent discussion of the effect of compositional mixing upon a reflection spectra. This effect arises when the material whose reflectivity is being recorded consists of a variety of mineral phases. It would be hoped that the absorption band features might correspond to the relative abundances of the compositional minerals in a simple relationship. However, though relative abundances play a role in determining the significance of an absorption band, the relationship is not a simple one. Gaffey resolves the following theorem: "The relative strength of an absorption feature is a function of the mean optical path length of a photon passing through the crystalline medium in relation to the variation of the optical density of the transmitting medium over the whole wavelength range under consideration." To paraphrase, if the optical mean path length is large with respect to the particle size and the optical density(ability of the material to absorb a photon) of the material outside the absorption bands is low, then the material will be characterized by a low albedo over the range of wavelengths used in the study. Similarly, if the optical path length is long relative to the optical density of the material at the absorption wavelengths, but short relative to other wavelengths, then the absorption bands will contrast significantly with the continuum. Finally, if the optical path length is short relative to both the optical density at the absorbing and nonabsorbing wavelengths, then the absorption bands

will appear weak and the reflection spectrum will appear bright with no significant absorption anomalies(Gaffey, 1973). Gaffey concludes that reflectivity spectra and their absorption features are also functions of the number of mineral phases in the material, the nature of these phases(dielectric versus metallic), and the ratio of the optical density to particle size(these are causes that supplement those explained by crystal field theory).

The effects of metallic impurities in dielectric samples and the reflectivity spectra of various opaque minerals have been studied by Hunt and Salisbury(1970-1971). Opaque minerals have featureless spectra with low albedo. The metallic impurities were found to decrease the overall reflectivity of dielectric mineral samples.

Crystal field theory accounts for absorption bands' positions as a function of the crystallographic optical axis along which the light was transmitted and absorbed. However, in relation to the reflectivity spectra of powders, etc., the material usually consists of various sizes of particles with crystal axis randomly oriented. This random orientation results in absorption features that are basically the summation of the features characterizing the spectra obtained from each orientation of the crystal. Gaffey(1973) observes that there is no simple relationship; that is a simple linear summation of spectral features from each axis of the subject crystal. Gaffey finds that a reflectivity spectra is the sum of the components of electronic transitions along all crystal axis of the medium multiplied by

the number of transitions for each given energy. This relationship may seem reasonable; however considerable trouble may be anticipated when quantitative probability is applied to determine the amount of absorption as a function of the degree of random crystal orientation.

It was not originally intended to paraphrase the literature on theory related to absorption spectra of crystalline materials in the ultraviolet through near-infrared spectral range. However, besides presenting both the complex and simple aspects of the theory, this review will make the discussions and interpretations of various spectral features referred to in this study more understandable. It might be noted that though various physical parameters effecting reflectivity spectra were discussed(eg., packing, emphasis on powdered samples, etc.),the samples used in this study were selected on the basis that their physical features were typical of geologic outcrops. Never-the-less, the studies of powders, packing, particle size, etc., are all useful in the determination of information from reflectivity spectra and filtered two-dimensional vidicon imagery of rocks in situ.

Figure: G-1

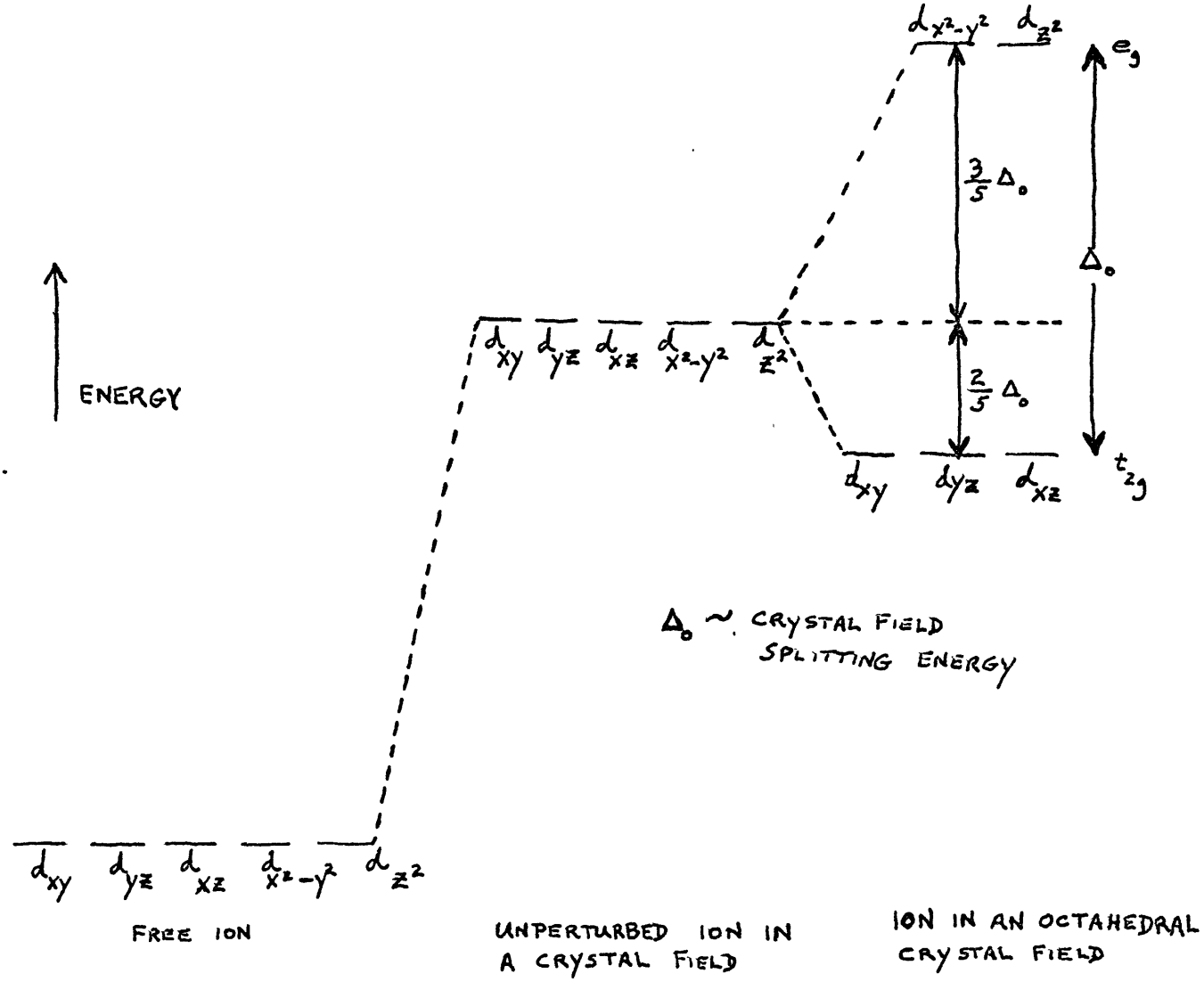

Figure G-1 : Relative energy levels of d orbitals of a transition metal ion in octahedral co-ordination site

(Burns, 1970)

Figure: G-2

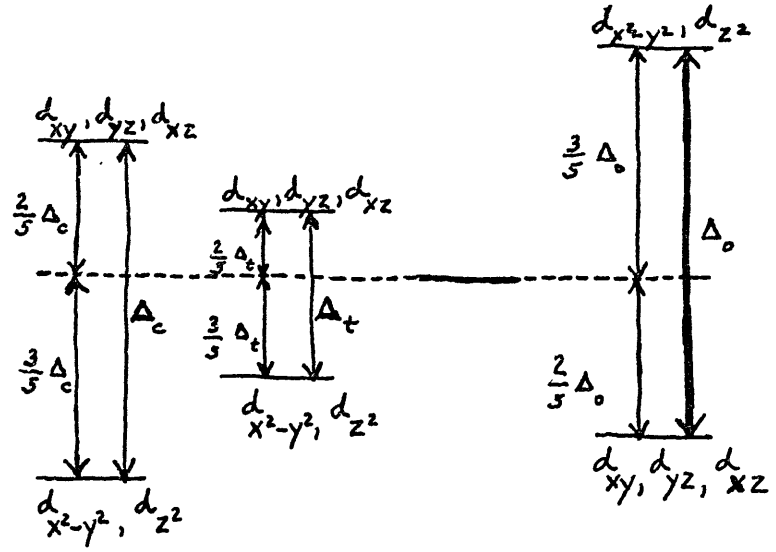

Figure G-2 : Relative energy levels of d orbitals of a transition metal ion in a cubic, tetrahedral and octahedral co-ordinations.
(Burns,1970)

Figure: G-3

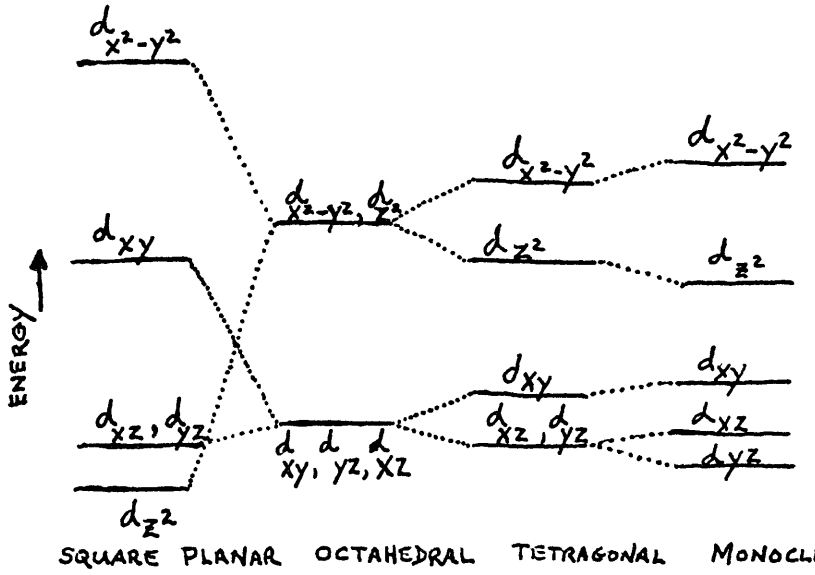

Figure G-3 : Relative energy levels of d orbitals of a transition metal ion in co-ordination sites of various symmetries
(Burns,1970)

TESTING ABILITY TO DIFFERENTIATE MINERALOGY

Background

An experiment was performed in a laboratory environment in which the ability of the vidicon system to differentiate mineralogy was tested. For this experiment, powdered samples of two distinct minerals were obtained. In order that the powders could be viewed by the vidicon system, a simple device involving a mirror mounted at forty-five degrees to the plane on which the samples would rest was constructed. This device is illustrated in Figure S-2 along with the basic vidicon system equipment set up for this experiment. The illustration shows only one light source, a 300 watt tungsten bulb with a reflector hood; this was replaced with symmetrically placed light sources(two-150 watt tungsten bulbs with reflector hoods).

The two mineral samples studied were plagioclase feldspar and a pyroxenite - websterite. The feldspar is a single mineral having the formula $NaAlSi_3O_8$. Websterite is a pyroxenite, $(Mg,Fe)_2Si_2O_6$, which in this sample's case would be termed 'En_{89}' of the enstatite-ferrosillite solid solution series(Pieters,1972). Pyroxenites are generally a coarse grained ultramafic consisting of hypersthene and some subordinate diopside(text description of the pyroxenite, websterite). Pyroxenites may have accessory minerals of biotite, hornblende and olivine. The plagioclase feldspar sample was determined to be albite-the sodic member of the plagioclase solid solution series.

Both mineral samples were ground to a powder in a nonmetallic mortar and sieved. The two samples were sieved to particles

less than 125 microns in diameter(the effects of particle size on the reflected light intensities relative to a MgO standard were not a concern in any of the experiments; however these effects are known - Hunt and Salisbury, 1970-1971). The mineral samples were placed on a 3/4" square, pale green glassine paper. The paper and the powder samples were then carefully placed on a 3" square glass slide which had been coated with the highly reflective MgO a few minutes before the experiment was performed. The samples-MgO-glass stage mount was placed beneath the mirror of the horizontal viewing assembly. Both the pictures and respective dark fields(Kunin,1972) were taken by the vidicon system.

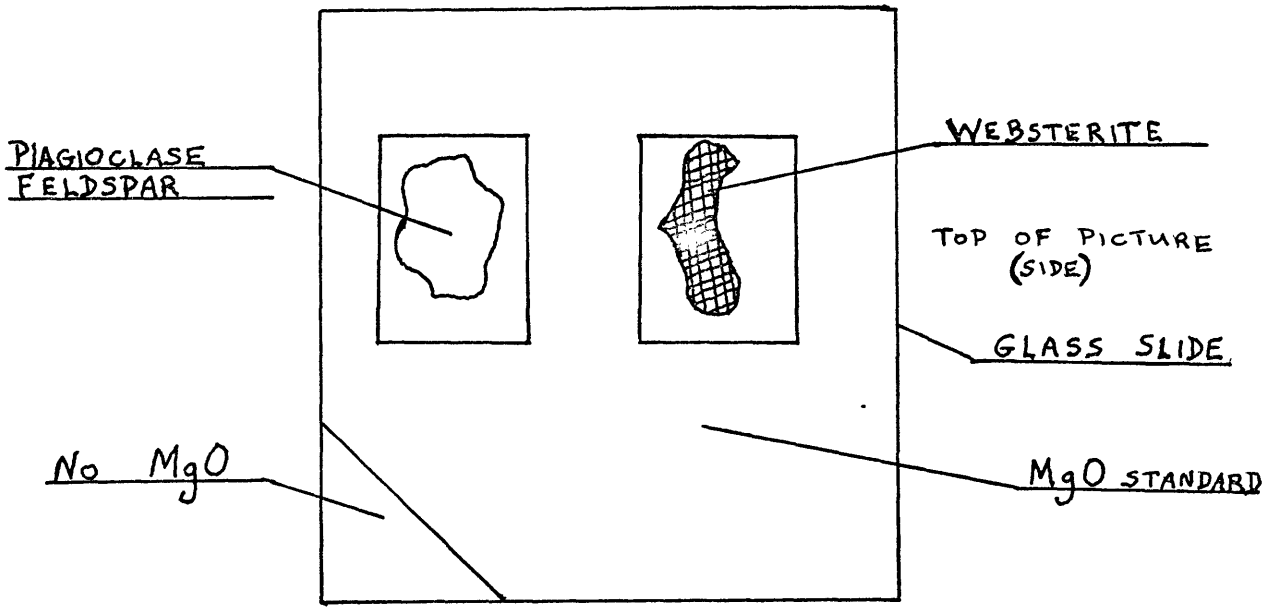

Figure: S-1

Websterite-Plagioclase Mount Orientation

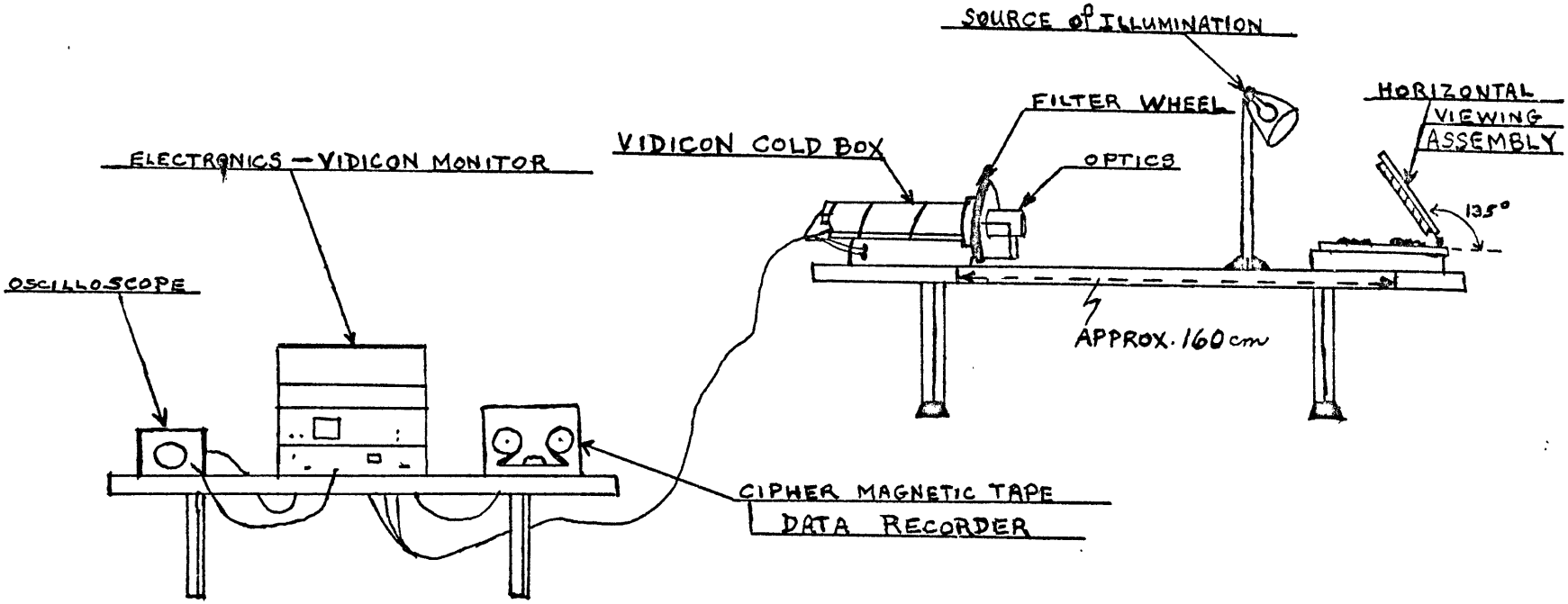

Comments:- Light Source: 150 Watt Tungsten Bulb

- Vidicon Cold Box(Dewar) cooled with CO_2 ice
- Most efficient laboratory procedure was to have (1) technician operating the vidicon while the other technician manipulated the rock samples, filter wheel, and made a log of the experiment(for the purposes of data processing)
- The only means of illumination was the light source; room was masked and dark; the filter wheel mount, dewar, and auxillary power supply unit was hooded to prevent saturation of the vidicon tube

LABORATORY SETUP FOR WEBSTERITE-PLAGIOCLASE POWDER EXPERIMENT

Figure: S-2

DISCUSSION

Experimental data was routinely processed; ie: obtain SC4020 pictures, obtain print-out of intensities(for both pictures and dark fields), subtract dark fields from pictures, perform desired intensity ratios with computer, and obtain the final Polaroid pictures (Kunin, 1972). The final pictures are displayed in Figures P-1, P-2, and P-3. The numeric results are summarized in Figure T-1. The table presents the vidicon system's capabilities in terms of intensity ratios. For each picture taken over a narrow spectral range, the average 60 point intensity matrix of the websterite is divided by the average 60 point matrix of the feldspar. This is similar to a ratio of ratios technique (McCord, 1968); except that the additional bother of ratioing the respective minerals average intensities to that of a given 60 element matrix of MgO is neglected. This step is omitted because the MgO intensity denominators cancel out upon ratioing the ratios.

Table T-1 illustrates that for all wavelengths(380.0Nm, 700.0 Nm, 900.0Nm), the websterite was less reflective than the plagioclase feldspar. The table infers that the degree of absorption is dependent upon wavelength. The diffuse reflection spectrum of websterite, made on a Cary 17 spectrometer, shows distinct absorption at 910.0 Nm(See Figure: G-4)(Pieters,1972). Crystal field theory explains the band as due to the spin allowed absorption band for Fe^{2+}(Pieters, 1972). Table T-1 shows that the vidicon system was able to resolve the absorption at 900.0 Nm for websterite as a result of this cation effect. To be sure that this absorption is centered at 910.0 Nm, vidicon

pictures must be taken at wavelengths surrounding the absorption band. The resultant intensity ratios should increase for wavelengths at plus and minus the 910.0 Nm band. This proof is demonstrated in a later experiment(experiment to identify mineralogy without ground truth) using other minerals.

Reflectivity spectra have been recorded for feldspars, including albite(Figure: G-4). In general, these spectra are flat with absorption increasing toward the blue end of the spectrum and are highly reflective with respect to MgO(Hunt and Salisbury, 1970). These characteristics assist in the differentiation of websterite from feldspar. There is a wavelength where the reflectivity of the two minerals is identical with respect to MgO. It is this unique wavelength that is used in some of the later experiments to act as a normalization base. Vidicon pictures are ratioed to the pictures taken at this unique wavelength so that enhancement of subtle absorption features may be accomplished. In this experiment, the normalization wavelength was closely satisfied at 380.0 Nm. Ratios of websterite to plagioclase feldspar at 700.0 Nm and 900.0 Nm are ratioed to the ratios made at 380.0 Nm. Though the information provided does not add to the first set of ratios' results, the discussion and technique is mentioned here for later reference.

The information provided by Table T-2 serves as warning with respect to the linearity of the vidicon system. A linear system is characterized by a consistency of intensity ratios for two areas of vidicon imagery as a function of exposure time, without changing filters, light source, or target areas. For the

pictures taken at 900.0 Nm and exposures of 0.02 and 0.04 seconds, the ratios of websterite to plagioclase intensities vary by approximately fifteen percent -- suggesting the possibilities of a nonlinear vidicon system or high electric noise levels within the system. A nonlinear vidicon system would be limited in its usefulness to the remote detection of mineralogy, photometry, and the mapping of composition. The possibility of nonlinearity or high noise levels will be investigated more carefully in a later experiment. Past work with the vidicon system has cited excellent linearity of the system(McCord and Westphal,1972), (McCord and Bosel, 1973).

CONCLUSIONS

In this first experiment, the vidicon system quite adequately differentiated the minerals websterite and plagioclase feldspar by using the absorption bands of these minerals as predicted and explained by crystal field theory.

PLAGIOCLASE, VAR. ALBITE 66B AMELIA, VA.,

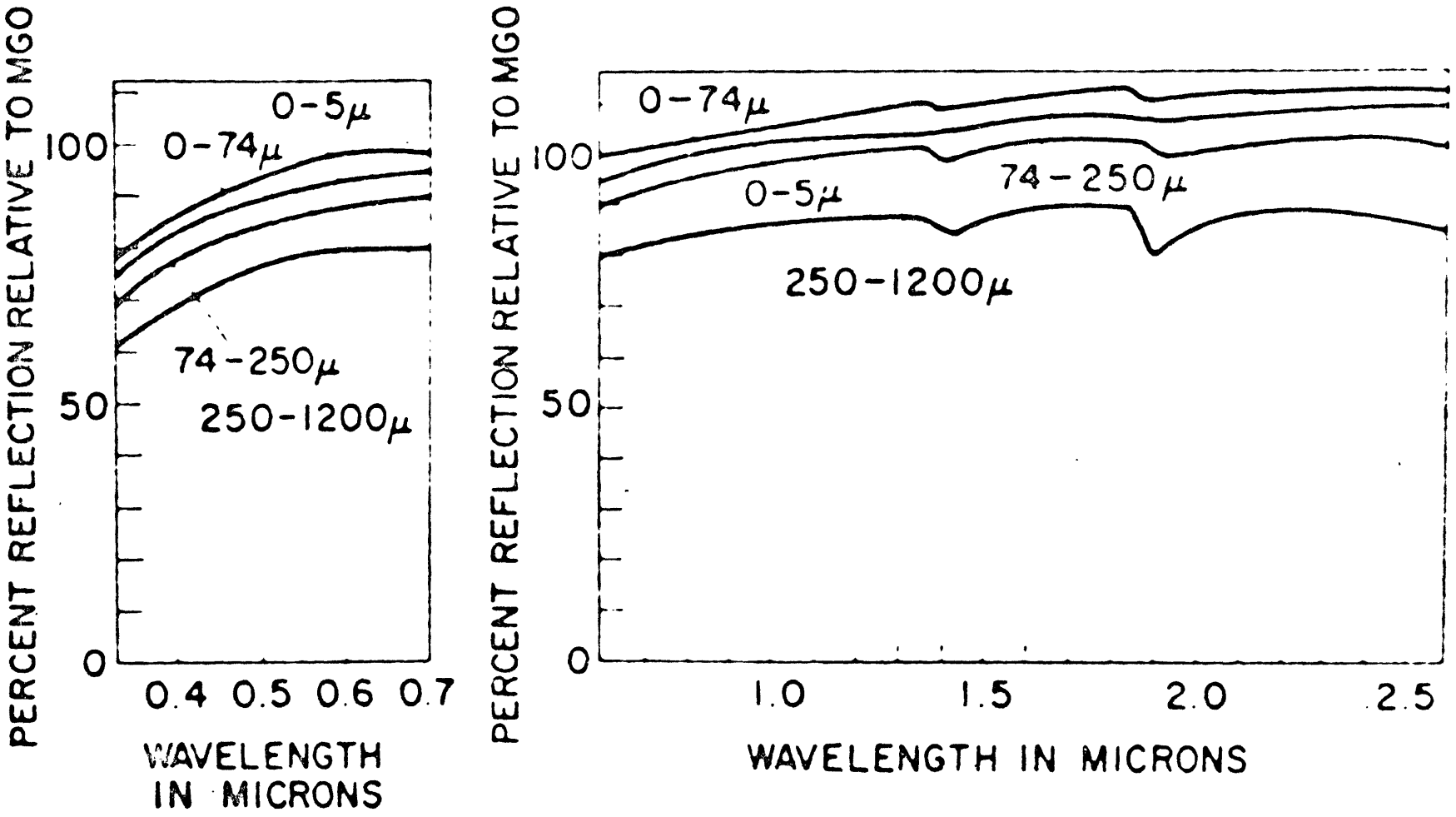

Figure: G-4

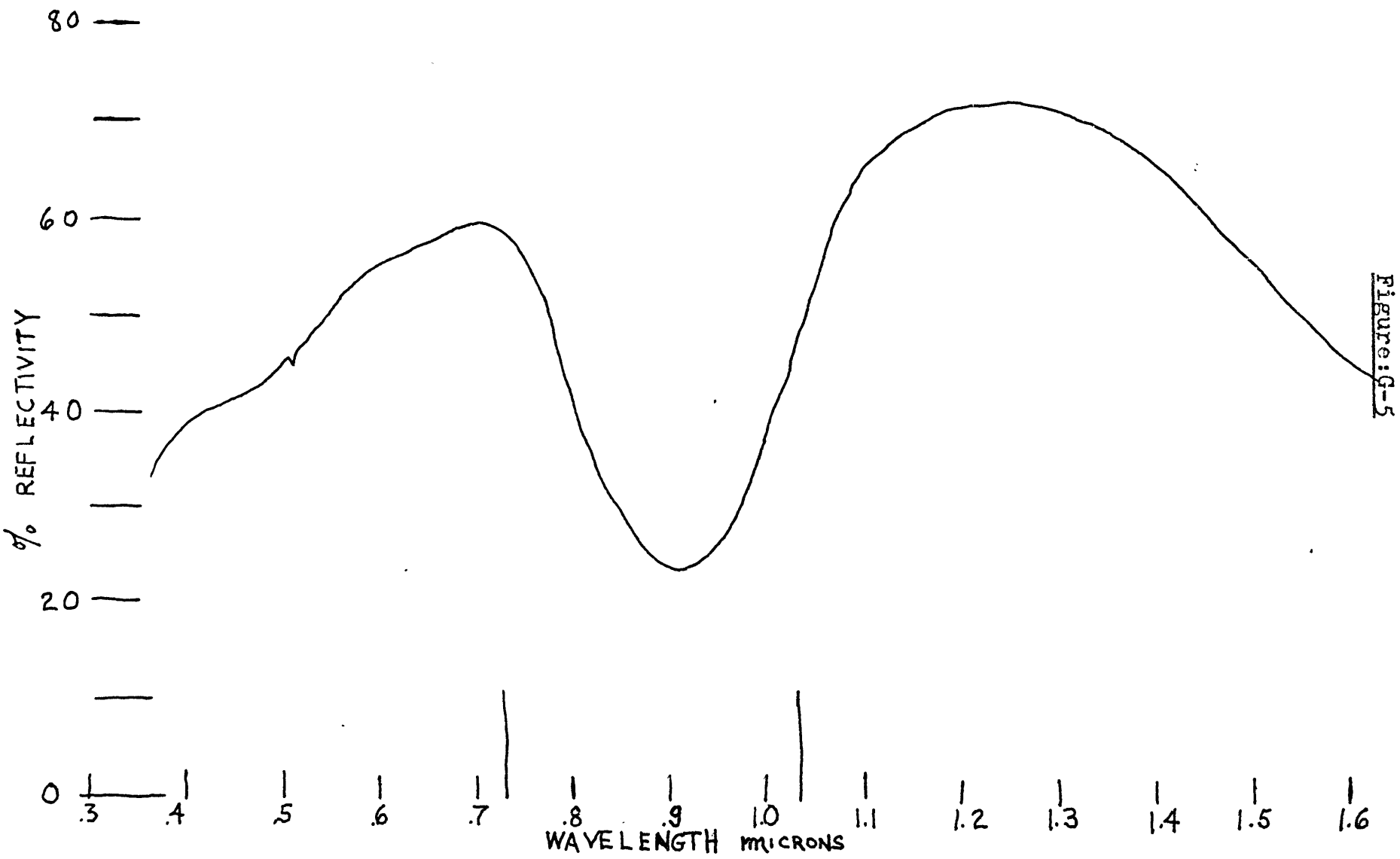

Figure: G-5

DIFFUSE REFLECTION SPECTRA of En_{89} — WEBSTERITE, PARTICLE SIZE LESS THAN 125 MICRONS

Figure: G-5

[PIETERS, 1972]

Figure: T-1: Ratios in Mineral Differentiation Test*

Wavelength	Mineral Ratio	Ratio Result
380.0Nm	Websterite/Plagioclase	74.24%
700.0Nm	Websterite/Plagioclase	65.02%
900.0Nm (Exposure-0.02sec)	Websterite/Plagioclase	48.82%
900.0Nm (Exposure-0.04sec)	Websterite/Plagioclase	33.85%

Figure: T-2: Ratio of Ratios**

(Websterite/Plagioclase,700Nm)//(Websterite/Plagioclase,380Nm)

Result: 87.7%

(Websterite/Plagioclase,900Nm)//(Websterite/Plagioclase,380Nm)
Exp.-0.02sec

Result: 65.5%

(Websterite/Plagioclase,900Nm)//(Websterite/Plagioclase,380Nm)
Exp.-0.04sec

Result: 45.6%

*NOTE: These ratios are based on average of mineral target matrix elements; sixty for the websterite and sixty for the plagioclase feldspar.

**NOTE: These ratios obtained from dividing the results in the preceeding table.

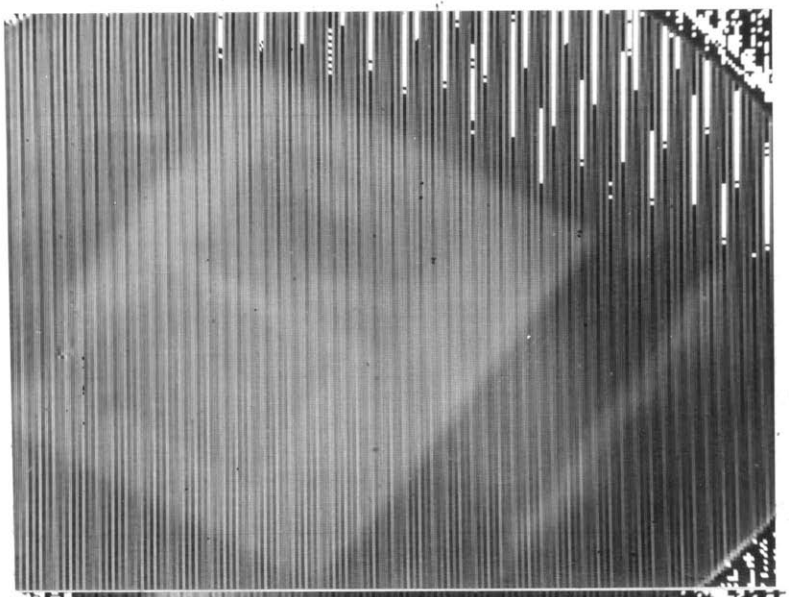

Figure: P-1

Websterite-
Plagioclase

380.0 Nm

Exp.-6.0 sec.

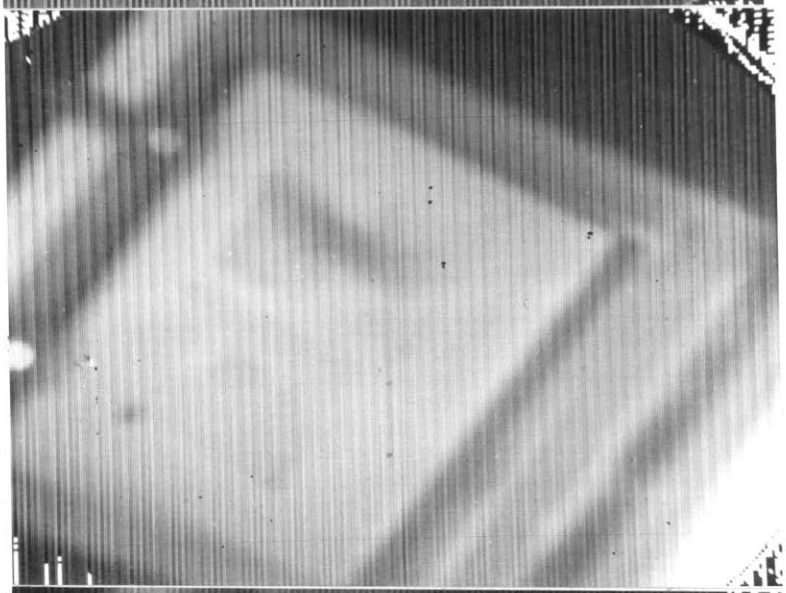

Figure: P-2

Websterite-
Plagioclase

700.0 Nm

Exp.-0.02 sec.

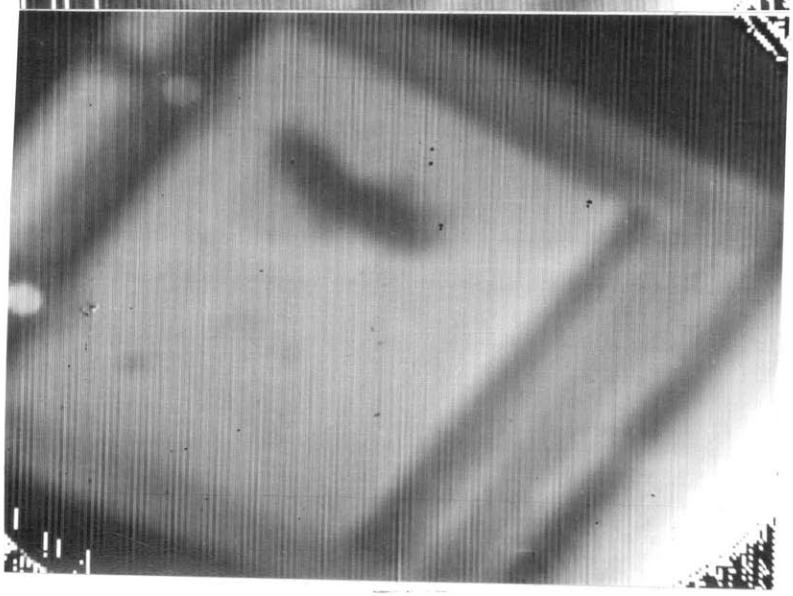

Figure: P-3

Websterite--
Plagioclase

900.0 Nm

Exp.-0.04 sec.

TESTING ABILITY TO DIFFERENTIATE MINERALOGY AND STRUCTURE OF LARGE ROCK SAMPLES

Background

Applying the theory and the results from the previous experiment, an experiment was performed to illustrate the vidicon system's ability to differentiate both mineralogy and structure of large rock samples under laboratory conditions. The laboratory environment is illustrated in Figure S-3. The rock samples varied from 20 to 60 centimeters along their greatest dimension. An area of approximately 30 centimeters in diameter could be adequately resolved by the vidicon system at a distance of approximately 3.15 meters(target to detector). The rocks were illuminated by a 150 watt tungsten bulb because its spectral characteristics are similar to that of the sun(except that it is shifted toward the infrared region of the spectrum due to the coolness of the bulb). The means of evenly illuminating the target were constructed with available materials; however pains to insure uniform illumination were not taken, because in nonlaboratory applications, a uniform illumination could not be depended upon(due to shadows, random clouds, etc.).

The rock samples were selected on the basis of mineralogy, structure, and their abilities to best illustrate the capabilities of the vidicon system. Five rocks were chosen from the collections of the geology department of the Massachusetts Institute of Technology: Jointed Dolomite, Orbicular Granite, Glacial Tillite, Folded Marble, and an Olivine Basalt. Each of these will be discussed separately with regard to their physical nature and experimental results.

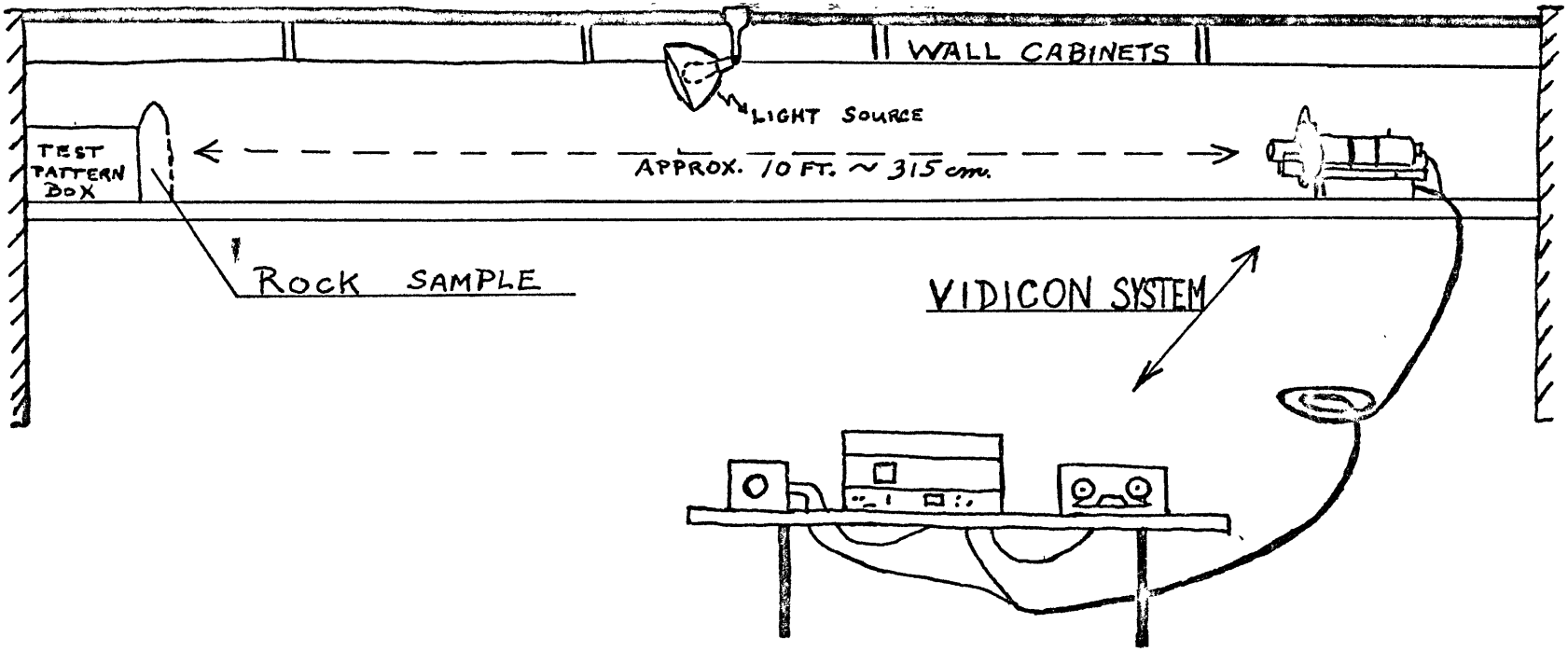

Comments:- Light Source: 150 Watt Tungsten Bulb
- Vidicon Cold Box(Dewar) Cooled with CO_2 ice
- Most efficient laboratory procedure was to have 1 technician operating the vidicon system while the other technician manipulated the rock samples, filter wheel, and made a log of the experiment(for the purposes of data processing)
- The only means of illumination was the light source; room was masked and dark; the filter wheel mount, dewar, and auxillary power supply unit was masked and hooded to prevent saturation of the vidicon tube
- Initial focusing was performed by using the test pattern box,replacing the test pattern with surface of the rock or target being "photographed" by the vidicon system, and then fine focusing by observing the vidicon monitor.

LABORATORY SETUP FOR LARGE ROCK SAMPLE, PORPHYRY COPPER,AND RELATED EXPERIMENTS

Figure: S-3

DISCUSSION

Probably the most interesting rock sample used in this experiment, because of its nature of illustrating the potential of the vidicon system in differentiating mineralogy and mapping structure, was a jointed dolomite(Figures P-4,P-5, and P-6). This jointed dolomite(general formula:$(Ca,Mg)CO_3$) had a red-brown matrix coloration due to the presence of an oxidized iron cation, Fe^{3+}. This sample had undergone tensional stress which formed a joint network in the rock matrix. These joints were gradually mineralized by dolomite containing reduced iron(Fe^{2+}) impurity. The Fe^{2+} cation and the mineral it was contained in are the cause for the joints to appear green to the eye(Billings,1954;Burns,1970).

Vidicon pictures were taken at 400.0 Nm and 950.0 Nm. After the dark fields had been subtracted(Kunin,1972), the images were enhanced by simply adding or subtracting picture intensities (eg.:picture at 400.0Nm subtracted from the 950.0 Nm picture yields Figure P-8). Before discussing the various computer techniques found to assist in enhancing imagery, a comparison of the two original pictures must be made(Figures P-4,5,6). The filters used in these photographs were selected on the basis of the reflectivity spectra of pure dolomites(Hunt and Salisbury,1970). According to those spectra, the dolomite should appear brighter relative to the MgO standard(located at the bottom right corner of the pictures) at 950.0 Nm than at 400.0 Nm. Though this seems to be the case in the pictures, it cannot be known for sure until the pictures are scaled. Separate pictures are scaled by equalizing the intensity of the MgO for the two pictures. A scaling factor

could be employed by the computer to adjust the intensities of the entire picture(whichever is chosen), so that the two pictures are comparable. This scaling technique assumes that the system is linear in its response to reflected light intensity as a function of time.

Linearity of the system was checked by taking ratios of regional reflected intensities of the dolomite and comparing them to those obtained from pictures taken at different exposure times (filter and light source constant). The results are listed in Figure T-3. Clearly there is a variation of ratios with exposure of 6 to 10%. This infers that the vidicon system is either nonlinear or has excessive noise problems. These results emphasized the need for a controlled linearity test to be performed.

By using the 950.0 Nm filter, the absorption band due to Fe^{2+} is illustrated by the low albedo of the joint. At 400.0 Nm, the joint pattern appears brighter than the matrix because Fe^{3+} ion, in its coordination with the dolomite, has caused absorption; while the Fe^{2+} ion of the joints has no absorption features. In the practical world, these pictures illustrate the vidicon system's potential in mapping structure and identifying which ions are causing the coloration of the target with the help of ground truth (knowledge of a target's characteristics prior to its formal exploration).

If the 400.0Nm and 950.0Nm pictures are not suitable for distinguishing structure, various computer techniques may be employed to enhance the imagery. For example, Figure P-8 results from subtracting the 400.0Nm picture from the 950.0 Nm picture.

The process involved no theory but enhancement of joint pattern is obvious. Printing the negative image of Figure P-6 clearly enhances the contrast between the joint pattern and the matrix (Figure P-7). Using the SC4020 plotting routines(Kunin,1972), produced a contour enhancement of intensities of the joint-matrix regions and illustrated numeric anomalies in regions assumed to have uniform absorbing properties(this enhancement technique is not illustrated in figure format due to difficulties in reproduction).

In order to obtain the relative albedo of the dolomite at the two wavelengths, either a ratio technique that compares the regions of the dolomite to the MgO standard or a ratio process that compares two regions of the dolomite at each wavelength would have to be employed. This would show whether the joint and matrix pattern are brighter at 950.0 Nm or 400.0 Nm. Using more filters, it would be possible to determine if the material is a dolomite or a sandstone(by plotting ratios versus wavelength) (See Figure G-9 and discussion on page 51).

Tentative conclusions from this experiment are that the vidicon system can determine the ions causing the absorptions despite the uniformity of the sample's general composition. The vidicon's ability to enhance imagery features was illustrated and discussed. In actual geophysical surveys, points common to both vidicon pictures and a topographic map might be known. If the two are superimposed, the structure could be mapped onto the topographic map. This concept is applied to aerial photography and is a great tool in mineral exploration.

Figure: T-3: JOINTED DOLOMITE LINEARITY RESULTS

CATION	REGION Coordinates	#Intensity Elements Averaged	Exposure (sec)	Intensity Average
Fe2+	(65-68,165-171)	28	3	4244/28
Fe3+	(81-84,170-176)	28	3	4834/28
	Ratio: Fe2+/Fe3+ = 0.87			
Fe2+	(65-68,165-171)	28	2	1290/28
Fe3+	(81-84,170-176)	28	2	1600/28
	Ratio: Fe2+/Fe3+ = 0.80			
	Ratio Variation: 7.0%			
Fe2+	(81-85,103-107)	25	3	3740/25
Fe3+	(90-94,130-134)	25	3	4689/25
	Ratio: Fe2+/Fe3+ = 0.79			
Fe2+	(81-85,103-107)	25	2	1137/25
Fe3+	(90-94,130-134)	25	2	1628/25
	Ratio: Fe2+/Fe3+ = 0.69			
	Ratio Variation: 10%			
Fe2+	(129-133,193-198)	30	3	4559/30
Fe3+	(161-165,161-166)	30	3	5797/30
	Ratio: Fe2+/Fe3+ = 0.78			
Fe2+	(129-133,193-198)	30	2	1421/30
Fe3+	(161-165,161-166)	30	2	1956/30
	Ratio: Fe2+/Fe3+ = 0.72			
	Ratio Variation: 6.0%			

RESULT: 6-10% Variation in reflected intensity ratios with exposure time holding all other parameters constant....infers nonlinearity of the vidicon system.

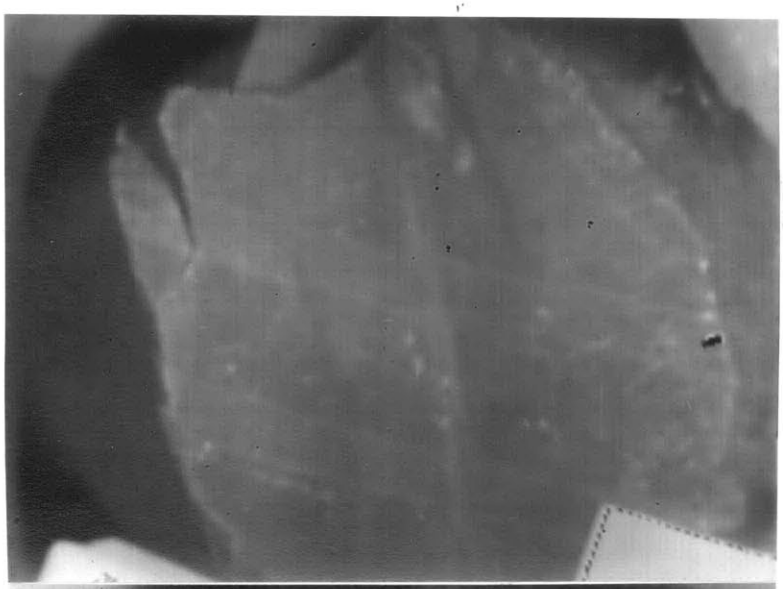

Figure: P-4

Jointed Dolomite

400.0 Nm

Exp.-20 sec.

Figure: P-5

Jointed Dolomite

950.0 Nm

Exp.-0.02 sec.

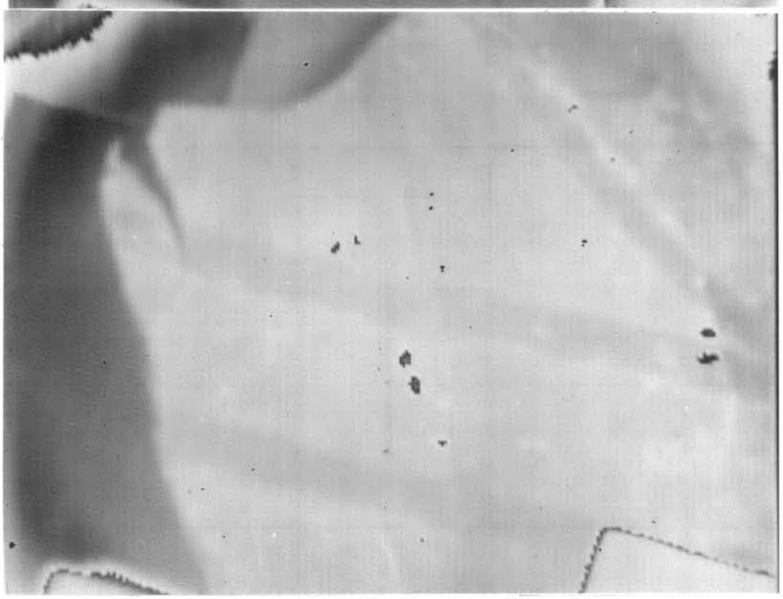

Figure: P-6

Jointed Dolomite

950.0 Nm

Exp.-0.04 sec.

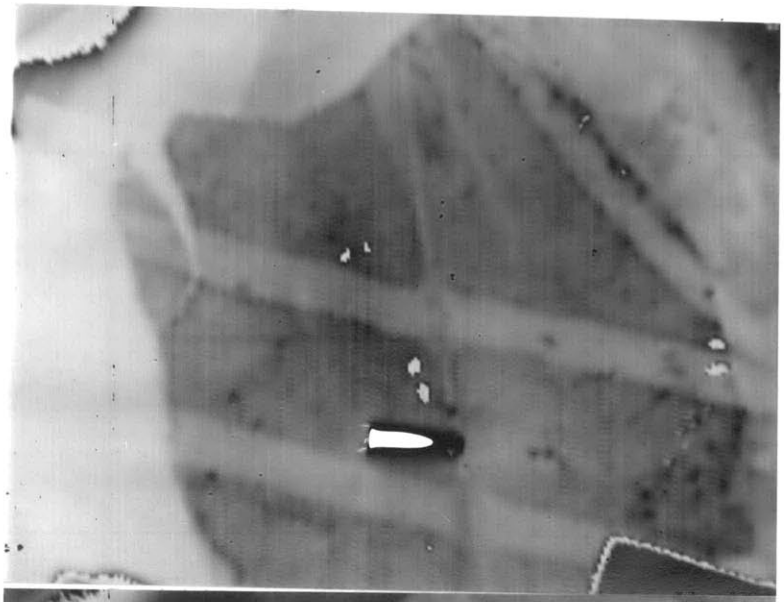

Figure: P-7

Jointed Dolomite with features enhanced (Negative, P-6)

950.0 Nm

Exp.-0.04 sec.

Figure: P-8

Jointed Dolomite with features enhanced by subtracting Figure P-4 from Figure P-6.

To assist in a rough determination of the vidicon system's resolving power, an orbicular granite(Figure P-9,10,11) was chosen because of its unusual structure and the number of mineral phases in its composition. The circular structures in this granitic rock are segregations of minerals that are explained by various differentiation processes(Johannson,1931) in the granitic magma. With reference to the picture taken at 950.0Nm (Figure P-11), a brief mineral description is in order. Orthoclase feldspar appears snow white. Plagioclase feldspar and quartz appears as splotches of grey intermixed with white feldspar. The more massive dark grey to black regions(inner orbicles) are composed of fine feldspar and biotite crystals. The matrix of the rock is coarse biotite, augite, and hornblende. Despite the picture's poor focus((due to the crude means available for focusing the image upon the vidicon detector(to be discussed in the section on field performance)), rock features having minimum linear dimensions of 0.15 mm could be resolved from 3.15 meters with perfect focusing conditions.

Pictures were taken at 400.0 Nm, 800.0 Nm and 950.0 Nm to illustrate how the absorption of photons allows the differentiation of minerals. However, this was accomplished without using the absorption bands. If two minerals are spectrally flat and featureless(quartz and plagioclase-labradorite), then the mineral that has greater reflectivity over a spectral range(quartz in this case) should be distinct from the other mineral at any wavelength. This explains the consistent differentiation of biotite from orthoclase feldspar in all vidicon pictures. However, problems

Figure:T-4: ORBICULAR GRANITE
Mineral Differentiation and Texture Results

Mineral	Location on Picture	Intensity Averages at: 400.0Nm	800.0Nm	950.0Nm
Orthoclase Feldspar	(170-175,131-136)(36)	175.4	236.0	111.0
Quartz	(157-160,198-203)(26)	117.6	134.3	64.7
Quartz	(136-140.229-235)(35)	120.9	144.0	70.0
Fine Biotite (Minor qtz) (" feldspar)	(144-148,177-183)(35)	84.0	72.0	39.6
Coarse Biotite (No Mixture)	(64-69,130-133) (20)	42.5	40.6	28.3

****

Figure: T-5: RATIO OF MINERAL INTENSITIES*

Subjects of Ratio (Relative to Quartz)	Wavelengths: 400.0Nm	800.0Nm	950.0Nm
Orthoclase/Quartz	1.49	1.75	1.71
Fine Biotite/Quartz	0.71	0.53	0.61
Coarse Biotite/Quartz	0.36	0.30	0.43
(Relative to Orthoclase)			
Quartz/Orthoclase	0.67	0.56	0.58
Fine Biotite/Orthoclase	0.47	0.30	0.35
Coarse Biotite/Orthoclase	0.24	0.17	0.25

*NOTE: Bottom table of results is based on the average intensities listed in the preceeding table.

Figure: P-9

Orbicular Granite

400.0 Nm

Exp.-10 sec.

Figure: P-10

Orbicular Granite

800.0 Nm

Exp.-0.05 sec.

Figure: P-11

Orbicular Granite

950.0 Nm

Exp.-1.0 sec.

arise when the reflection spectra are similar; eg: Rhodochrosite versus Magnesite (Hunt and Salisbury, 1971). To differentiate minerals with similar spectral reflectivity levels, use of their absorption bands' differences is necessary.

The orbicular granite could be anologized to the intrusive structures observed from an aircraft over the south-western region of the United States. In applying the vidicon system to the mapping of particular structures, ground truth of the target would have to be obtained. This would basically call for the determination of the lithology that comprises the structure and the region surrounding the structure. With the latter knowledge, interference filters that occupied the mineralization's absorption bands and continuum would be selected for the vidicon survey. If the absorption bands are distinctive and not shared by other minerals and/or rock units of the region, then a particular lithology or structure may be mapped. Such a procedure would have considerable value in mining exploration.

Another rock sample that depicted terrestrial surface features was a glacial tillite; Precambrian Gondwana Conglomerate-Tillite, of the Cobalt Series-obtained by Robert Shrock near Kirkland Lake, Ontario. This tillite consists of granitic clasts of variable composition(Figure P-13, Table T-6) in a chloritic clay matrix(greywacke(?)). The main compositional minerals were determined prior to the experiment. Filters for differentiating minerals were selected using the latter information and the Hunt and Salisbury reflectivity spectral curves(1970-1971). Unfortunately, the minerals were not the type that could be differentiated by

the subtle use of absorption bands. Instead, according to the reflectivity spectra of Hunt and Salisbury(1970-1971), the structure and mineralogy should appear distinct at any wavelength. Pictures were taken at 400.0, 560.0, 800.0, and 1100.0 Nms.(Figures P-12,13,14,15). If the obvious poor focus and saturation is ignored(to be discussed in a later section), it is obvious that the key structures of the granites in the chloritic matrix are distinguishable. The average albedo of each granitic clast is a function of the distinct compositional differences of each granite relative to the others. Because of the poor quality of the 400.0 Nm and 1100.0 Nm pictures, the SC4020 plot routine that was discussed earlier(Kunin,1972) was employed. The plotting of the pictures was a more concise means of determining which mineralogy was most directly effecting the albedo of the granites.

At 400.0 Nm, Granite II(Figure S-4) had the highest albedo due to its significant quartz composition(Table T-6). The other three granites' low quartz compositions and amphibole content made their reflectivities comparable to the matrix(Hunt and Salisbury,1970) which resulted in poor contrast. The intensity plots illustrated that at 560.0 Nm, Granites II and III have the highest albedo. Reflectivity spectra of Hunt and Salisbury(1970-1971) suggest that the high concentrations of hornblende and quartz for Granite II and the high concentrations of hornblende for Granite III are the minerals responsible for the high albedo. At 800.0 Nm the chlorite is absorbing due to Fe^{3+} ion in its coordination state(Hunt and Salisbury,1970). This absorption permits contrast between the four granites relative to the matrix; however

to differentiate the granites relative to each other is difficult. The reason for the difficulty is that only Granite I has enough quartz content to give it a distinct albedo relative to the others; but the composition of the remaining granites are similar in their quartz-poor nature. The 1100.0 Nm filter picture is very distorted and complicated by the difficulties in focusing the equipment; the intensity plots were of no real help in this case because of the overall picture quality.

The remaining two rock samples observed were a banded marble and an olivine basalt. The marble exhibited a fold structure that is a common terrestrial crust feature. The marble's structure was resolved adequately(no figures because of the saturated nature of the pictures). The olivine basalt contained olivine phenocrysts; these have absorption bands at 1000.0Nm due to Fe^{2+}in six-fold coordination. The olivine-feldspar matrix experienced similar absorptions at 1000.0 Nm for the same reasons. The latter similarity may account for the inability of the vidicon system to dfferentiate phenocrysts from matrix material at 950.0 Nm; though the low contrast may be attributed to saturation(no figures). The low contrast phenomena is predicted by:crystal field theory; olivine reflectivity spectra(Hunt and Salisbury, 1970); and the reflectivity spectra for a grey basalt(Adams and Filice, 1967). A second experiment was performed on the basalt sample. The pictures were of poor quality again leaving this investigation of low contrast phenomena open to speculation.

Figure: S-4

Gondwana Glacial Tillite Reference Sketch (See Table T-6)

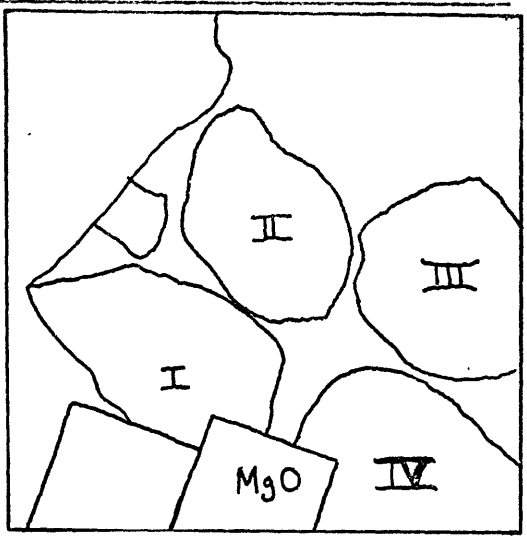

Figure: T-6:: Composition of Granite Clasts

Granite I :	80% Red-Pink Orthoclase Feldspar
	10% Weathered Hornblende
	10% Muscovite(?) and Quartz
Granite II:	25% Hornblende and Biotite
	40% Pink Orthoclase Feldspar
	35% Quartz
GraniteIII:	55% Weathered Hornblende(Biotite?)
	45% Pink Orthoclase Feldspar
	10% Quartz
Granite IV:	15% Hornblende and Biotite
	35% Pink Orthoclase Feldspar
	35% White Orthoclase Feldspar
	5% Quartz

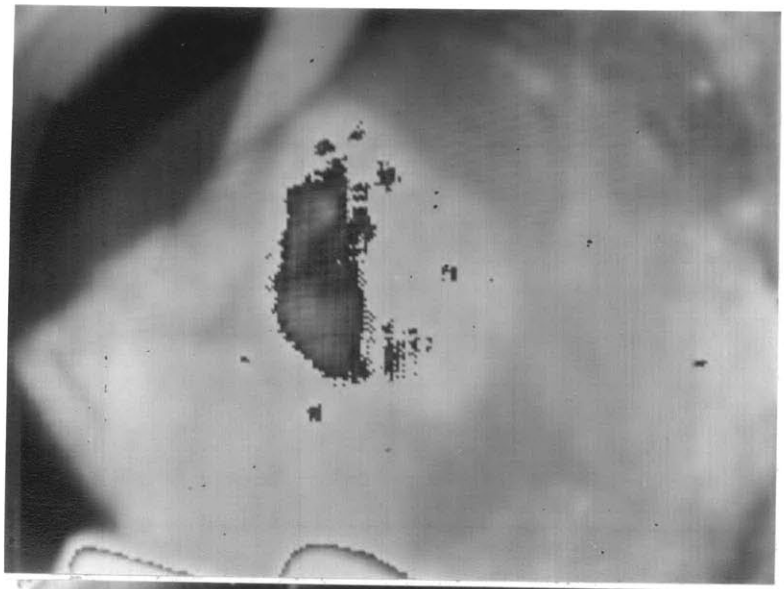

Figure: P-12

Gondwana Tillite

400.0 Nm

Exp.-5 sec.

Figure: P-13

Gondwana Tillite

560.0 Nm

Exp.-1.0 sec.

Figure: P-14

Gondwana Tillite

800.0 Nm

Exp.-0.4 sec.

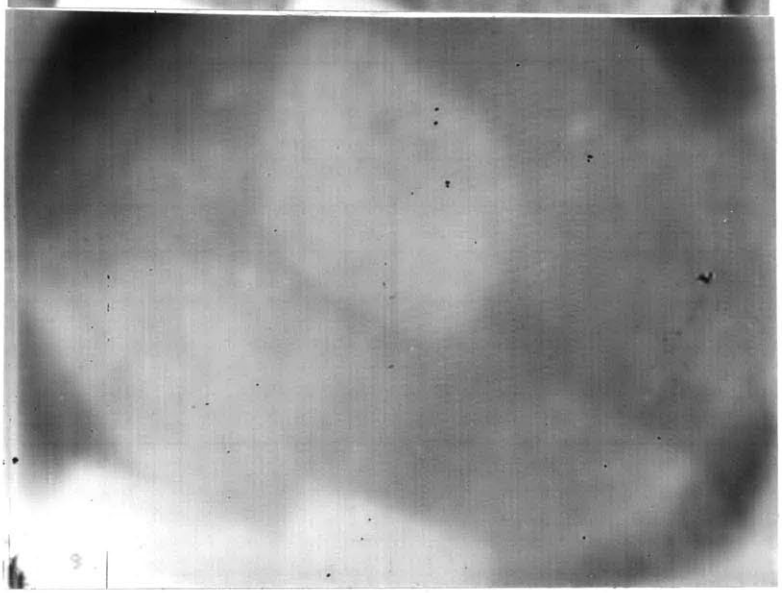

Figure: P-15

Gondwana Tillite

1100.0 Nm

Exp.-25 sec.

TESTING ABILITY TO IDENTIFY MINERALOGY WITHOUT GROUND TRUTH

Background

During a remote sensing survey with the vidicon system, there could conceivably occur a time when there was no available ground truth from which interference filters could be selected for a survey. If the vidicon system could identify mineralogy, with the assistance of computer processing and a library of absolute reflectivity spectra(eg. Hunt and Salisbury), then it would provide a valuable tool in ore mineral exploration that exceeded its proven value in detection, differentiation, and mapping of geologic material.

Absolute reflectivity spectra have been obtained for a variety of common minerals(Hunt and Salisbury). The process consists of plotting the ratio of the reflected intensity of a mineral to a standard's reflectivity(MgO, sandblasted gold) versus wavelength (Hunt and Salisbury,1970-1971; Adams and Filice,1967). An experiment was performed to obtain the ratio of the recorded intensities of minerals with respect to the subsaturation intensities of a MgO standard. These ratios were plotted versus wavelength. The resulting spectral curves were compared to published absolute reflectivity spectra in order to identify the minerals. This was basically a crude form of vidicon spectroscopy.

The laboratory setup is illustrated in Figure S-3 and the procedure followed is similar to the experimental procedures involving large rock samples(page 34). The minerals chosen in this study were cinnabar(HgS-mercury ore), rhodochrosite($MnCO_3$), and rhodonite($MnSiO_3$). Cinnabar was selected for its simple spectra;

CINNABAR 133B MANHATTAN, NEV.

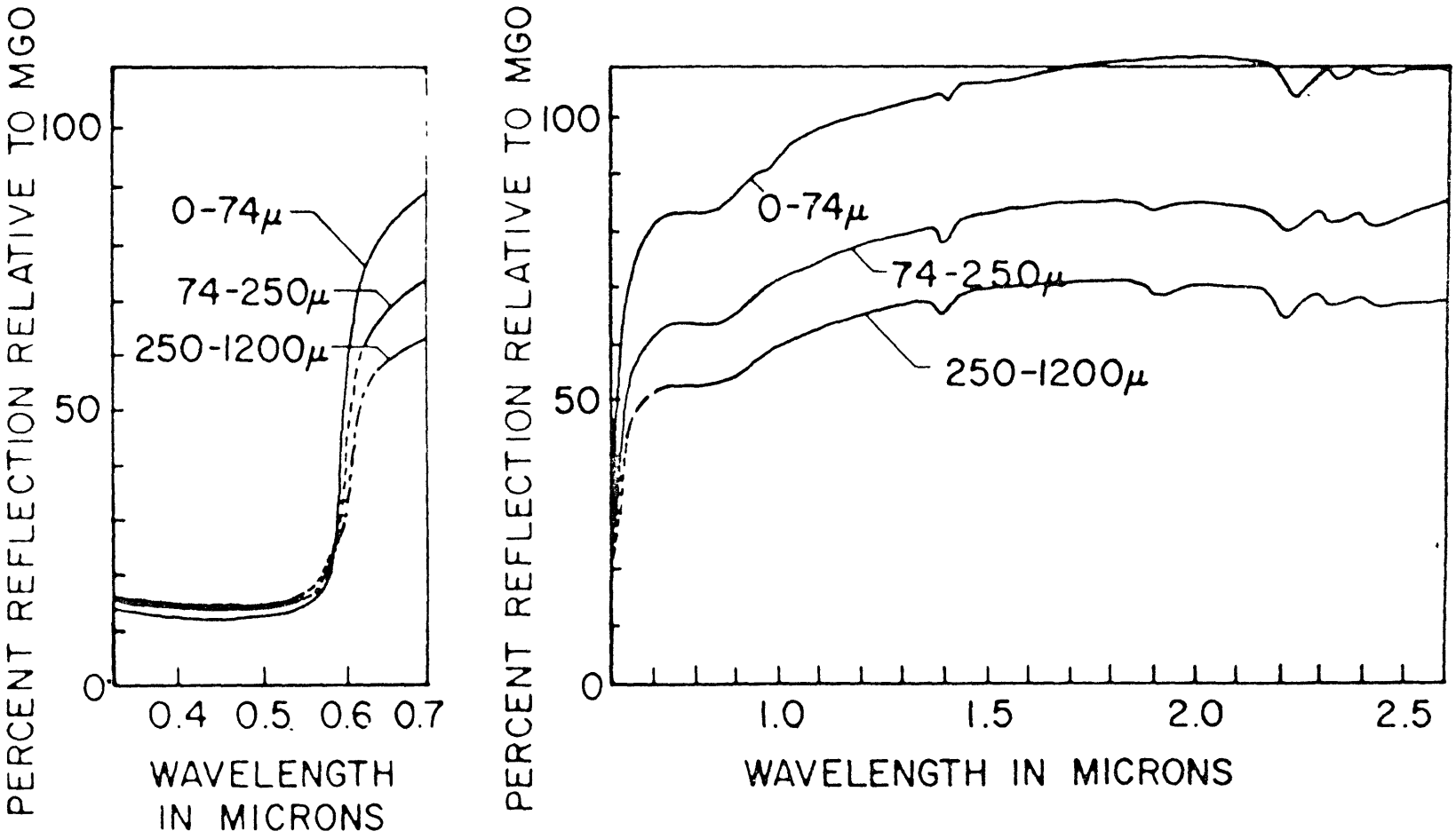

Figure: G-6

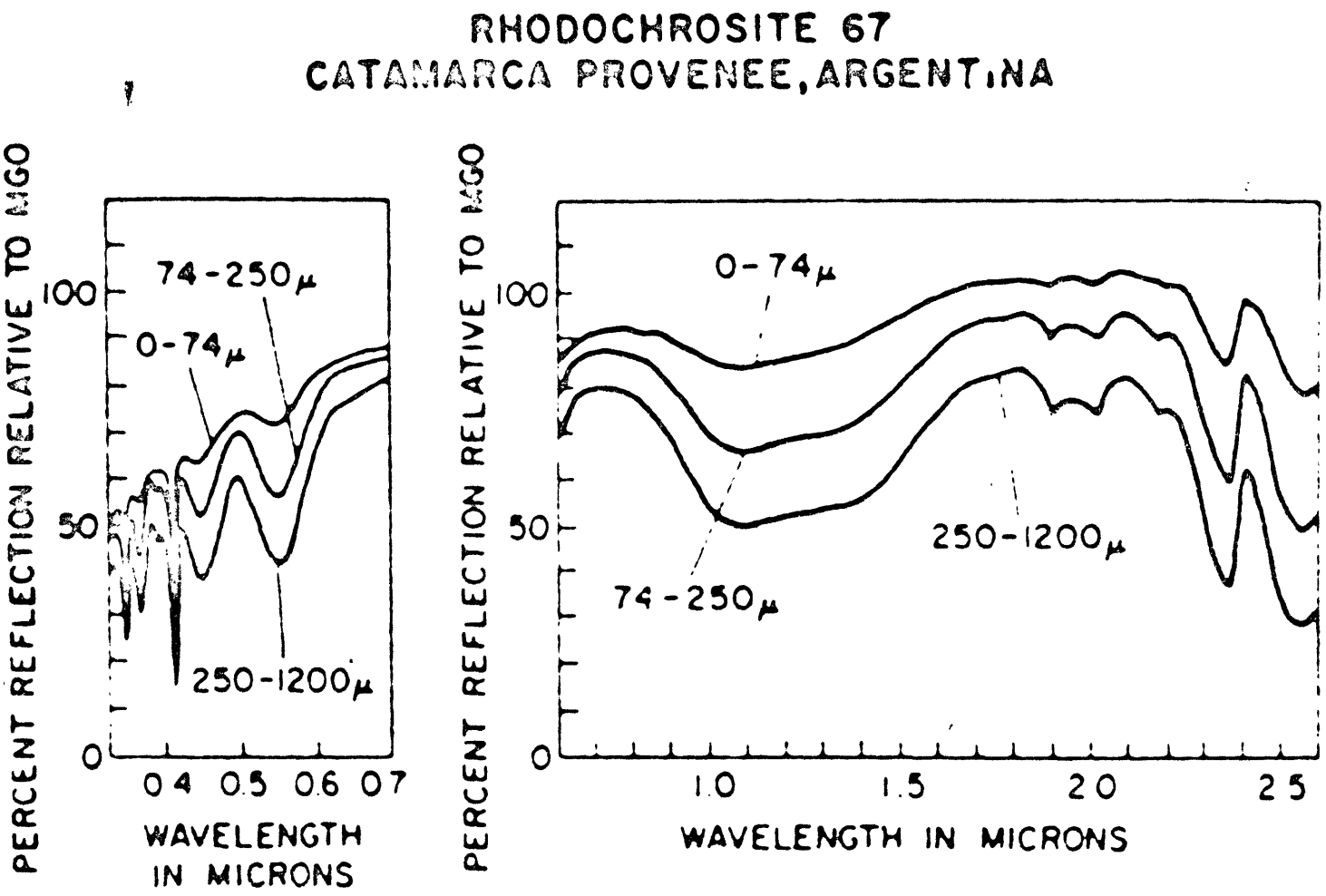
RHODOCHROSITE 67
CATAMARCA PROVENEE, ARGENTINA
PERCENT REFLECTION RELATIVE TO MGO
100
50
0
74-250μ
0-74μ
250-1200μ
0.4 0.5 0.6 0.7
WAVELENGTH IN MICRONS
PERCENT REFLECTION RELATIVE TO MGO
100
50
0
0-74μ
250-1200μ
74-250μ
1.0 1.5 2.0 2.5
WAVELENGTH IN MICRONS

Figure: G-7

Figure: G-8

Rhodonite ($MnSiO_3$) Reflectivity Spectra

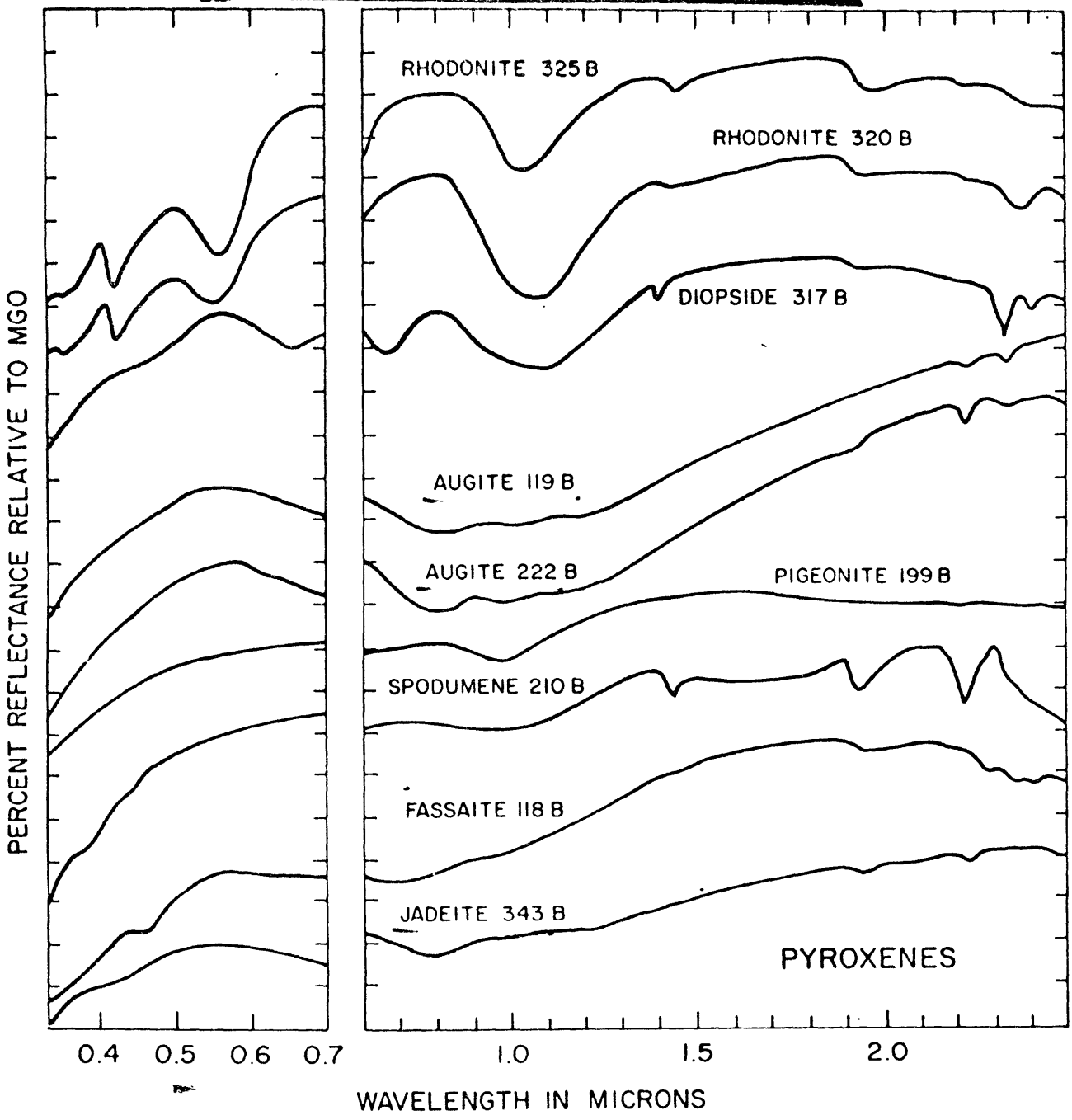

ie. conduction band at approximately 600.0 Nm causes low albedo from 400.0 Nm to 600.0 Nm and high albedo from 600.0 Nm to 1100.0 Nm(sharp increase in albedo at 600.0 Nm). Figures G-6, S-5, and P-16 illustrate cinnabar's absolute reflectivity spectra, position relative to the target pattern, and its appearance on a processed vidicon picture,respectively. Rhodochrosite and Rhodonite were selected because of the fine, distinct electronic absorptions that the Mn^{2+} ion in octahedral coordination produced at 340.0 Nm, 370.0 Nm, 410.0 Nm, 450.0 Nm, and 550.0 Nm. Figures P-7,8 are the absolute reflectivity spectra of rhodochrosite and rhodonite respectively; whereas Figure S-5 and P-16 illustrate the minerals' location on the target pattern and processed vidicon pictures.

DISCUSSION

In order to successfully perform a reasonable vidicon spectroscopy experiment, several interference filters had to be selected in order to adequately illustrate the minerals' absorption bands and/or conduction bands. Unfortunately, the filters available for the experiment did not adequately correspond to the absorption features of rhodonite and rhodochrosite. There were filters that covered the continuum but there was only one filter that corresponded to a Mn^{+2} absorption band(560.0Nm). Never-theless, nineteen filters were used and the resulting pictures and print-out of intensities(0 to 255 scale) permitted ratios of minerals' intensities to standard MgO intensity to be determined(Figure T-7). The averages of table T-7 are plotted in Figure G-9 relative to wavelengths of the visible and near-infrared spectra.

Comparison of Figure G-9 with Figures G-6,7,and 8 show some encouraging similarities. The cinnabar reflectivity spectra plotted in Figure G-9 has an overall low albedo due to the presence of opaque mineral impurities in the sample. The rise in reflectivity at 600.0 Nm marks the conduction band of cinnabar. Both of the spectra for rhodonite and rhodochrosite show a distinct absorption band at 550.0 Nm that may be attributed to the Mn^{2+} ion. The bands at 900.0 Nm and 1000.0 Nm may be due to the presence of Fe^{2+} ion in a contaminant mineral or trapped within the crystal structure of the rhodonite or rhodochrosite. The absorption band at 660.0 Nm and the broad band from 700.0 Nm to 800.0 Nm could not be explained because of their indistinct nature. As predicted by the absolute spectra(Figures G-7,G-8), rhodonite had a generally higher spectral albedo than rhodochrosite. This characteristic would be useful in differentiating the two distinct minerals having otherwise similar spectral characteristics.

In conclusion, if an ample number of vidicon pictures are processed, a mineral(or at least the key transition elements of the mineral) may be identified from the spectra generated from this crude spectroscopy technique. If too many pictrures are taken, a problem concerning the cost in computer processing must be considered. The answer to this problem may well be answered by the development of a prism spectrometer that has been designed for the vidicon system(George Silvas, telephone communication); a paper describing this device is anticipated to be written in the near future.

Figure: T-7: Spectral Curve Comparison Test Data

Mineral	Prime Coordinates	Number of Intensity Points Averaged
Cinnabar(HgS)	(81-85,100-104)	25
Rhodochrosite ($MnCO_3$)	(110-114,158-162)	25
Rhodonite ($MnSiO_3$)	(144-148,111-115)	25
MgO	(146-150,199-202)	20+

Ratios: Mineral/MgO ***

Wavelength (Nm)	HgS	$MnCO_3$	$MnSiO_3$	MgO
400.0	0.024	0.047	0.084	1.0
427.0	0.160	0.259	0.377	1.0
470.0	0.016	0.065	0.170	1.0
500.0	0.016	0.088	0.195	1.0
533.0	0.018	0.072	0.168	1.0
560.0	0.022	0.069	0.222	1.0
570.0	0.018	0.105	0.227	1.0
600.0	0.037	0.163	0.485	1.0
620.0	0.092	0.352	0.672	1.0
660.0	0.038	0.174	0.440	1.0
700.0	0.085	0.369	0.686	1.0
746.5	0.050	0.307	0.520	1.0
800.0	0.063	0.363	0.389	1.0
850.0	0.252	0.451	0.976	1.0
900.0	0.088	0.217	0.136	1.0
950.0	0.147	0.340	0.187	1.0
1000.0	0.073	0.149	0.081	1.0
1033.0	0.081	0.191	0.093	1.0
1100.0	0.266	0.438	0.380	1.0

****

Note: The ratios in this table are the data for Spectral Curve which may be compared Spectral Curve G-9 for the purposes of assessing the instrumentation's capability in determining mineralogy without prior groundtruth.

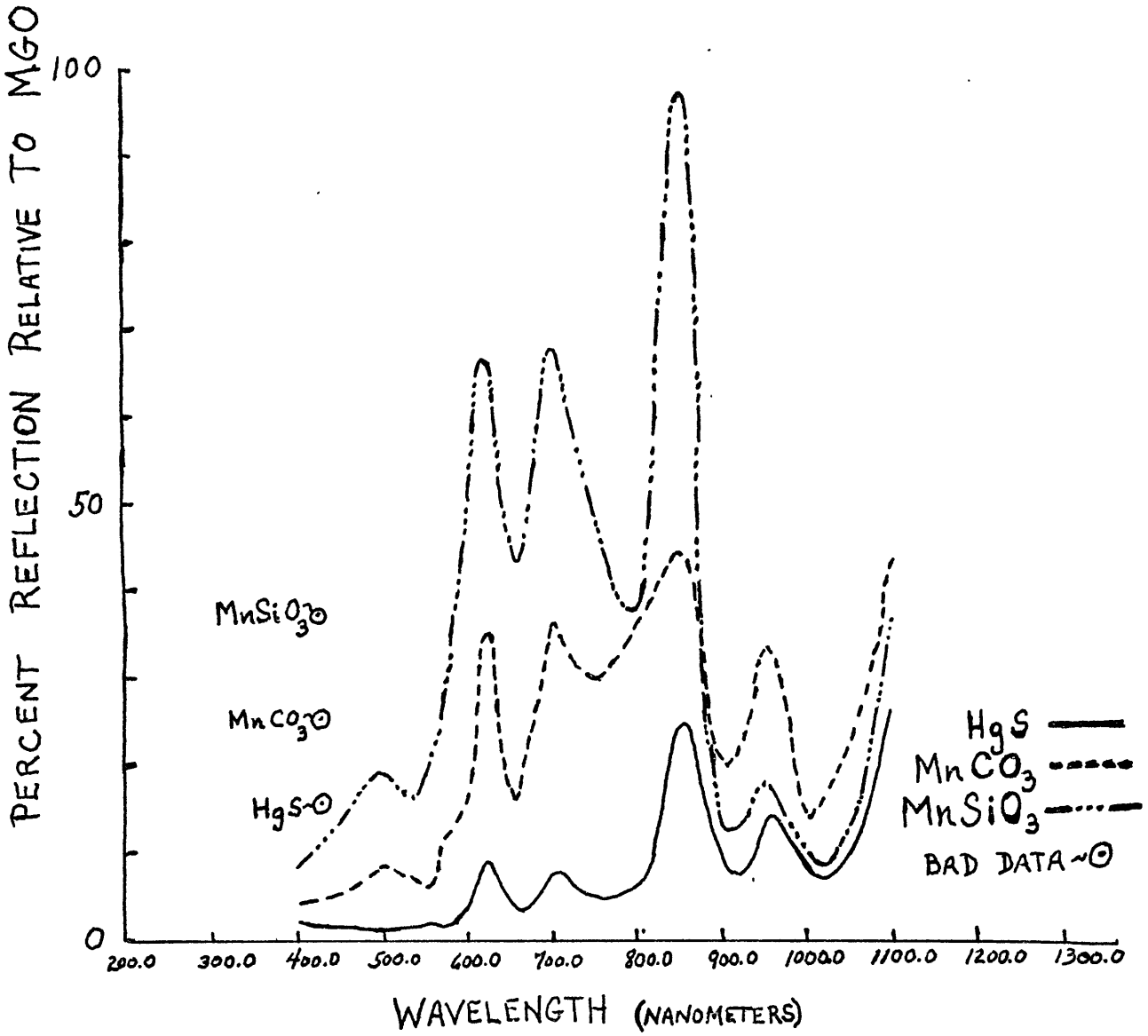

Figure: G-9

Vidicon Spectroscopy Experiment's Plot of Intensity Ratios versus wavelength(19 filters) for three minerals: Cinnabar, Rhodochrosite, and Rhodonite.

Figure: S-5

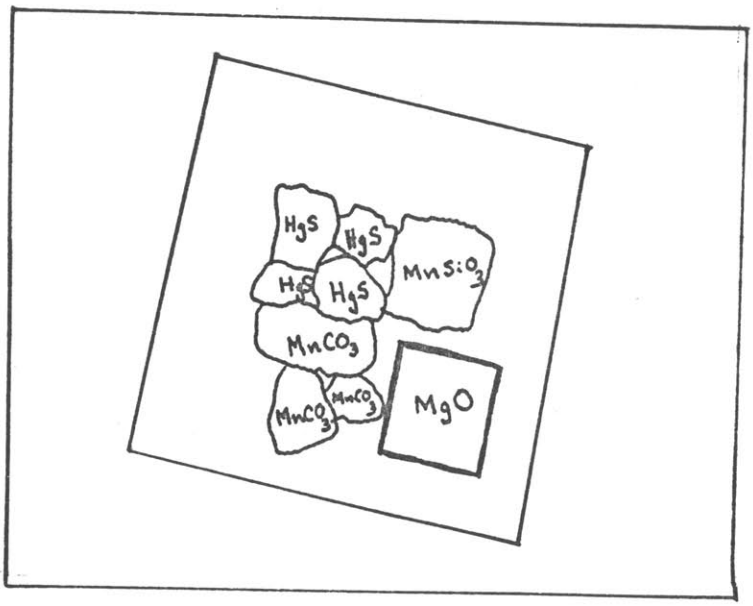

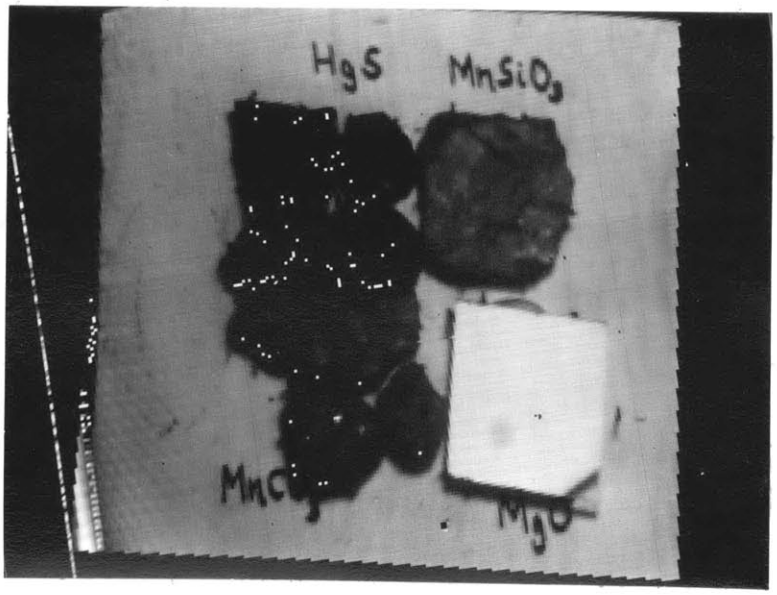

Figure: P-16

HgS-$MnCO_3$-$MnSiO_3$ Sample Imagery of the Vidicon Spectroscopy Experiment; 560.0 Nm, Exposure: 0.3 sec.

A CONTROLLED LINEARITY TEST OF THE VIDICON SYSTEM

Background

In the earlier experiments that illustrated the vidicon system's ability to differentiate minerals and discriminate structure in large rock samples, impromptu tests of the vidicon system's linear response were performed. Linear response means that the ratio of average intensities of two regions of a target's imagery is constant when a function of exposure time(holding light source, target, and interference filter constant). The initial tests' results(pages:32,39) inferred the possibility of a nonlinear response or a problem linked to excessive'noise'levels.

After the second experiment's results indicated a nonlinear and/or electrically noisy vidicon system, considerable discussion was initiated between the investigator and the technicians to determine the source of the problem. Since the vidicon tube's response is known to be linear(McCord,1972), there was the implication that the trouble was linked to the system's electronics or the technique used in the laboratory tests. If the vidicon picture had a subject material that absorbed to a degree that placed its recorded intensities in the same numeric range as the dark field and if another region of the same target had an albedo in excess of the dark field intensities(within the normal linear range of the tube), then upon increasing the exposure time, the normally reflective area would get brighter but the absorbing region would remain at the same intensity levels. This effect is characterized by light regions of the target becoming brighter and dark regions remaining just as dark. The phenomena might be

labelled as a 'light sink' effect(Huguenin, verbal communication). This effect would produce ratios that varied nonlinearly with the exposure time. The effect could be elliminated by taking precautions when performing the tests. The tests and any vidicon 'photography' should be conducted without saturating the regions of the target that are to be ratio analyzed. Similarly, pictures must be made that do not compete with the intensity of the dark fields associated with the picture.

Linearity tests have been performed by Ezell and Gettys (personal communication) which gave good, but ambiguous, results (performed prior to this experiment). Their results did instruct the fact that there is an operational technique to follow when employing the vidicon system. For example, if a picture was not recorded within a few minutes of having been taken, then variable regions of the image brighten due to electric noise. This phenomena is the source of nonlinear results when ratioing regional intensities. On the basis of this information, a careful, yet practical test in a geologic sense, was performed to test linearity.

During a vidicon experiment in which porphyry copper rock sample suites were being 'photographed'(see next section,page 66), the Christmas District rock samples(Figures P-31 to P-37) were used to conduct a linearity test of the vidicon system. The test was performed under controlled conditions using an 800.0 Nm interference filter and exposures of 0.1, 0.2, and 0.3 seconds.

DISCUSSION

The results of the linearity experiment are recorded in Figure T-8. The experiment consisted of a single linearity experiment; however the results are determined from the ratios of three distinct regions of the target. Ratios were performed on the average intensities of three pairs of rock samples. The samples'locations and the actual pictures are illustrated in Figures S-9 and P-35 respectively.

The degree of variation of the ratios is best explained by the variance percentages of table T-8. These percentages are obtained by subtracting the ratios for separate exposures and calling this a percentage of variance. These percentages are representative of variance because under linear conditions the ratios should agree to within 1 or 2 %. The results indicated that there is usually an agreement between two of the separate exposures but the third exposure gives considerably different results. The latter phenomena follows no pattern. An exposure made at 0.1 seconds and 0.2 seconds do not have consistently agreeable ratios while the 0.3 second exposure is the consistent oddball; instead there is random agreement of ratios as function of exposure time. This is fortunate because the random variation in ratios infers that the problem is with the electric noise levels of the vidicon system rather than a problem of nonlinearity. The noise levels can be remedied but the nonlinearity problem would be permanent.

On the basis of these results(and with consideration to the fact that the experiment was performed in a manner that should have elliminated technique-induced nonlinearity), it is concluded

with reservation, that the vidicon system has nonlinear features that are linked to noise problems within the system. The reservation of the conclusion is that the possibility of a nonlinear vidicon system has not been elliminated on the basis of these tests. The fluctuation of intensity ratios may be attributed to some aspect of experimental technique that has not been determined at this time. Recommendations for remedying these problems will be made in a later section.

Figure: T-8:: Linearity Test: Data and Results
Wavelength - 800Nm

Porphyry Copper Rock Sample	Exposure(sec)	Prime Coordinate	25 Point Average	Ratio
13B	0.1	(112,119)	81/25	0.4850
12A	0.1	(169,193)	167/25	
13B	0.2	(112,119)	746/25	0.569
12A	0.2	(169,193)	1311/25	
13B	0.3	(112,119)	1492/25	0.4858
12A	0.3	(169,193)	3071/25	
	Variance - 0.08% to 8.4%			
10A	0.1	(124,140)	129/25	0.488
13A	0.1	(81,111)	63/25	
10A	0.2	(124,140)	1315/25	0.333
13A	0.2	(81,111)	438/25	
10A	0.3	(124,140)	2495/25	0.359
13A	0.3	(81,111)	895/25	
	Variance - 2.6% to 15.5%			
10A	0.1	(124,140)	129/25	0.534
12B	0.1	(89,143)	69/25	
10A	0.2	(124,140)	1315/25	0.454
12B	0.2	(89,143)	598/25	
10A	0.3	(124,140)	2495/25	0.495
12B	0.3	(89,143)	1236/25	
	Variance - 4.1% to 8.0%			

Note: Linearity Test results are based on the averaging and ratioing of matrix regions of 25 elements of two distinct rock samples of the viewed target; these matrix regions were selected as representative of the average albedo of the rock sample and were located as close as possible to the center of the picture because the resolution of the vidicon detector decreases towards the periphery of the picture(due to thickening of the silicon wafer for mounting purposes).

QUOTEABLE QUOTES ON THE SUBJECT:

REMOTE-SENSING OF PORPHYRY COPPER DEPOSITS

"The best signature for a porphyry copper deposit that I know of is the image of trucks running around in a hole in the ground."

Spencer R. Titley
Professor of Geology
The University of Arizona

VIDICON APPLICATIONS IN THE DETECTION OF PORPHYRY COPPER DEPOSITS

Background

The abilities of the vidicon system to detect, differentiate and map mineral resources that are economically feasible to mine are investigated in this experiment. Porphyry copper deposits were chosen as the subject of this experiment for two reasons: their low grade ore provides a challenge to modern mining firms' remote sensing techniques; and rock sample suites from three porphyry copper mining districts were available for the study. Despite their low grade ore, porphyry copper deposits are worth the time and effort in detecting, mining, and ore processing because these deposits are a major source of copper for industry and are a source of considerable profit to an enterprising firm.

A porphyry copper deposit, by a strict geological definition, is a well-disseminated copper mineralization in an acid, igneous intrusive(Titley and Hicks,1966). However, an economic geologist would define the deposit as low grade, mass mined(pit mine), formed later than the host rocks and was mineralized below the surface(Titley and Hicks, 1966).

In order that the reader develop a better appreciation of this experiment, a brief description of the nature of porphyry copper deposits is in order. The lower half of Figure S-6 illustrates a generalized cross-section of a porphyry copper deposit. In the western hemisphere, these deposits occur along the Cordilleran mountain chain that extends from Alaska to the southern end of South America. The deposits are typically associated with monzonitic porphyry or granodiorite-type intrusives of late Mesozoic

to early Tertiary age. Porphyry copper deposits are not particular about the host rocks that they occupy; eg. Paleozoic carbonates, shales, volcanic material, etc. Usually these deposits have their emplacement controlled by structure; ie. emplaced in folded or faulted host material. The intrusions bring about thermal and chemical changes in the host material making contact with the intrusion. Contact metamorphic minerals are found along the contact. Carbonates and sandstones are recrystallized and shales are often silicified. Faulting and emplacement of breccia pipes usually follow the emplacement of intrusives. It is during these processes of emplacement and breccia pipe formation that the intrusive and associated host rock experience hydrothermal solutions which mineralize and alter the rock(Jerome--Titley and Hicks,1966).

The hydrothermal solutions alter the intrusives and the host rock into three categories of rock that are differentiated by the minerals that characterize them. The alteration divisions are: Potassium Silicate Facies - muscovite, sericite, biotite, potassium feldspar, and some nondiagnostic minerals; Argillic Facies - muscovite(sericite), clay minerals; Propylitic Facies - muscovite(sericite), epidote, chlorite, and carbonate minerals (Jerome, Creasey - Titley and Hicks, 1966). The potassium silicate facies and the argillized facies are usually found associated with the zone of primary copper sulfide mineralization. The propylitically altered material is found bordering the contact between the central zone and the alteration zone(Figure S-6).

The copper mineralization may be differentiated into four types: hydrothermal primary sulfide mineralization - pyrite,

molybdenite, chalcopyrite, bornite, enargite, sphalerite, galena and other sulfides; zinc-lead deposits; copper sulfide replacement zones(found in silicified carbonates surrounding intrusion); and secondary copper mineralization deposits. The secondary copper mineralization is more relevant to this study because this is the type of deposit that would have the greatest probability of being detected through remote sensing with the vidicon system. Secondary mineralization is developed by acid leaching of surficial material's copper sulfide minerals followed by redeposition of these sulfides below the water table. These deposits will not be detected by an airborne vidicon survey because they are overlain by hundreds of feet of leached caprock. This oxidized material displays colors of buff-tan, brown, green, blue, and maroon because of oxidized iron(limonite) primarily. However, coloration may be due to abundances of oxidized copper mineralization: cuprite, malachite, azurite and chrysocolla. If carbonates and silicates are not the host rock material, oxidized minerals of copper and iron may not be found(iron oxides are always present in some quantity). Surface rocks of a porphyry copper deposit will have copper mineralization in very low, practically undetectable, concentrations(Schwartz - Titley and Hicks, 1966). Therefore, the ability of the vidicon system to dectect copper in the surface rocks of a porphyry copper deposit will be nil.

For detail beyond this superficial account of porphyry copper deposits, Titley and Hicks(1966) provide an excellent and comprehensive source book of information on these deposits and

the nature of the mining districts of the south-west. All material in the preceding synthesis were derived from its text.

The rock samples that were photographed by the vidicon system in this experiment were from three porphyry copper mining districts: Christmas, Silver Bell, and Tucson Mountain. Each district had eight rock samples associated with it; consisting of four rock suite pairs per district. Each pair member had a lithology that was fresh and relatively unaltered. The remaining four pair complements were of the same lithologies but were altered propylitically. Without going into repetitious detail, the rock samples are listed and described in ample detail in Figures T-9, T-10, T-11. The mining district's inferred geologic history, sample location((based on the Bureau of Land Management's cadastral system(Compton, 1962)), and approximation to the present day cross-section of the mining district are illustrated in Figures S-10, S-11, and S-12. Prior to the actual experiment, representative rock samples(approximately one inch in diameter) were subjected to absolute reflectivity measurements made with a ratio--recording spectroreflectometer(procedure described by Adams and Filice, 1967). These absolute reflectivity spectra are figured in numeric sample order for each mining district in Appendix I.

The next step in preparation for the vidicon experiment with the porphyry copper samples was to examine the absolute reflectivity spectra by sample pairs(altered versus unaltered). Absorption band positions and peak reflectivity(relative to MgO) were noted. Using the library of reflectivity spectra of common

minerals(Hunt and Salisbury,1970-1971) and employing crystal field theory(Burns,1970), the absorption bands of the sample spectra were explained with a few exceptions(this spectra comparison required identification of the minerals in each sample so that the appropriate library spectra could be selected for comparison). The library spectra and the absolute reflectivity spectra of the sample were compared over the 400.0 Nm to 2500.0 Nm range. However, due to the spectral range of detection of the vidicon tube, emphasis was made on comparisons from 400.0 Nm to 1100.0 Nm. By applying table T-15 to the reflectivity spectra of Appendix I, the transition elements and ligands responsible for the absorption bands of the porphyry copper deposit sample spectra may be determined. All absorption bands at wavelengths greater than 1300.0 Nm were explained as vibrational features of water, hydroxyls, or carbonate ligands. Absorption bands below 1300.0 Nm were usually attributed to electronic transitions due to either Fe^{2+} or Fe^{3+} ions. Despite the help of available references, two absorption bands' genesis could not be determined. These bands at 470.0 Nm and 660.0 Nm may be associated to epidote, $Ca_2(Al,Fe)_3(SiO_4)_3(OH)$; a propylitic-alteration mineral. Referencing Hunt and Salisbury(1971) spectra, it was discovered that the known electronic absorption bands due to Cu^{2+} are few in number, two of the known Cu^{2+} bands overlap Fe^{3+} bands(Table T-15), and confidence in the remaining bands is weak because of the weak nature of the bands. Therefore, the absolute reflectivity spectra of the rock samples could not be interpreted in terms obvious spectral features that corresponded to copper content.

Because of the difficulties in determining the presence of copper in the porphyry copper rock samples from their reflectivity spectra, this experiment was designed to test the vidicon system's ability to differentiate the altered from the unaltered rock samples. This was to be accomplished by: using the spectral differential that arises when absorption bands are not shared by elements of the rock sample pair; comparing the average albedo considered over the entire spectral range of 400.0 Nm to 1100.0 Nm.

The laboratory setup for this experiment is illustrated in Figure S-3. Laboratory procedures were similar to the procedures used in the experimentation with the large rock samples (page 34). The distinction between this experiment and previous experiments was the procedures observed in the experiment practically insured that the pictures were taken below the saturation level of the detector. The freshly coated MgO standard was omitted because this experiment was concerned with differentiation of lithologies and not with aspects of vidicon spectroscopy. In order to ratio intensities of vidicon pictures taken under field conditions, a large MgO standard in the field would be impractical. A chopping technique,similar to that employed in astronomical photometry, could be used in vidicon surveys. Another possibility might be to reference all target reflectivities to the brightest object of the target(whose reflective response over the wavelengths considered is known). Fortunately, in a field survey with the vidicon system, only relative reflectivity is a concern-as opposed to absolute reflectivity.

Figure: S-6

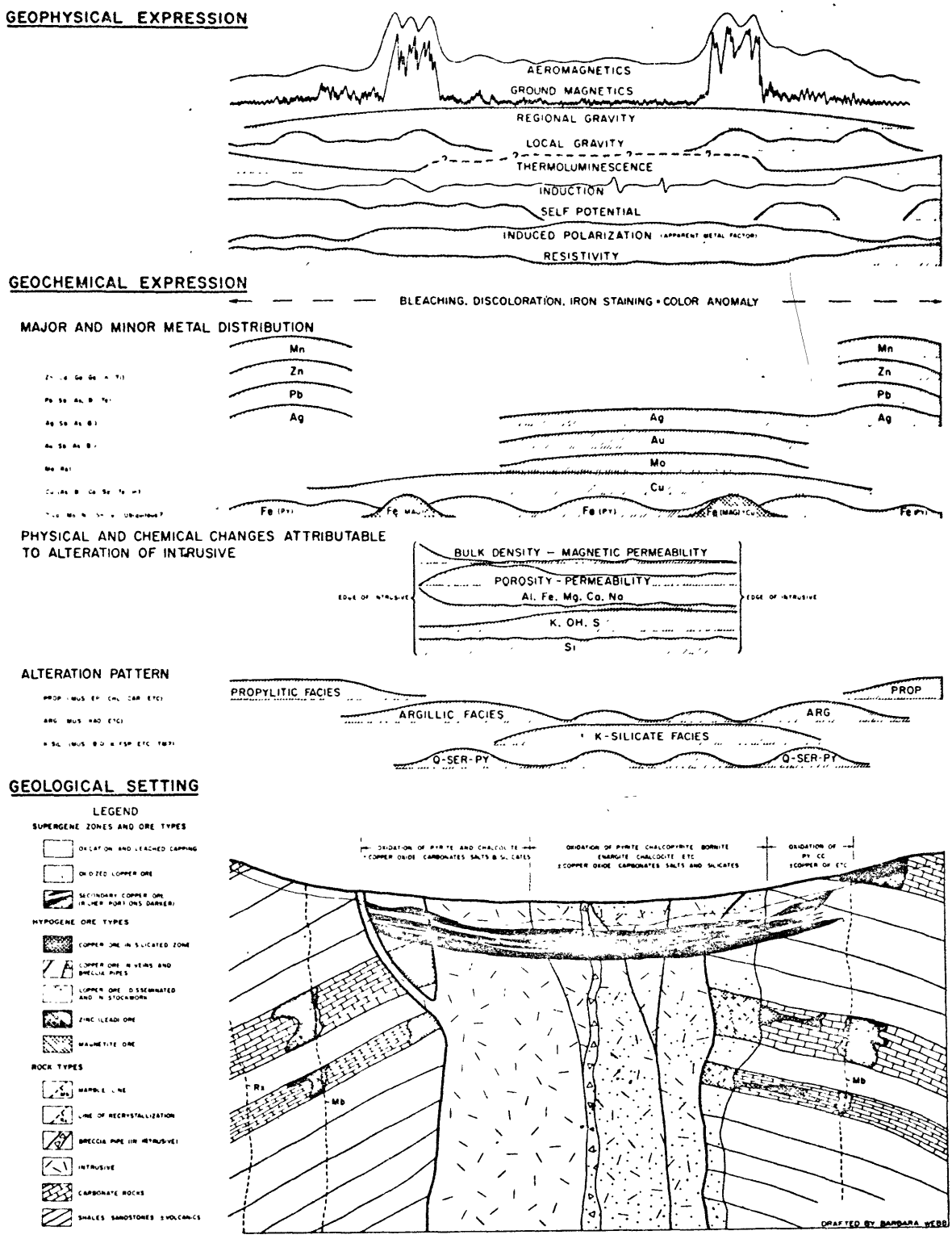

Figure: S-6:: Geophysical, Geochemical, Geological Expression of a model Porphyry Copper Deposit

(Figure taken from: Jerome, Titley and Hicks, 1966)

SILVER BELL DISTRICT

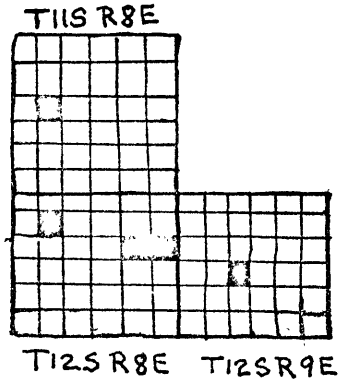

Samples: 15A) Unaltered Dacite
15B) Propylitic Altered Dacite
16A) Unaltered Latite
16B) Propylitic Altered Latite
17A) Unaltered Latite Porphyry
17B) Propylitic Altered Latite
18A) Unaltered Dacite
18B) Altered Dacite

Comments: Host Rocks-Alaskite,Dacite,Quartz-Monzonite Porphyry
Alteration types- Potassic, Argillic, Propylitic,Qtz.-Sericite
Critical Assemblages-Muscovite Muscovite Chlorite Quartz
K-Feldspar Kaolinite Calcite Sericite
Montmorillinite

Propylitic Alteration Silicates: Chlorite, Calcite,Sericite,
Hydromica,Montmorillinite

Primary Sulfides: Pyrite,Chalcopyrite,Bornite,Tetrahedrite,
Molybdenite.

(Information from: Creasy, Titley and Hicks,1966)

Sketch implies possible genesis: Limestone was intruded by latite and alaskite/ the latter was intruded by dacite/ the complex then intruded by monzonite/ hydrothermal mineralization and alteration followed.

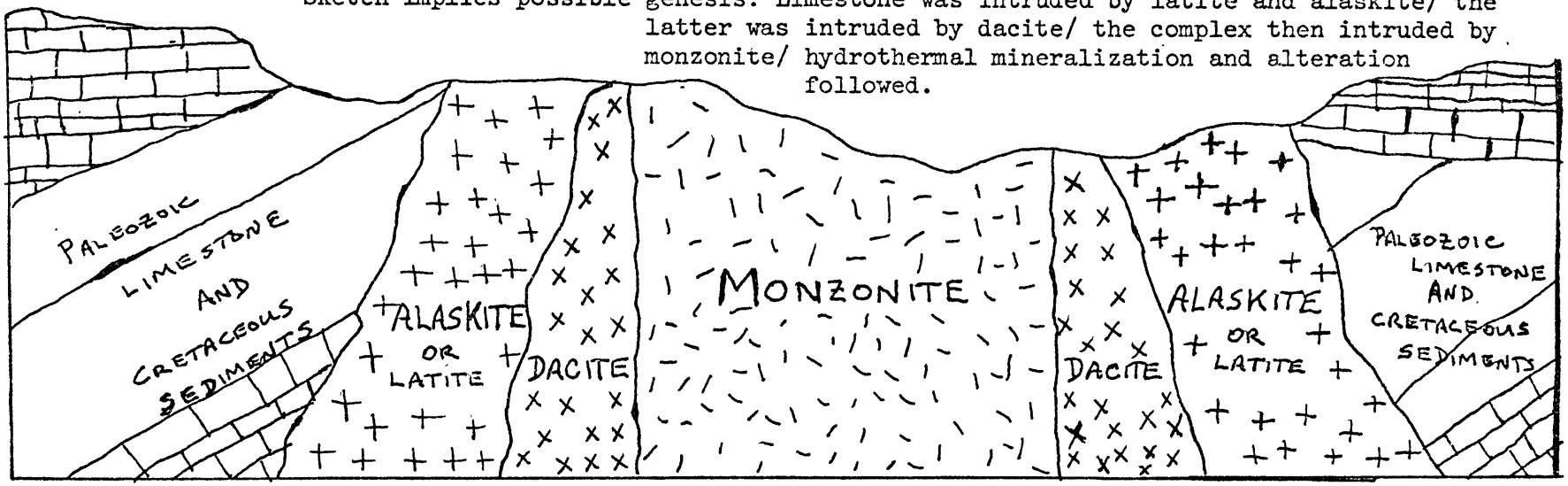

Figure: S-10

Figure: T-9:: SILVER BELL DISTRICT

Sample Listing and Description

Sample Number	LOCATION	Description
15A	SEC08,T12S,R8E Pima Cnty,Ariz.	Relatively Unaltered Dacite(?) Porphyry...Light to Medium Grey Matrix with tan splotches(initial stages of alteration).... Mineralogy:Epidote, weathered Biotite,Limonite,Plagioclase feldspar in excess of quartz
15B	SEC14,T12S,R8E Pima Cnty,Ariz.	Propylitic Altered Dacite(?) Porphyry...Tan-brown matrix with white feldspar phenocrysts (small), feldspar phenocrysts weathered out-leaving cavities-weathered Biotite,Epidote.... Feldspars altered to orange clay
16A	SEC21,T12S,R9E Pima Cnty,Ariz.	Relatively Unaltered Latite(?) ...fresh surface is a dark grey matrix with grey phenocrysts of Plagioclase feldspar...weathered surface is light orange(limonite) and feldspar phenocrysts are bleached white...some crystals of Augite and Hornblende have weathered out of the rock... phenocrysts stained by Epidote
16B	SEC21,T12S,R9E Pima Cnty,Ariz.	Propylitic Altered Latite(?).. Weathers to a pinkish brown... Contains Orthoclase and Plagioclase feldspar,Quartz, Hornblende, Epidote, and Biotite.. Pink feldspar on fresh surface but doesn't have good cleavage
17A	SEC17,T11S,R8E Pima Cnty,Ariz.	Relatively Unaltered Latite Porphyry...Sanidine and Na or K(?)Orthoclase feldspar phenocrysts in a green-grey matrix. ...weathers to light grey-brown and reddish brown material... Hornblende and Augite have we weathered from surface..samples have dark brown(burnt?)zones with perimeters characterized by the orange-brown(Fe3+)zone.

Figure: T-9:SILVER BELL DISTRICT
Sample Listing and Description

Sample Number	Location	Description
17B	SEC21,T12S,R9E Pima Cnty,Ariz.	Propylitic Altered Latite Porphyry...Fresh surface has become powdery(sericite) and the feldspar phenocrysts have become less distinct....pink clay penetrates rock sample...Epidote is replacing the iron-bearing pyroxenes...Brown weathered crust is contaminated by rouge clay(Fe3+)
18A	SEC13,T12S,R8E Pima Cnty,Ariz.	Relatively Unaltered Dacite... Phenocrysts of plagioclase in excess of quartz...Epidote,Orthoclase feldspar,quartz in dark grey plagic(?)matrix...Epidote in considerable quantities... Weathered matrix is a lighter grey than the fresh surface... Hornblende weathers to maroon clay and Biotite...Feldspar are weathered to a tan-white.
18B	SEC13,T12S,R8E Pima Cnty,Ariz.	Propylitic Altered Dacite... No obvious Epidote...Biotite is weathering golden brown... Feldspars bleached to a grey-white...pyroxenes occur as inclusions in the Orthoclase feldspar phenocrysts

TUCSON MOUNTAIN DISTRICT

PIMA COUNTY, ARIZONA

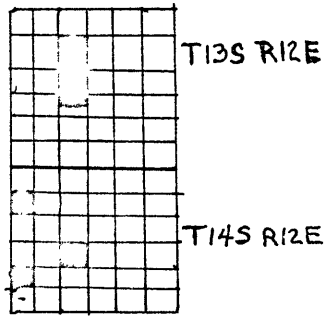

Samples: 5A)Propylitic Altered Tv Rhyolite Breccia
5B)Unaltered Tv Rhyolite Breccia and Tuff
6A)Unaltered Cretaceous Siltstone
6B)Propylitic Altered Limy Siltstone(Cretaceous)
7A)Unaltered Cretaceous Arkose
7B)Propylitic Altered Cretaceous Arkose
9A)Unaltered Cretaceous Andesite
9B)Propylitic Altered Cretaceous Andesite

Comments: No published information could be found

Sketch implies a possible genesis(unfounded): Arkose and Siltstone are deposited and intruded by Andesite/ Andesite is intruded by rhyolitic breccia pipes/ hydrothermal alteration and mineralization takes place(theory proposed on basis of known characteristics of Porphyry Copper Deposits)

Figure: S-11

Figure: T-10: TUCSON MOUNTAIN DISTRICT
Sample Listing and Description

Sample Number	Location	Description
5A	SEC30,T14S,R12E Pima Cnty,Ariz.	Propylitic Alteredd Tertiary Rhyolite Volcanic Breccia... Considerable Rouge Material-believed to be cuprite with associated limonite..Minor obvious amounts of quartz, hornblende, and jarosite(?).. Some zones appear black as if burnt...considerable light-tan clay dusting the surface... white feldspar phenocrysts approximately 0.5cm in size.
5B	SEC30,T14S,R12E Pima Cnty,Ariz.	Unaltered Tertiary Rhyolite Volcanic Breccia and Tuff... Primarily rouge-mineralized weathered surface...distinct from (5A)..cuprite and/or limonite responsible...tiny flakes of what appeared to be native copper-after close examination, these may be weathered biotite
6A	SEC7,T14S,R12E Pima Cnty,Ariz.	Fresh,Relatively Unaltered Cretaceous Siltstone...carbonized...black alternating with light grey banding... weathers to a muddy,milky grey mineralization...limestone is responsible for $CaCO_3$ icing. ...tiny mica flakes visible
6B	SEC21,T14S,R12E Pima Cnty,Ariz.	Propylitic Altered Limy Siltstone(Cretaceous)...rock is silicified(chertlike)...weathers brown,yellow, orange... possible traces of pyrite... alteration coloration penetrates the rock...epidote is observed along with stain attributed to Fe^{3+}minerals... quite distinct from 6A.

Figure: T-10: TUCSON MOUNTAIN DISTRICT
Sample Listing and Description

Sample Number	Location	Description
7A	SEC7,T14S,R12E Pima Cnty,Ariz.	Unaltered Arkose(Cretaceous) Fresh exposure shows striated Calcium-Plagioclase and white orthoclase feldspar in a grey matrix...pink feldspar and clay predominate on weathered surface...dusted by a rouge material(Cuprite(?))..some pyroxenes
7B	SEC21,T14S,R12E Pima Cnty,Ariz.	Propylitic Altered Arkose... Weathered surface shows milky quartz particles distinct along with the white feldspar crystals ...Light-brown limonite stain with occasional patches of zones of weathered pyroxenes..rouge staining is absent..some samples have a limonite stained, baked shell with pink feldspars-some regions burnt black...Limonite staining is spotty on fresh piece.
9A	SEC9,T13S,R12E Pima Cnty,Ariz.	Unaltered Cretaceous Andesite. Na-Ca Plagioclase lava..by definition...Sanidine crystals in matrix...dark brown,weathered inclusions surrounded by feldspar crystals...fine textured matrix weathers to medium grey ...splotches of white material (clay(?)) on surface..Fe^{3+} stain on feldspar crystals..Epidote formed from amphiboles present Some feldspar crystals are green (microcline)(?)
9B	SEC16,T13S,R12E Pima Cnty,Ariz.	Propylitic Altered Cretaceous Andesite...Bleached effects.. Considerable epidote...glass chards and some pyroxenes are visible in weathered zones... high clay content and apparent staining due to limonite and possibly cuprite.

CHRISTMAS DISTRICT

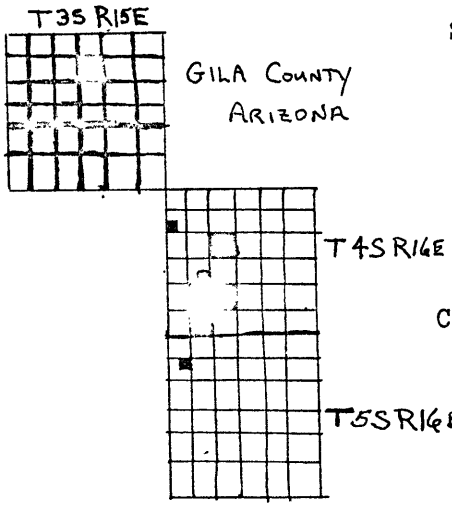

Samples:
10A) Unaltered Upper Paleozoic Limestone
10B) Propylitic Altered Paleozoic Limestone
11A) Unaltered Quartz-Monzonite Porphyry
11B) Propylitic Altered Quartz Monzonite Porphyry
12A) Unaltered Diorite(?) Porphyry
12B) Propylitic Altered Diorite(?) Porphyry
13A) Unaltered Cretaceous Andesite
13B) Propylitic Altered Cretaceous Andesite

Comments: Mineralized zone - composition of quartz monzonite
Texture - porphyry only
Host Wall Rock Structure - Passive

(Information obtained from: Stringham,Titley and Hicks,1966)

Sketch implies a possible genesis(founded): Paleozoic Limestone intruded by diorite/ diorite intruded by andesite/ complex intruded by quartz - monzonite porphyry(theory proposed on basis of known characteristics of Porphyry Copper Deposits)

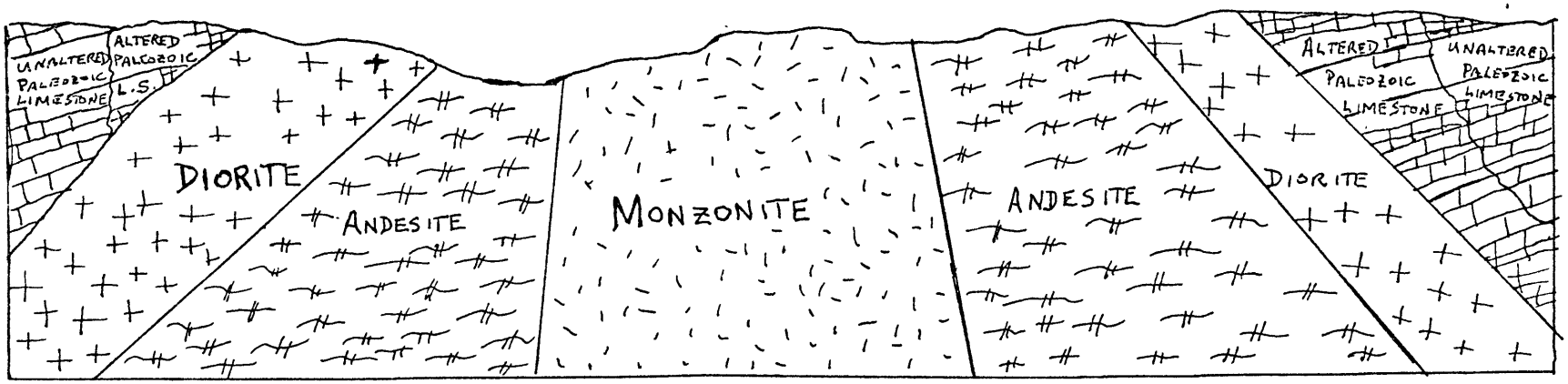

Figure: S-12

Figure: T-11: CHRISTMAS DISTRICT
Sample Listing and Description

Sample Number	Location	Description
11A	SEC16,T4S,R16E Gila Cnty,Ariz.	Relatively Unaltered Quartz-Monzonite Porphyry...by definition,approximately equal amounts of alkaline and calcium feldspars...Biotite altering to Chlorite-no significant quantities..Hornblende and Augite present along with Muscovite..weathered surface contains abundance of rouge clay(stained by limonite)
11B	SE1/4,SEC20, T4S,R16E Gila Cnty,Ariz.	Propylitic Altered Quartz-Monzonite Porphyry...same description as for 11A with the following exceptions: epidote is developed in the rock from the iron bearing amphiboles,etc...hand specimen shows the plagioclase to be Albite..feldspars alter to a light tan clay.
10A	Dripping Spring Mountains SEC10,T3S,R15E Gila Cnty,Ariz.	Relatively Unaltered Upper-Paleozoic Limestone...Light grey,medium-crystalline lime stone with dull red hematite and/or cuprite(?)coating on weathered surface..feldspar particles..Limonite stain on other samples-light brown... small muscovite particles
10B	Winkelman Area SW1/4,Sec7 T4S,R16E Gila Cnty,Ariz.	Propylitic Altered Upper-Paleozoic Limestone...altered to a chalky-white powder exterior...veryfine muscovite(sericite)...has become more coarsely crystalline... light, pinkish cast observed due to either hematite or cuprite...presence of a green mineral in slight concentration observed(malachite or chlorite)

Figure: T-11: CHRISTMAS DISTRICT
Sample Listing and Description

Sample Number	Location	Description
12A	SEC32,T4S,R16E Gila Cnty,Ariz.	Relatively Unaltered Diorite(?) Porphyry...by definition, contains less than 10% quartz and consists primarily Na-Plagioclase feldspar...the latter mineral makes up the grey matrix...20% of rock consists of hornblende and biotite...weathers grey(light) to tan-presumably due to to Fe3+..appears to have a baked crust
12B	SEC29,T4S,R16E Gila Cnty,Ariz.	Propylitic Altered Diorite(?) Porphyry...considerable amounts of Epidote..evidence of clay from alteration processes but not to any great extent... white feldspars in light green matrix-pyroxenes are less numerous(fresh surface).
13A	NE1/4,SEC7, T5S,R16E Gila Cnty,Ariz.	Relatively Unaltered Cretaceous Andesite...by definition, it is a lava consisting of primarily Na to sub-calcic plagioclase feldspar...weathering to a light tan color enhances phenocrysts of feldspar and pyroxenes...some epidote... limonite and possible cuprite staining...fresh surface is dark grey matrix(feldspar).
13B	SEC28,T4S,R16E Gila Cnty,Ariz.	Propylitic Altered Cretaceous Andesite...greater concentrations of epidote, chlorite, and limonite stain. Vugular glass pods found... no other obvious differences from 13A;however,sample is distinct due to alteration.

DISCUSSION

The tables and processed vidicon pictures are divided into three parts according to mining district: Table T-12 and Figures P-17 to P-23 correspond to the rock samples of the Silver Bell District; Table T-13 and Figures P-24 to P-30 correspond to the rock samples of the Tucson Mountain District; and Table T-14 and Figures P-31 to P-37 correspond to the rock samples of the Christmas District. To identify the rock samples in the pictures of the mining district suite, reference sketches, Figures S-7,8, and 9, should be referred to.

Seven vidicon pictures were made of each rock suite. The filters selected were the minimum number that seemed adequate to differentiate an altered rock from its unaltered complement. The tables of intensity averages were derived from the print-out of the vidicon pictures. If the reader refers to any picture of a rock suite and observes that two samples of a common lithology have different albedos, then the tables(T-12,13,14) give the average numeric intensity of the samples(based on a 0 to 255 scale). By performing ratios of the average intensities, a ratio representing the reflectivity of one sample relative to the other is determined. This information would be useful in mapping a porphyry copper deposit using vidicon pictures. If one of the samples had a reflectivity that was known over a spectral range, then by ratioing other samples' intensities to the average intensity of the standard sample unit, determination of the unknown samples' lithologies could be possible(by spectra interpretation). This procedure is feasible because rocks have characteristic re-

flectivity spectra from which they may be identified(supported by Adams and Filice, 1967).

There is one comment to be made for vidicon picture interpretation; it can be misleading. For the first example, refer to the absolute spectra in Appendix I for the Silver Bell samples 17A and 17B. The two spectra are totally distinct and possess different reflectivities at all wavelengths under consideration - except one wavelength at 600.0 Nm. At 600.0 Nm the two curves intersect (if overlayed). The intersection marks a wavelength of equal reflectivity at which the altered and unaltered lithology could not be differentiated. This phenomena is illustrated in Figure P-19. Now suppose two rock samples of different lithology are compared; ie: 7B and 9B of the Tucson Mountain District(Appendix I). Despite the fact that sample 9B has a broad band absorption from 800.0 Nm to 1100.0 Nm(due to Fe^{3+} and Fe^{2+} absorptions(table T-15)) and sample 7B has no absorptions in that spectral region, the two samples could not be differentiated. This failure to differentiate is due to the samples having similar albedo on an absolute scale(ratio of sample intensity to standard MgO intensity plotted versus wavelength). This problem is illustrated in Figure P-21; a vidicon picture at 850.0 Nm(wavelength at which the absolute spectra predict minimum differences in albedo).

There are several cases where the absolute spectra predict differentiation of a sample pair at all wavelengths; ie. Tucson Mountain District: samples 6A and 6B(verified by referring to Figures P-24 to P-30). Such information would be invalu-

able if porphyry copper deposits consisted only of rock types 6A and 6B; however in actual survey operation, consideration would have to be given to the spectral nature of all rock units that might be found in the region to be mapped by the vidicon system. Such an operation would necessitate having a ground truth program. This program would take regional rock samples (like those used in this experiment) and would perform absolute reflectivity measurements of them. The resultant spectra would be used in picture interpretation, mapping, and filter selection.

It might be concluded then that the vidicon system illustrates significant promise in differentiating distinct rock units and rocks of the same lithology that have been altered as opposed to those which were left unchanged. It is concluded that the vidicon system would be useful in the mapping and detection of a porphyry copper deposit(with the help of some ground truth). These conclusions naturally lead to an experiment in which the vidicon system is taken into the field(after ground truth measurements have been made) and used to map a geologic outcrop on the basis of mineralogy, structure and genesis. This experiment is discussed in the following section.

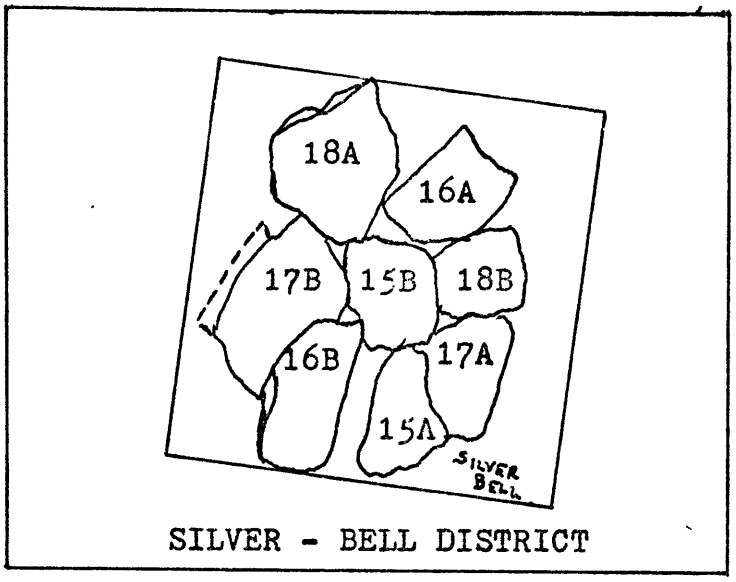

TOP OF PICTURES (SIDE)

Figure: S-7

Silver Bell District Target Reference Sketch

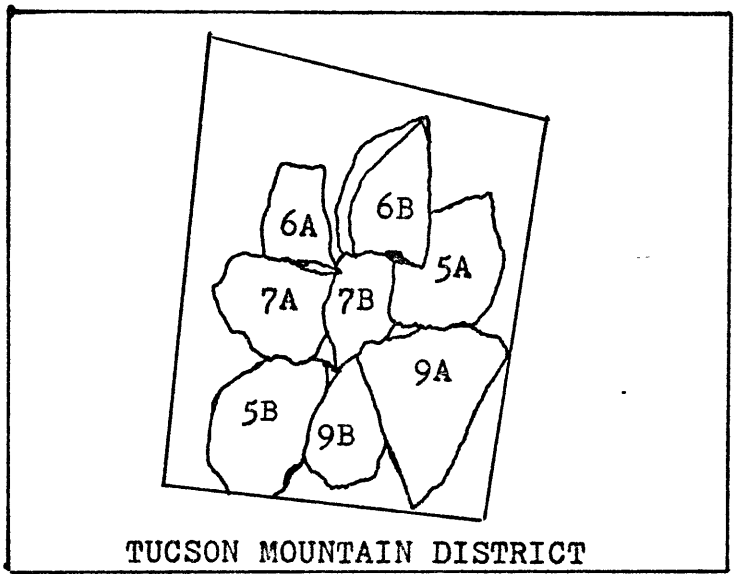

TOP OF PICTURES (SIDE)

Figure: S-8

Tucson Mountain District Target Reference Sketch

Figure
T-12:: Silver Bell: Petrologic Differentiation Data*

Sample=	Wavelength	Average	Sample	Wavelength	Average
15A	470.0Nm	7.48	15A	850.0Nm	42.96
15B	"	13.24	15B	"	141.12
16A	"	11.76	16A	"	136.28
16B	"	4.80	16B	"	28.92
17A	"	3.92	17A	"	43.88
17B	"	3.32	17B	"	76.16
18A	"	6.92	18A	"	104.08
18B	"	6.12	18B	"	54.52
15A	500.0Nm	14.84	15A	900.0Nm	82.76
15B	"	40.04	15B	"	122.88
16A	"	27.50	16A	"	117.96
16B	"	8.08	16B	"	38.0
17A	"	4.52	17A	"	74.16
17B	"	5.16	17B	"	36.48
18A	"	15.0	18A	"	67.68
18B	"	13.68	18B	"	46.76
15A	600.0Nm	76.12	15A	1100.0Nm	91.60
15B	"	134.0	15B	"	105.76
16A	"	99.56	16A	"	102.16
16B	"	35.40	16B	"	44.56
17A	"	32.88	17A	"	83.88
17B	"	34.84	17B	"	50.00
18A	"	55.96	18A	"	64.28
18B	"	42.36	18B	"	69.96
15A	700.0Nm	29.08			
15B	"	73.84			
16A	"	52.12			
16B	"	12.76			
17A	"	16.68			
17B	"	13.32			
18A	"	19.44			
18B	"	15.83			

* The data averages are the mean value of 25 intensity values (on a(0 to 255)scale) corresponding to 25 points of target imagery which appeared representative of the particular rock sample.

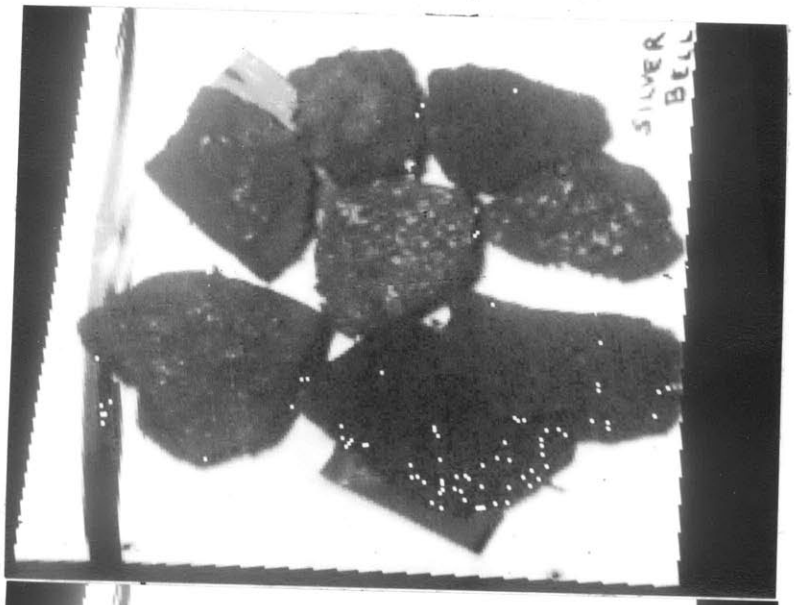

Figure: P-17

Silver Bell
District

470.0 Nm

Figure: P-18

Silver Bell
District

500.0 Nm

Figure: P-19

Silver Bell
District

600.0 Nm

Figure: P-20

Silver Bell
District

700.0 Nm

Figure: P-21

Silver Bell
District

850.0 Nm

Figure: P-22

Silver Bell
District

900.0 Nm

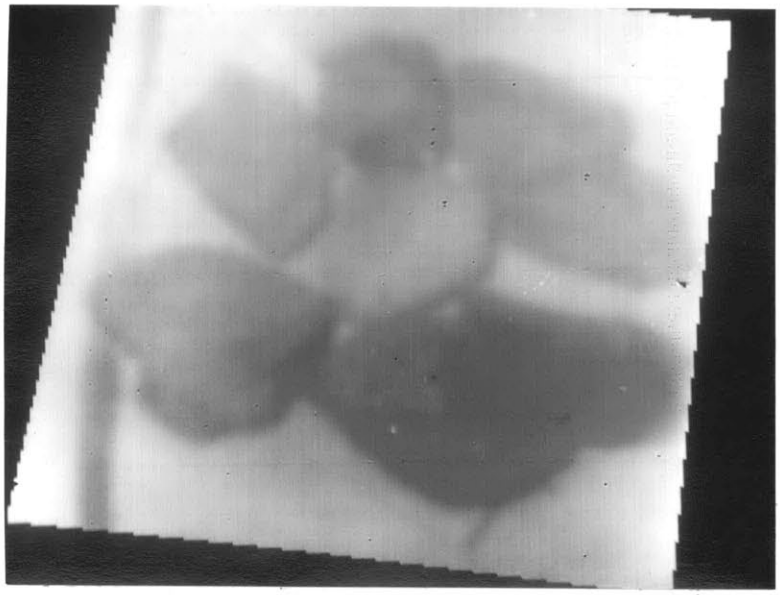

Figure: P-23

Silver Bell
District

1100.0 Nm

Figure T-13:: Tucson Mountain: Petrologic Differentiation Data*

Sample	Wavelength	Average	Sample	Wavelength	Average
5A	470.0Nm	12.52	5A	746.5Nm	118.56
5B	"	6.36	5B	"	62.68
6A	"	12.00	6A	"	62.56
6B	"	81.80	6B	"	201.04
7A	"	17.64	7A	"	89.28
7B	"	5.36	7B	"	55.36
9A	"	7.80	9A	"	64.0
9B	"	8.76	9B	"	69.04
5A	600.0Nm	32.60	5A	850.0Nm	75.24
5B	"	6.80	5B	"	13.8
6A	"	10.72	6A	"	50.36
6B	"	117.64	6B	"	254.12
7A	"	17.0	7A	"	39.84
7B	"	4.52	7B	"	21.84
9A	"	6.96	9A	"	15.96
9B	"	10.44	9B	"	12.76
5A	660.0Nm	33.20	5A	900.0Nm	62.20
5B	"	6.80	5B	"	25.20
6A	"	8.08	6A	"	18.0
6B	"	120.30	6B	"	124.36
7A	"	18.2	7A	"	33.0
7B	"	4.00	7B	"	17.40
9A	"	5.32	9A	"	26.76
9B	"	9.76	9B	"	29.68
5A	700.0Nm	74.68			
5B	"	28.24			
6A	"	26.88			
6B	"	163.32			
7A	"	49.88			
7B	"	14.68			
9A	"	23.68			
9B	"	36.36			

* The data averages are the mean value of 25 intensity values (on a(0 to 255)scale) corresponding to 25 points of target imagery which appeared representative of the particular rock sample.

Figure: P-24

Tucson Mountain District

470.0 Nm

Figure: P-25

Tucson Mountain District

600.0 Nm

Figure: P-26

Tucson Mountain District

660.0 Nm

Figure: P-27

Tucson Mountain District

700.0 Nm

Figure: P-28

Tucson Mountain District

746.5 Nm

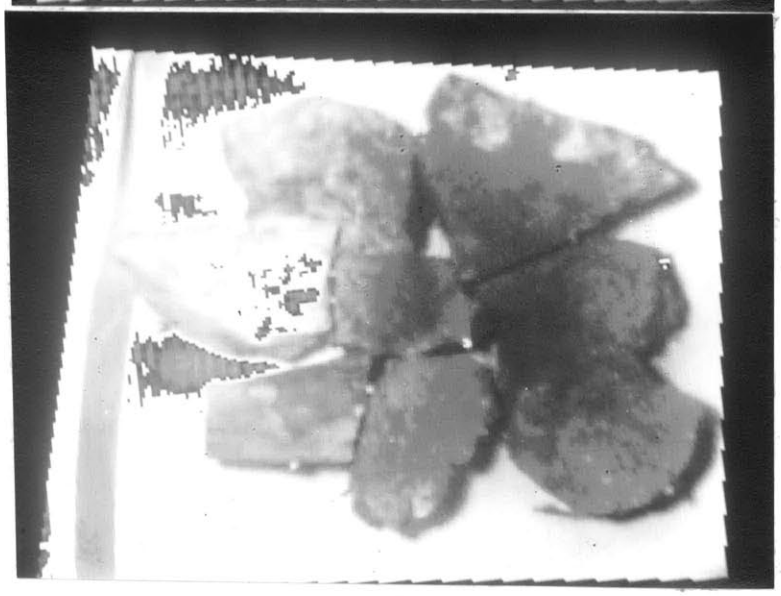

Figure: P-29

Tucson Mountain District

850.0 Nm

Figure: P-30

Tucson Mountain District

900.0Nm

Figure: T-14::

Christmas District: Petrologic Differentiation Data*

Sample	Wavelength	Average	Sample	Wavelength	Average
10A	470.0Nm	1.72	10A	800.0Nm	39.96
10B	"	5.52	10B	"	68.16
11A	"	3.64	11A	"	43.76
11B	"	6.84	11B	"	71.44
12A	"	3.84	12A	"	60.16
12B	"	1.92	12B	"	30.24
13A	"	1.96	13A	"	26.16
13B	"	3.68	13B	"	48.12
10A	560.0Nm	3.80	10A	850.0Nm	41.92
10B	"	44.64	10B	"	36.80
11A	"	11.88	11A	"	52.48
11B	"	49.52	11B	"	119.16
12A	"	16.96	12A	"	43.32
12B	"	7.80	12B	"	25.32
13A	"	7.92	13A	"	39.76
13B	"	18.40	13B	"	98.24
10A	660.0Nm	23.76	10A	1000.0Nm	32.72
10B	"	86.92	10B	"	53.48
11A	"	30.40	11A	"	38.36
11B	"	73.16	11B	"	55.0
12A	"	60.28	12A	"	39.8
12B	"	20.72	12B	"	18.6
13A	"	19.80	13A	"	18.48
13B	"	42.44	13B	"	35.80
10A	746.50Nm	36.32			
10B	"	82.04			
11A	"	30.92			
11B	"	66.16			
12A	"	59.12			
12B	"	21.40			
13A	"	19.04			
13B	"	39.36			

* The data averages are the mean value of 25 intensity values (on a (0 to 255) scale) corresponding to 25 points of target imagery which appeared representative of the particular rock sample.

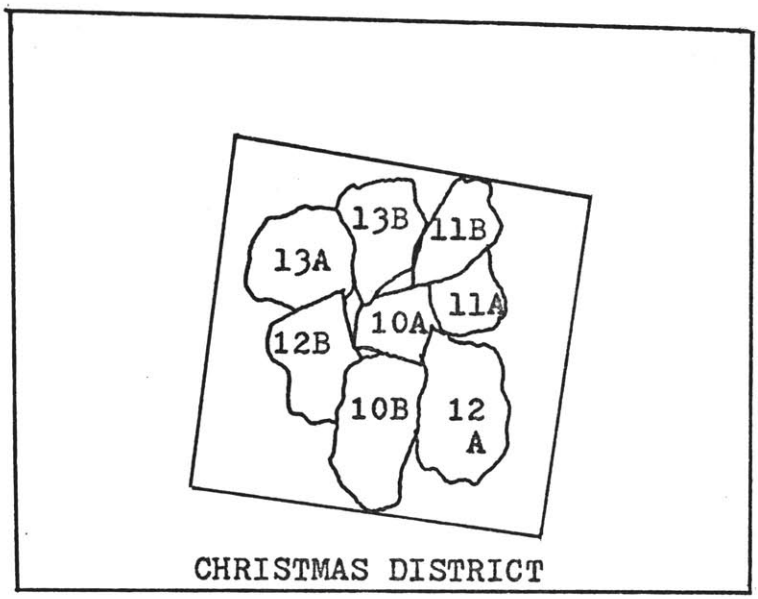

TOP OF PICTURES (SIDE)

Figure: S-9

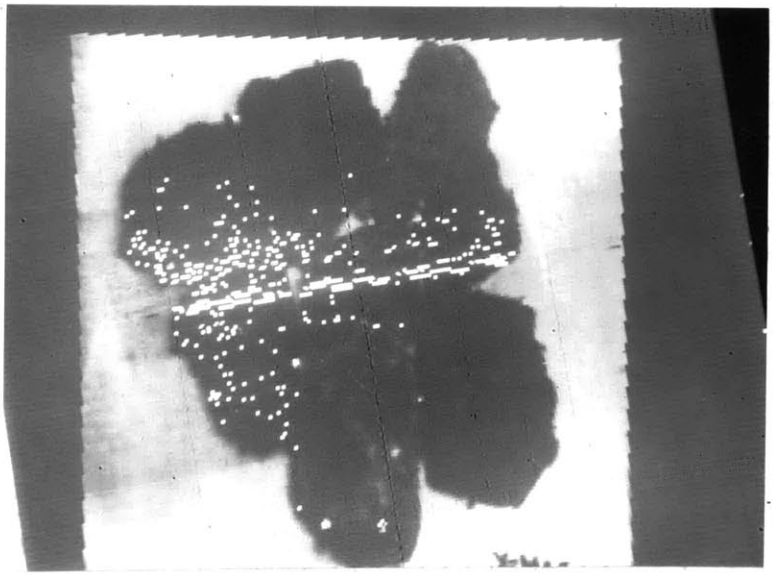

Figure: P-31

Christmas District, 470.0 Nm

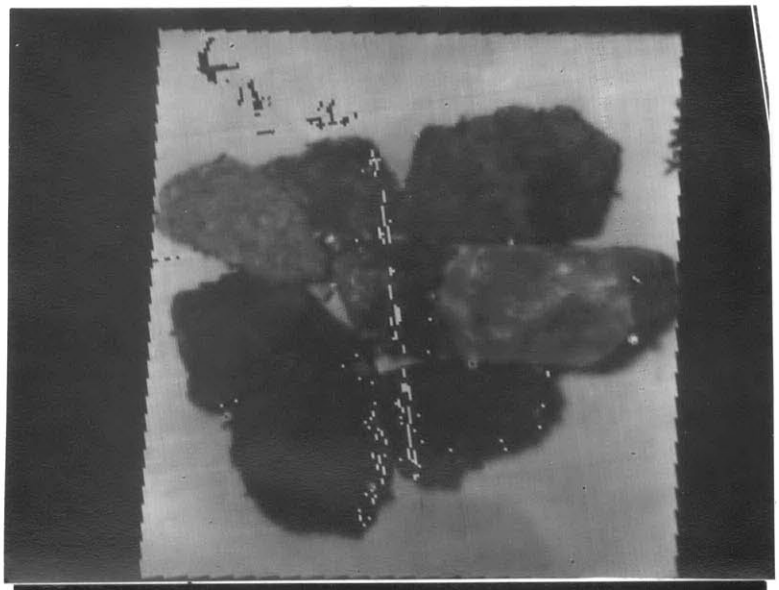

Figure: P-32

Christmas District

560.0 Nm

Figure: P-33

Christmas District

660.0 Nm

Figure: P-34

Christmas District

746.5 Nm

Figure: P-35

Christmas District

800.0 Nm

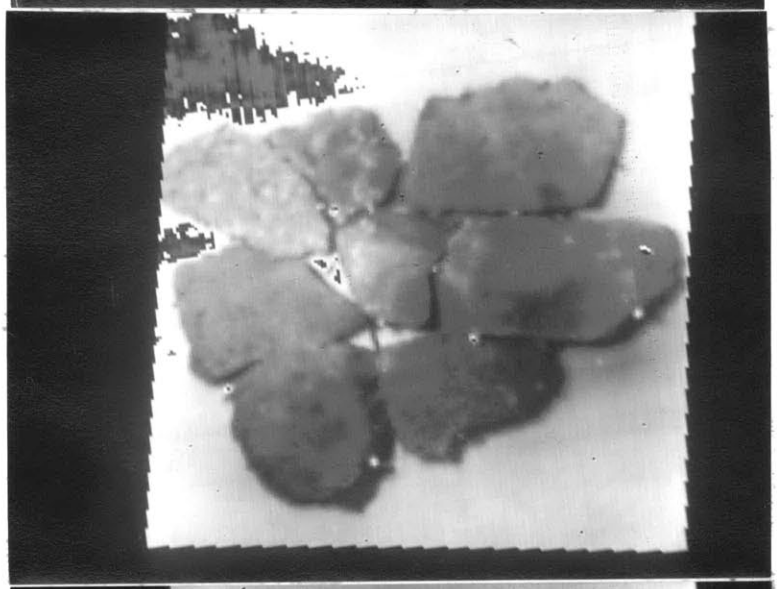

Figure: P-36

Christmas District

850.0 Nm

Figure: P-37

Christmas District

1000.0 Nm

THE VIDICON SYSTEM IN THE FIELD

Background

As a consequence of the vidicon system's proven capabilities to identify and differentiate both mineralogy and structure of rocks under laboratory conditions, an experiment was conducted to test the system in nonlaboratory environments. Nonlaboratory conditions is synonymous with field work to the geologist or geophysicist. To accomplish this study, considerable field work was performed in eastern New York, western Vermont, and south-eastern Massachusetts. The outcrops were selected on the basis of composition , structure, accessibility,and compatibility with the optical system of the vidicon equipment.

Figures S-13 and S-14 illustrate the location and setting of the formational contact that was selected as the site for this last experiment. The site marks the contact between the Paleozoic Blue Hills Granite and the late Paleozoic Pondville Conglomerate. The outcrop is located approximately three miles north of Randolph, Massachusetts on Route 28 North at the intersection of Route 28 and Route 128(north-west quadrant of intersection).

This rock exposure actually consists of two contacts : the contact between the Blue Hills Granite and a welded transition zone(metamorphosed Pondville Conglomerate); and the latter welded transition zone makes contact with the Pondville Conglomerate formation(Figure S-14). Besides being compatible with the conditions of the experiment, this outcrop is well known for its geological uniqueness. The uniqueness is founded upon the mystery which shrouds the genesis of the contact units and the absolute ages of the rock units. For a thorough discussion of this outcrop and

the local geology, a thesis(in print) by Sayer is recommended for enhancing the reader's understanding of the regional setting of this experiment(Sayer,1973; Emerson,1917).

The Blue Hill Granite is a porphyritic-textured Carboniferous granite(Emerson,1917) containing large rectangular to roughly circular green clasts. The blue matrix of this granite contains 74% SiO_2 (30% of which is quartz), 48% sodic feldspar (perthitic anorthoclase), and 6-8% riebeckite, arfedsonite, and aegerite. The blue coloration of the granitic matrix is due to the amphibole riebeckite, $Na_2(Mg,Fe,Al)_5Si_8O_{22}(OH)$, in concentrations of up to 3% (Sayer, telephone communication). The green clasts are composed of feldspar(with altered sericite) and quartz.

The Pondville Conglomerate is thought to be a rhyolitic volcanic mud flow, a lahar(Sayer, telephone communication), deposited in contact with the Blue Hill Granite during the late Paleozoic or Triassic periods(the absolute ages are still being investigated at this time). The conglomerate consists of: approximately 4% black slate boulders; 90% rhyolitic boulders(5 to 100 cm. in diameter), containing quartz and feldspar in an aphanitic texture that bleaches white on exposed surfaces; and some granitic boulders that are the same composition as the Blue Hill Granite (Sayer, telephone communication; personal inspection). The matrix of the conglomerate consists of coarse feldspars and quartz that are stained maroon by hematite. The matrix contrasts significantly with the boulders which appear light green or white(due to chlorite or sericite(?)).

The welded zone that separates the Blue Hill Granite from the Pondville Conglomerate has the appearances of the Pondville Conglomerate. The key difference is that the Pondville Conglomerate is a loose chunky conglomerate; whereas the clasts of the welded zone appear baked into the matrix(lumpy texture is absent). The boulder clasts appear to have the same composition as the Blue Hill Granite. Hematite, formed from the oxidation of riebeckite from the granite, is the staining agent of the welded transition zone (Figure S-14). The riebeckite has its origin in the Blue Hill Granite clasts that were captured by the proposed Pondville volcanic mud flow. A possible dike network is being investigated to determine if it could be the source of heat responsible for the welded nature of the central transition zone of the outcrop(See Sayer, 1973).

The conglomerate weathers to give the appearance of a maroon matrix cementing a green clastic material. The granite has a weathered surface that is predominately limonite stained (limonite: $FeO(OH)\cdot nH_2O$). Pyrolusite(MnO_2) is more abundant near the contacts of the outcrop and is the source of the purple cast of the weathered material.

On the basis of the mineralogy of the rock units, interference filters were selected for a vidicon survey of the outcrop. These filters were selected after the available reflectivity spectra of the outcrop's minerals were studied(Hunt and Salisbury, 1970-1971)(filter selection was limited by an inadequate filter library). Since the outcrop displayed different degrees of limonite staining, variable texture, and distinct lithologies, it

was concluded that the greatest differentiation of units should occur in the 800.0 Nm to 1100.0 Nm spectral range. The latter wavelengths would enhance the outcrop's features because of the absorption of Fe^{2+} and Fe^{3+} in their respective reduced and oxidized states(present in the weathered rock material). A series of pictures,at wavelengths ranging from 400.0 Nm to 1100.0 Nm, was proposed for the experiment,so that the minerals like riebeckite and pyrolusite might be distinguished.

A discussion of the logistics and the equipment required to conduct a vidicon survey is now in order. The closest utility pole was a mile away. This required the vidicon equipment to be powered by a portable generator. For the first attempt of this experiment, a 115 volt-60cyle-2.5kilowatt generator was borrowed from the M.I.T. electrical shop. The electric noise of this first power source proved to be a problem with respect to the magnetic tape recorder and its ability to record data(despite the use of a low-band pass filter in the experiment). In the second attempt, the power source was a 3.75kilowatt generator. It proved to be satisfactory with the help of considerable electric signal filters. In order to transport the basic vidicon system, a table, chair, generator(200 to 400 lbs.), 200 feet of cable, transformers, one assistant, and other accessories, an "Econoline" type van was rented. The van proved to be quite adequate for performing as an observation post during the vidicon survey of the outcrop.

DESCRIPTION OF THE VIDICON SURVEY EXPERIMENT(S)

The conditions that caused the first survey attempt to fail and those which permitted the second attempt to be a partial success will be discussed in this section. Figures S-13 and S-14 illustrate the geographical conditions in which the first surveys were conducted. The problems in conducting a terrestrial survey with an astronomical device arose from four factors: excessive heat, excessive light, power sources, and a breakdown in communications.

During the first attempt, the equipment was assembled and manipulated from 9AM to 2PM on a day that was hazy, humid, and hot(85 degrees Fahrenheit by 10 AM). The only advantage of the weather was the diffuse illumination of the outcrop; no need to worry about shadows obscuring important structures. The disadvantages of the weather were: that the coolant for the detector cold box was melting more rapidly; that the time during which the vidicon tube was cool for useful data gathering was shortened to slightly greater than one hour; the discomfort and frequency of collapse(due to heat prostration) became a serious impedance to the surveyors' progress.

The problems with the portable, gasoline-driven electric generators were two-fold: failure to operate properly; and poor signal qualities. As a result of the usual vibrations inherent in transporting equipment by truck, the generators either failed to start (first attempt) or were so badly flooded that considerable tact had to be employed to start them. Despite special precautions to provide a 'clean' power source signal to the equipment

and magnetic tape unit, problems with generator electric noise and signal discontinuity were witnessed by the processed vidicon pictures(Figures P-38, P-39) from the second experimental survey attempt.

The second attempt progressed enough for excessive illumination to pose a problem. After making the best attempt possible to focus upon the contact between the Blue Hill Granite and the welded zone of Pondville Conglomerate(left contact, Figure S-14), it was discovered that using interference filters other than the 400.0 Nm and 433.0 Nm resulted in vidicon saturation. The tube was detecting so much light that it could no longer resolve contrasts(overexposure). Precautions for preventing light from leaking to the detector were taken by covering the dewar-filter wheel-optics assembly with a plastic cover and two blankets. The lens was stopped down(F-8) and the shutter was operating at the minimum exposure time of 0.1 seconds(switch that adjusted exposures to 0.01 seconds did not seem to be working during the experiment). Two pictures at 850.0 Nm and 900.0 Nm were taken with the interference filters in tandem with a neutral density filter which cut the light levels by 70% and 90% respectively. The actual effect of the neutral density filters could not be determined because the vidicon tube was warming up and the supply of ice and time had been exhausted(no figures illustrate these pictures).

To assist future survey work with the vidicon system, it is appropriate to mention the problem of communications' failure which was the primary reason for the first survey's failure to produce data. After considerable work had been performed in pre-

preparing for the survey experiment and a morning of trouble-shooting had been spent in the field, it was discovered(with all equipment operating normally) that there was no video signal from the vidicon tube. The survey was abandoned. The absence of video signal was traced to a wire that had been disconnected because of its loose nature on the evening preceding the day of the survey. The wire's disconnection occurred during a rash of impromptu modification sessions with the vidicon electronics. This would be acceptable except that no attempt to reconnect the wire had been made. This negligent act occurred despite posted schedules listing dates on which the system would be actively used for experimentation. Such costly errors can be elliminated by better management of personnel and equipment - as compared to explaining such experiment failures as due to equipment failures.

A final and most significant problem with the surveys was the difficulty in focusing an image of the outcrop. Due to extreme heat, the Polaroid film used for oscillographs was ruined. The daytime brightness prevented focusing by visually observing the vidicon monitor. Even with the help of an impromptu blanket tent(which was placed over the technicians and equipment), the attempt to focus by using the residual image on the vidicon monitor scope was foiled. Consequently, the optics system was aimed with a Brunton compass and the lens was focused at infinity (by educated guesswork). The resultant pictures at 400.0 Nm and 433.0 Nm are displayed in Figures P-38 and P-39. Recommendations for remedying the discussed problems will be made in the following section.

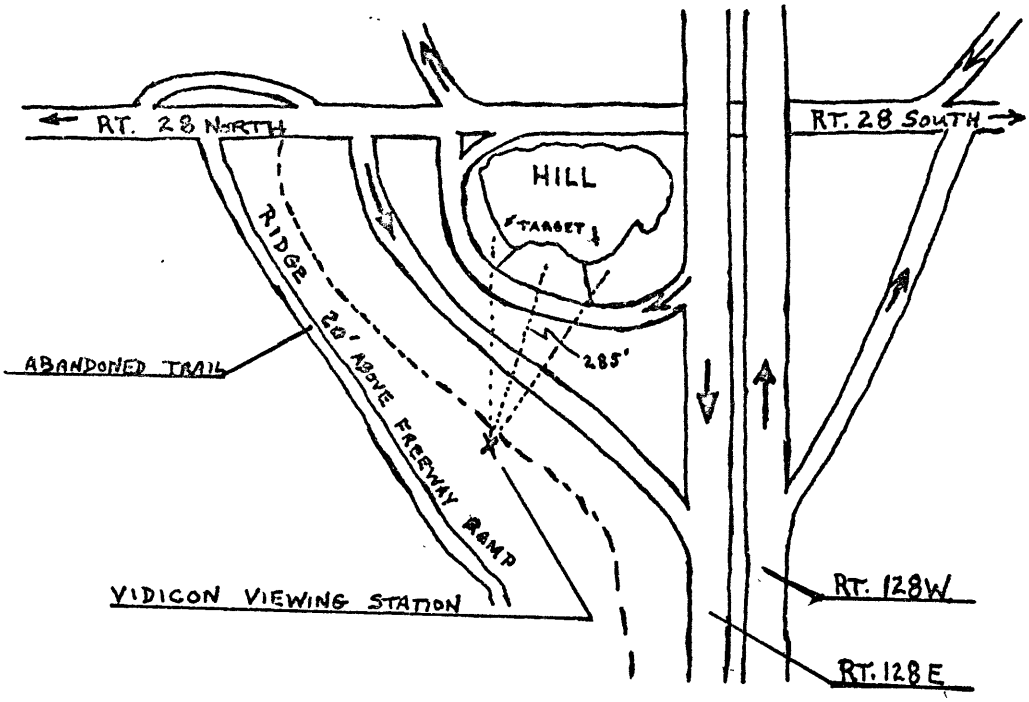

Figure: S-13

Location and Orientation of Field Experiment

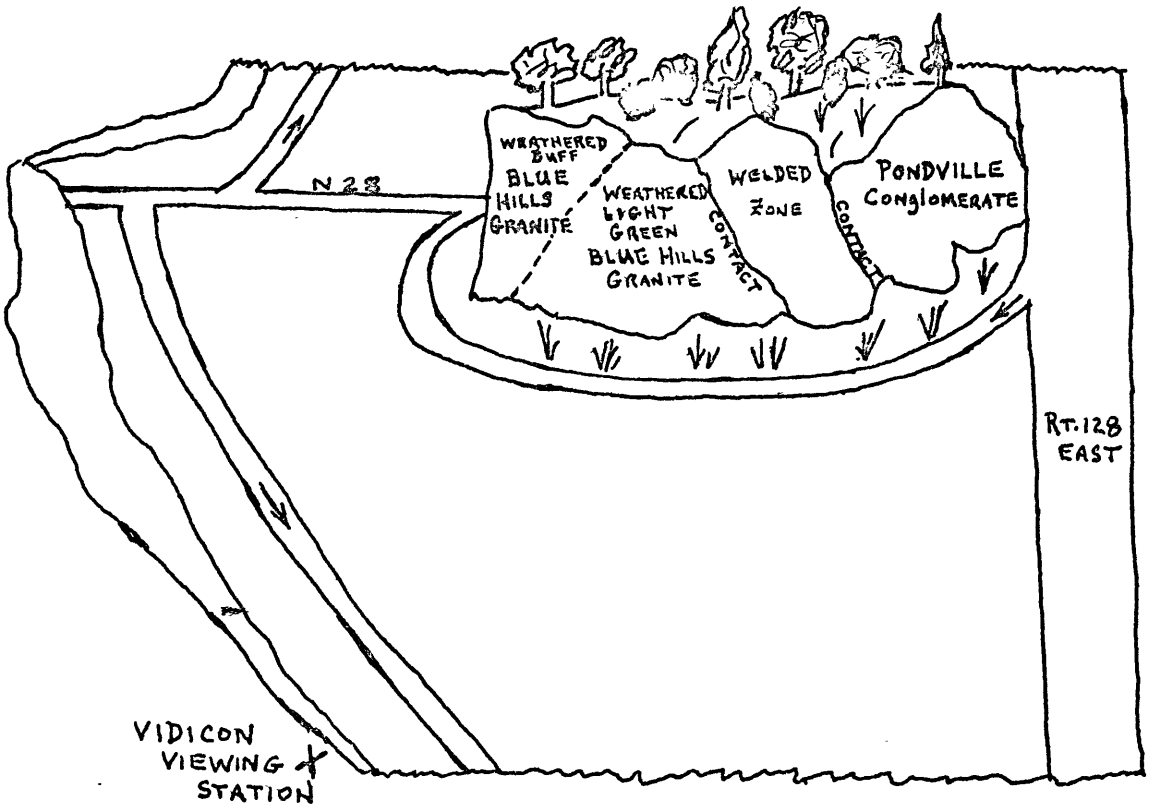

Figure: S-14

Sketch of Outcrop used in the Field Experiment

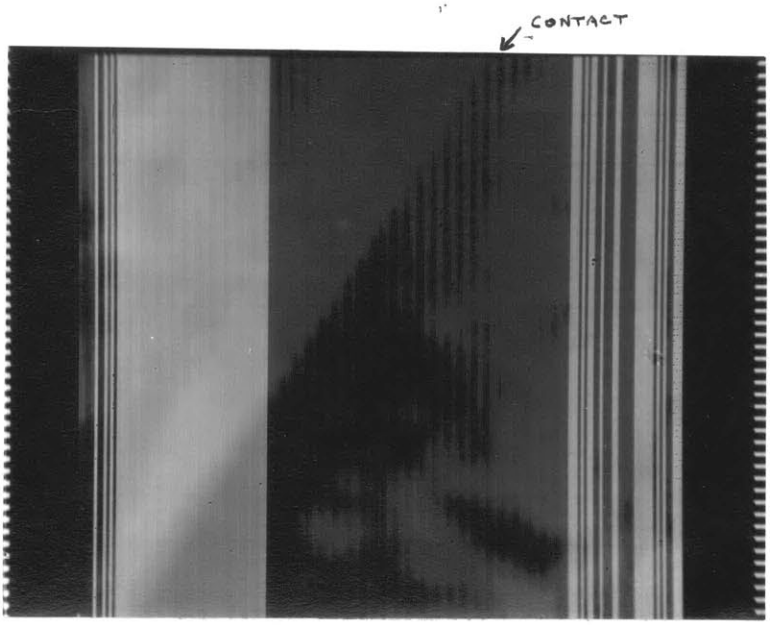

Figure: P-38

Contact of Blue Hill Granite and Welded Zone
of Pondville Conglomerate, 400.0 Nm, Exp. - 0.1 sec.

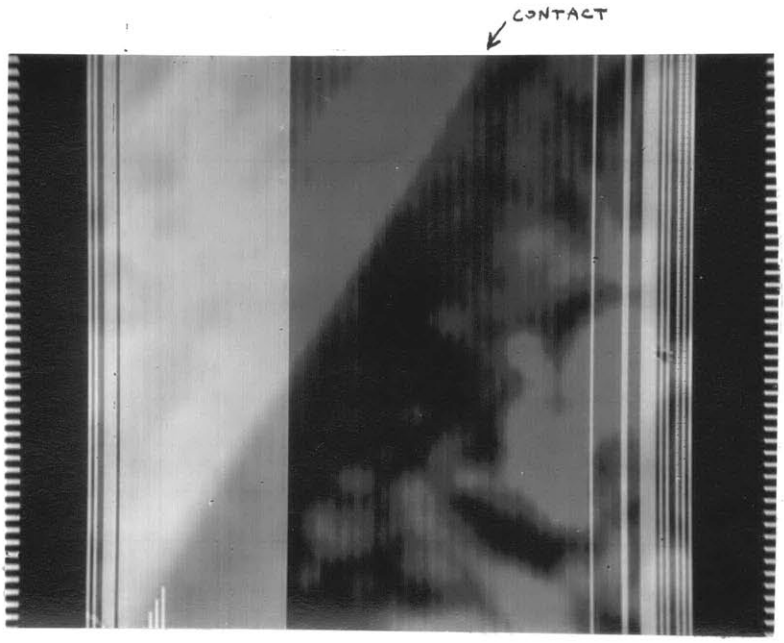

Figure: P-39

Contact of the Blue Hill Granite and Welded Zone
of Pondville Conglomerate, 433.0 Nm, Exp. - 0.1 sec.

RECOMMENDATIONS

During the course of this study, various technical problems with the vidicon system were found which require solutions. Several of the solutions relate directly to the vidicon system's geophysical applications; however some recommendations are made that also will improve the system's usefulness as an astronomical instrument.

Tests of the vidicon system gave results that inferred that the system was experiencing electric noise problems that were effecting the consistency of the data as a function of exposure time. However, it is strongly recommended that the system be tested by more sophisticated techniques so that the trouble may be resolved as either a nonlinearity problem or a noise problem. After identifying the problem, correct the problem.

While processing the data, two anomalous features(possibily noise generated) were observed in the data. Vidicon pictures occasionally had rectangular plateaus of block saturation recorded in various sectors of an image(which obliterated the true picture in that area). Sporadically, pictures were found to have random single point saturations positioned randomly on the image (Figures P-17 thru P-37)(film tape was elliminated as the source of the problem).

Another problem may be observed in Figures P-4 to P-15. The pictures show a circular area of resolution. Beyond the periphery of this region, the target appears to be out of focus. The phenomena is attributed to the vidicon tube's silicon detector which becomes thicker at its boundry for mounting purposes(Ezell,

personal communication). This inefficient use of the detector directly effects the vidicon system's field of view and its value as a geophysical tool. This problem will be corrected when the vidicon tubes are redesigned to remedy such problems. To recommend reconstruction of the vidicon tube at this time would be a fruitless effort.

It is recommended that the equipment and technique used for focusing the vidicon system in the field be significantly improved upon. A simple(but perhaps costly) solution to focusing problems is to devise a television monitor system that stores the vidicon picture for immediate reference. This would permit the sighting and focusing of the vidicon system in an efficient manner that would yield high quality vidicon pictures. This suggestion includes the redesign of the optical system. A redesigned optical system could substantially minimize the need to refocus the image each time a picture was taken at a different wavelength.

An insolated hood that would isolate the vidicon cold box-filter wheel assembly from daytime illumination and heat is desperately needed. Such a hood would grant the vidicon system a longer operation time because the solid CO_2 refrigerant would last longer. The hood would also elliminate saturation of the vidicon tube due to the leakage of light into the tube.

To elliminate trial and error picture sessions, it is requested that an electronic exposure meter be built into the vidicon system. Such a meter would prevent saturation by adjusting the shutter speed and exposure time before the vidicon picture was manually recorded.

In the interest of future field work with the vidicon system, a dependable, rugged and portable electric generator will be essential. The generator should be designed or modified so that the signal it generates will be noise free and compatible with the electronic controls and magnetic tape recorder of the system.

Before repeating the field studies with the vidicon system, it is recommended that some of the experiments performed in this study be repeated. This will allow the learned techniques for obtaining high quality pictures to be reapplied to the first experiments where any technique was practiced in crude form. Following the repetition of earlier experiments, the recommendations discussed should be acted upon. Upon completion of the suggested improvements, the vidicon system should be used in the field for mapping mineralization and structure. The development of the vidicon system as a geophysical tool may then take two courses of action. The vidicon system may be developed for satellite or airborne remote sensing applications and/or it can be developed for ground-based geophysical surveys.

CONCLUSIONS

This study presented a logical procedure for investigating an astronomical tool's applicability to terrestrial geological problems. For the 400.0 Nm to 1100.0 Nm spectral range, the vidicon system clearly illustrated its ability to: differentiate mineralogy; identify the transition element ions that are responsible for photon absorptions; enhance imagery and map mineralized structure of large rock units with the assistance of computer processing; resolve detailed structure and mineralization; identify minerals (without prior ground truth); differentiate propylitically altered versus unaltered rock units associated with porphyry copper deposits.

The field performance of the vidicon system to map a geologic outcrop's structure and mineralogy was promising. If the suggestions presented in the previous section of recommendations are acted upon, the vidicon system could be made into a durable, practical and extremely useful geophysical tool. The promise of this vidicon system as a remote sensing instrument is based on the premise that the discovered system problems will be categorically negated.

Figure: T-15 ::

GUIDE TO COMMON ABSORPTION BANDS IN REFLECTIVITY SPECTRA*

Approximate Wavelengths of Absorption Band Maxima		Source of Absorption Feature
370.0 Nm	Mn^{2+};	Octahedral-electronic energy level transitions
400.0 Nm	Fe^{3+}	Electronic energy level transition
410.0 Nm	Mn^{2+};	Same as above for Mn^{2+}
450.0 Nm	Cu^{2+}, Mn^{2+};	Same as above
470.0 Nm	(?),	Found in some porphyry copper reflectivity curves.
510.0 Nm	Fe^{2+};	Electronic energy level transition
520.0 Nm	Cu^{2+};	Octahedral electronic transitions
550.0 Nm	Fe^{3+};	Conduction band with sharp absorption edge/illustrates transparent-opaque transition
	Mn^{2+}, Fe^{2+};	Electronic energy level transition
570.0--620.0Nm	Cu^{2+};	Conduction band(Cuprite)
600.0 Nm	S, S^{2-};	Conduction band(Cinnabar)
660.0 Nm	(?),	Found in some porphyry copper reflectivity curves(diagnostic of propylitization)
700.0 Nm	Fe^{3+};	Electronic energy level transition(thic cation's strongest band)
800.0 Nm	Fe^{3+}, Cu^{2+};	Octahedral electronic energy level transitions(Azurite)
850.0 Nm	Fe^{3+}, Cu^{2+};	Octahedral electronic energy level transition(Cuprite)
900.0 Nm	Fe^{2+}, Fe^{3+};	Six-fold coordination energy level electronic transitions
970.0-1000.0 Nm 1000.0-1100.0 Nm	Fe^{2+};	Electronic energy level transition due to distortion of coordination
1350.0 Nm	(?),	Found in some porphyry copper reflectivity spectra; could be due to CO_3(?)-Vibrational
1400.0 & 1900.0 Nm		Undissociated water in lattice-Vibrational

GUIDE TO COMMON ABSORPTION BANDS IN REFLECTIVITY SPECTRA*

(continued)

Approximate Wavelengths of Absorption Band Maxima		Source of Absorption Feature
1400.0 Nm (without band at 1900.0Nm)	OH^-,	Presence of hydroxyl groups other than water in lattice - Vibration related absorption
1500.0 Nm	OH^-,	Same as above
1800.0-1900.0Nm	Fe^{2+},	Electronic energy level transition due to disordered octahedral orientation
2170.0 Nm 2180.0 Nm 2270.0 Nm 2420.0 Nm 2500.0 Nm (Other wavelengths depending on the cation)	$CO_3^=$	Overtone and combination tones of lattice vibrations
2200.0 Nm 2300.0	OH^-,	Vibrational combination tones

*NOTE: This tabulation is primarily derived from making reference to:(Hunt & Salisbury,1970-1971)

APPENDIX I

TUCSON MOUNTAIN DISTRICT

SAMPLE NUMBER	General Description
5 A	Propylitic Altered Tertiary Rhyolite Volcanic Breccia
5 B	Unaltered Tertiary Rhyolite Volcanic Breccia and Tuff
6 A	Fresh, Relatively Unaltered Cretaceous Siltstone
6 B	Propylitic Altered Limy Siltstone (Cretaceous)
7 A	Unaltered Arkose (Cretaceous)
7 B	Propylitic Altered Arkose
9 A	Unaltered Cretaceous Andesite
9 B	Propylitic Altered Cretaceous Andesite

Note: For detailed descriptions refer to Figure: T-10, pages 77-78.

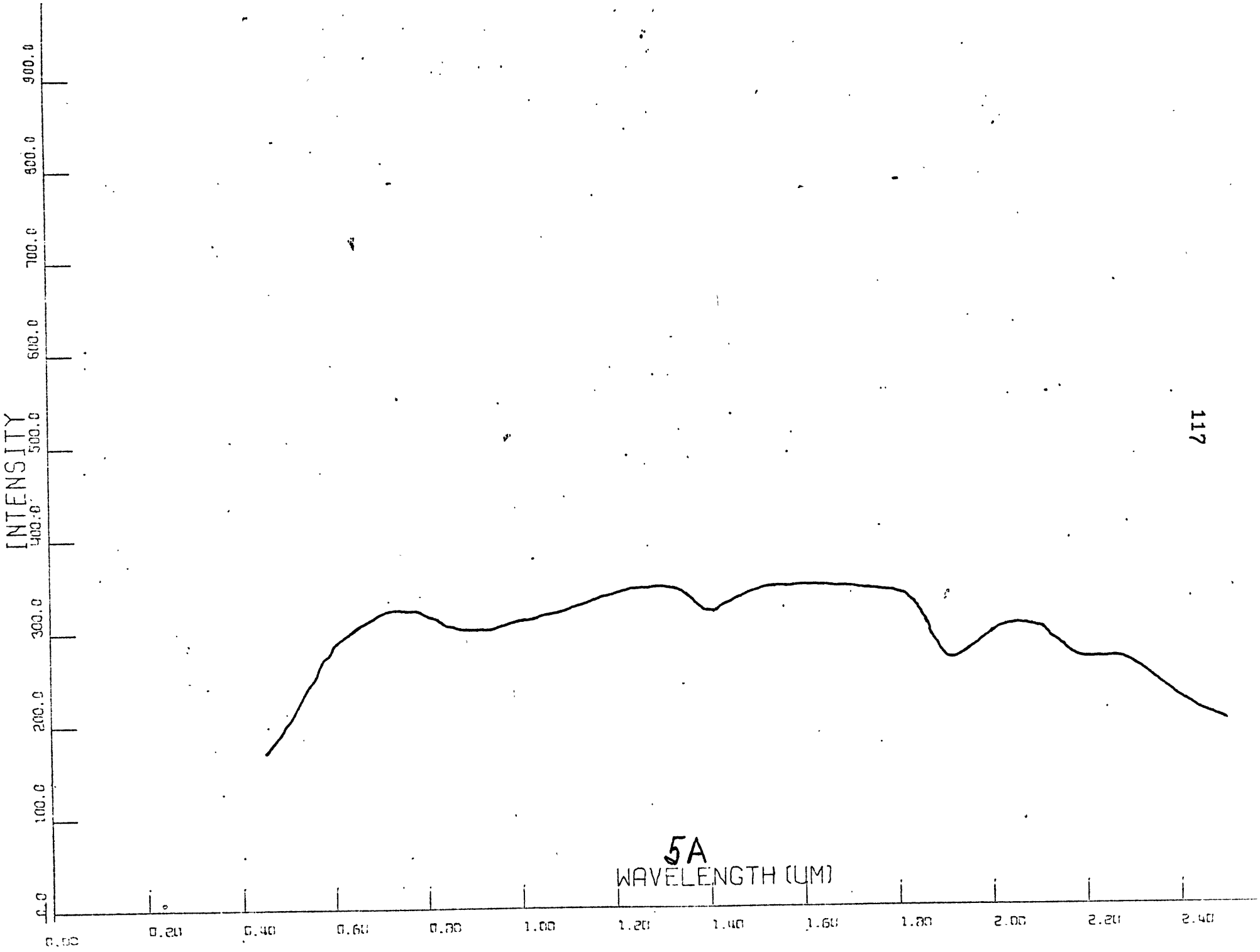
INTENSITY
900.0
800.0
700.0
600.0
500.0
400.0
300.0
200.0
100.0
0.0
0.00
0.20
0.40
0.60
0.80
1.00
1.20
1.40
1.60
1.80
2.00
2.20
2.40
WAVELENGTH (UM)

5A

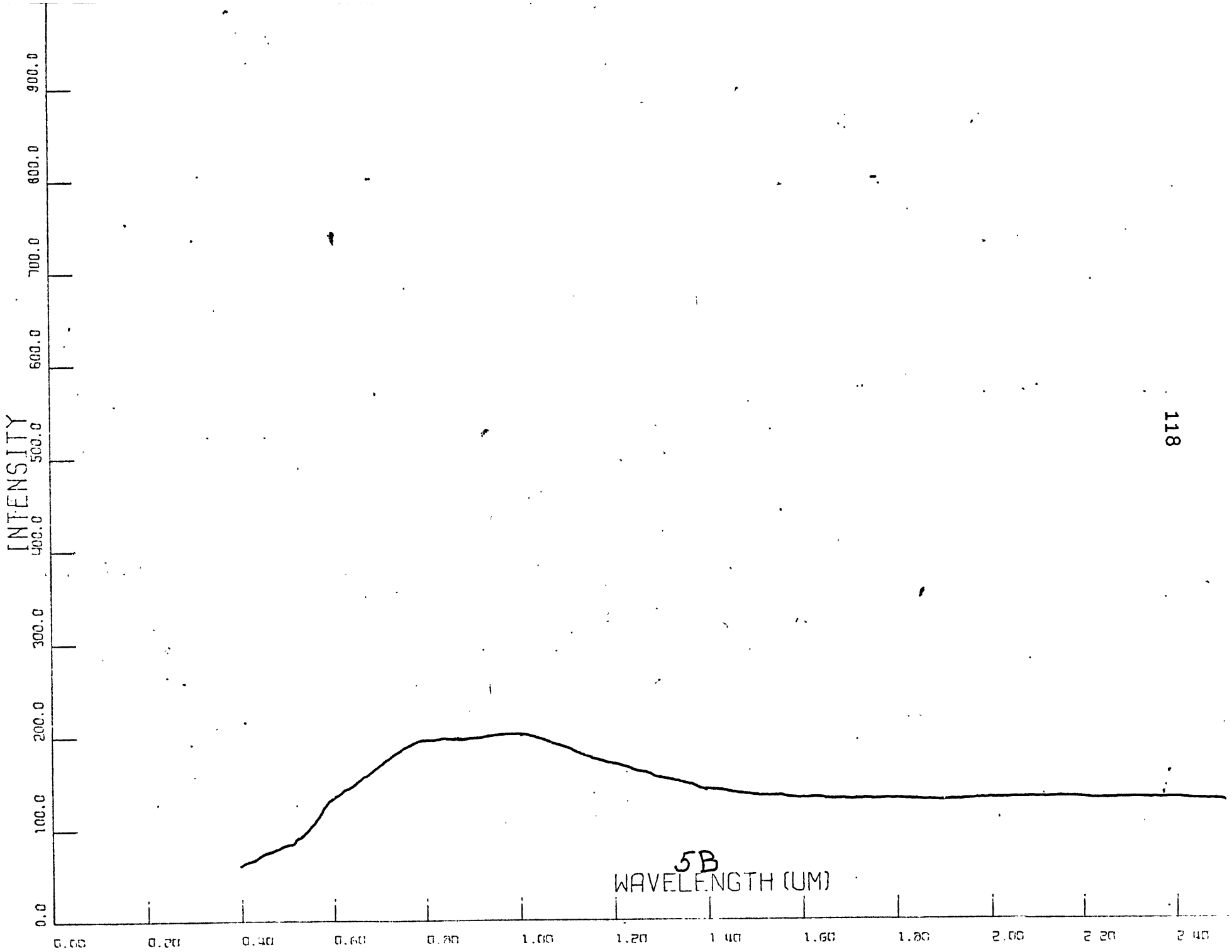
INTENSITY
0.0
100.0
200.0
300.0
400.0
500.0
600.0
700.0
800.0
900.0
0.00
0.20
0.40
0.60
0.80
1.00
1.20
1.40
1.60
1.80
2.00
2.20
2.40
WAVELENGTH (UM)

5B

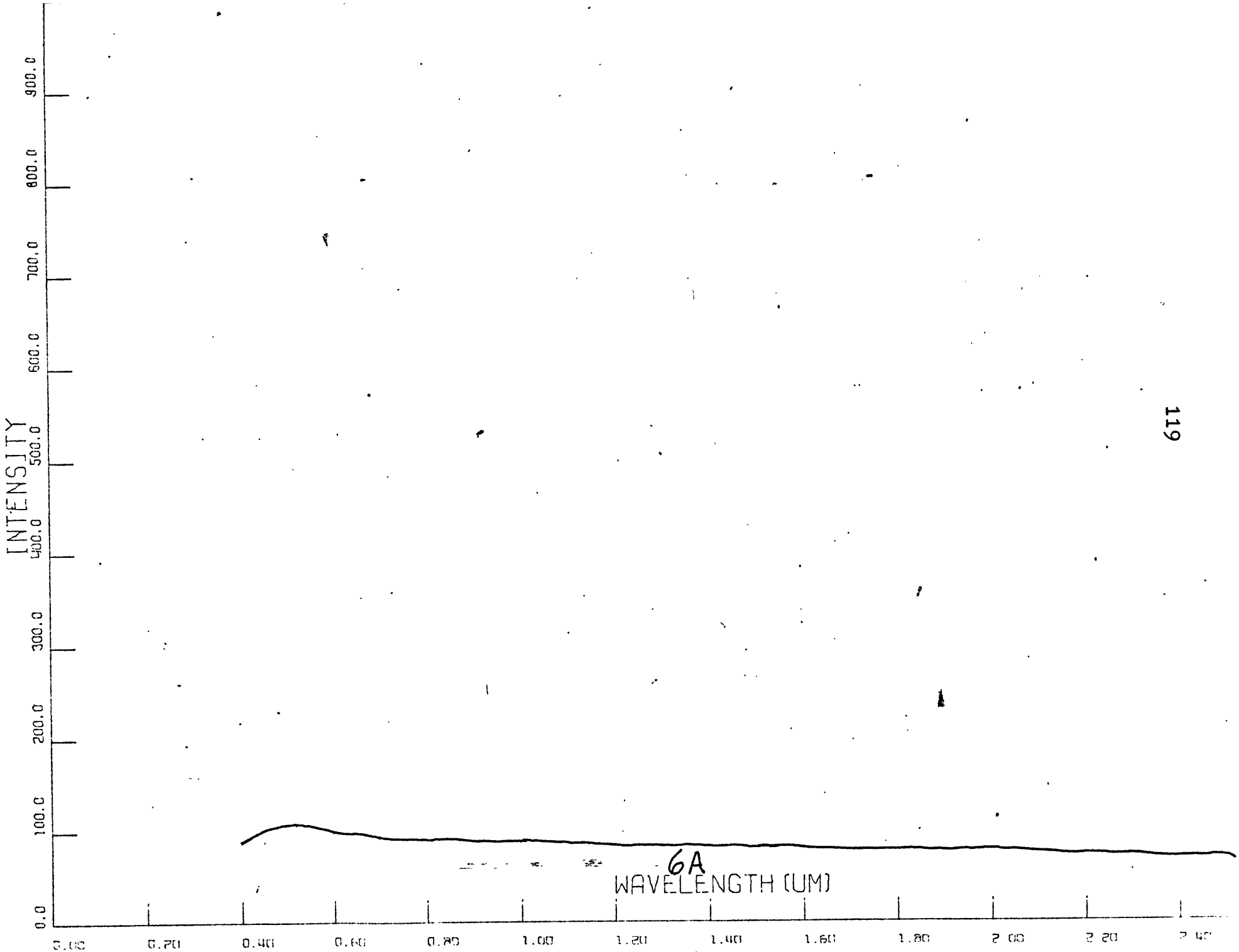
INTENSITY
900.0
800.0
700.0
600.0
500.0
400.0
300.0
200.0
100.0
0.0
0.00
0.20
0.40
0.60
0.80
1.00
1.20
1.40
1.60
1.80
2.00
2.20
2.40
WAVELENGTH (UM)

6A

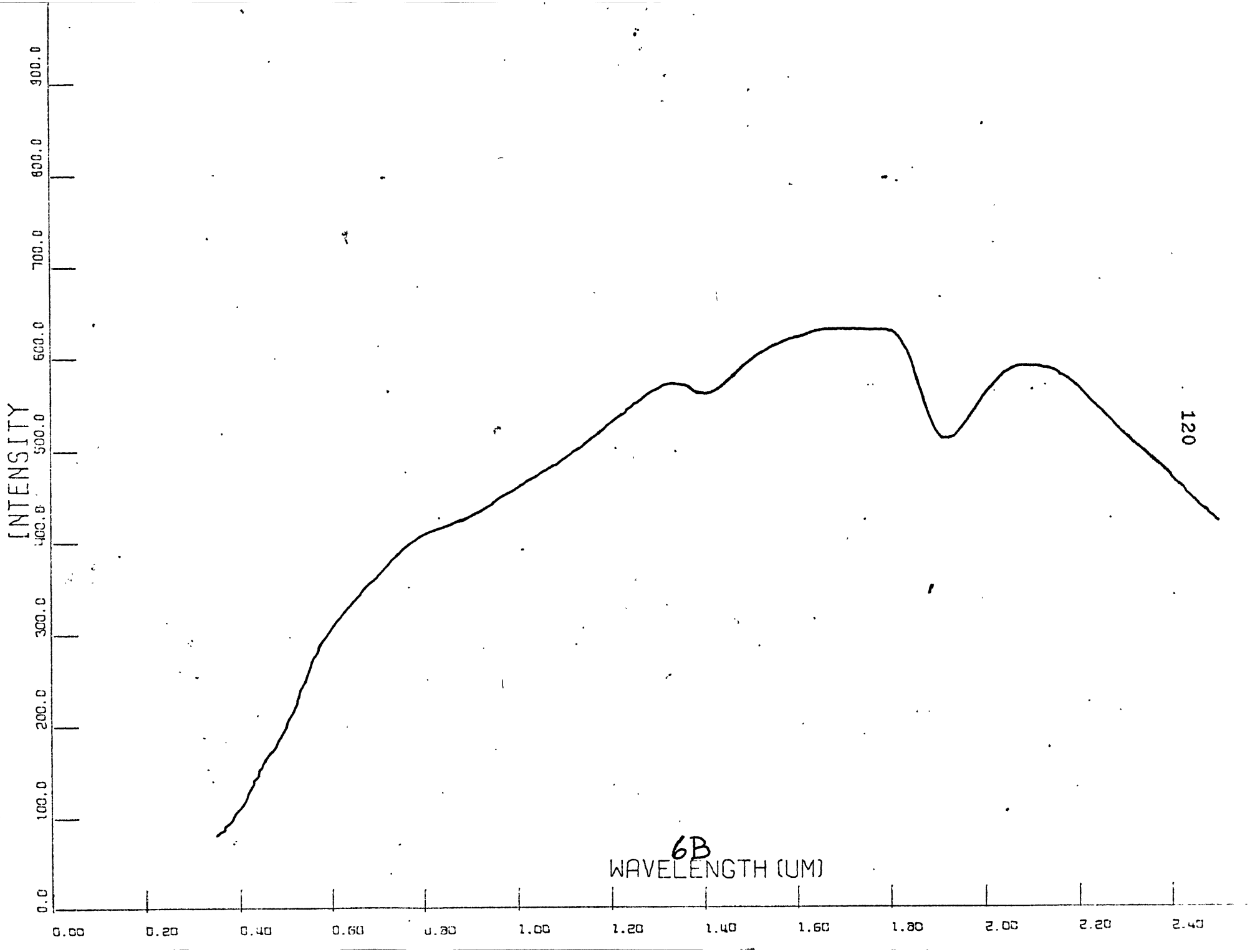
INTENSITY
900.0
800.0
700.0
600.0
500.0
400.0
300.0
200.0
100.0
0.0
0.00
0.20
0.40
0.60
0.80
1.00
1.20
1.40
1.60
1.80
2.00
2.20
2.40
WAVELENGTH (UM)
120

6B

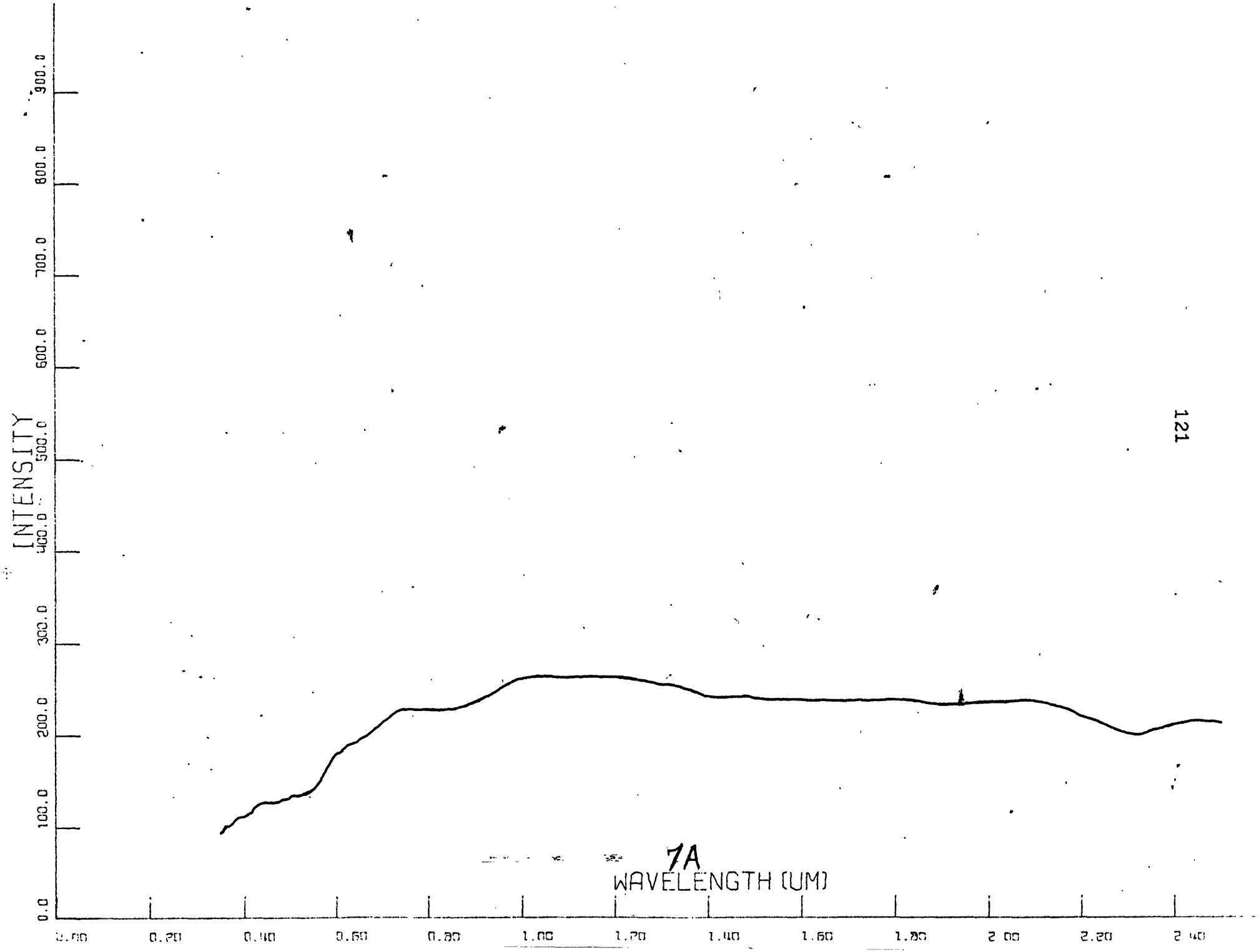
INTENSITY
0.0
100.0
200.0
300.0
400.0
500.0
600.0
700.0
800.0
900.0
0.00
0.20
0.40
0.60
0.80
1.00
1.20
1.40
1.60
1.80
2.00
2.20
2.40
WAVELENGTH (UM)
7A
121

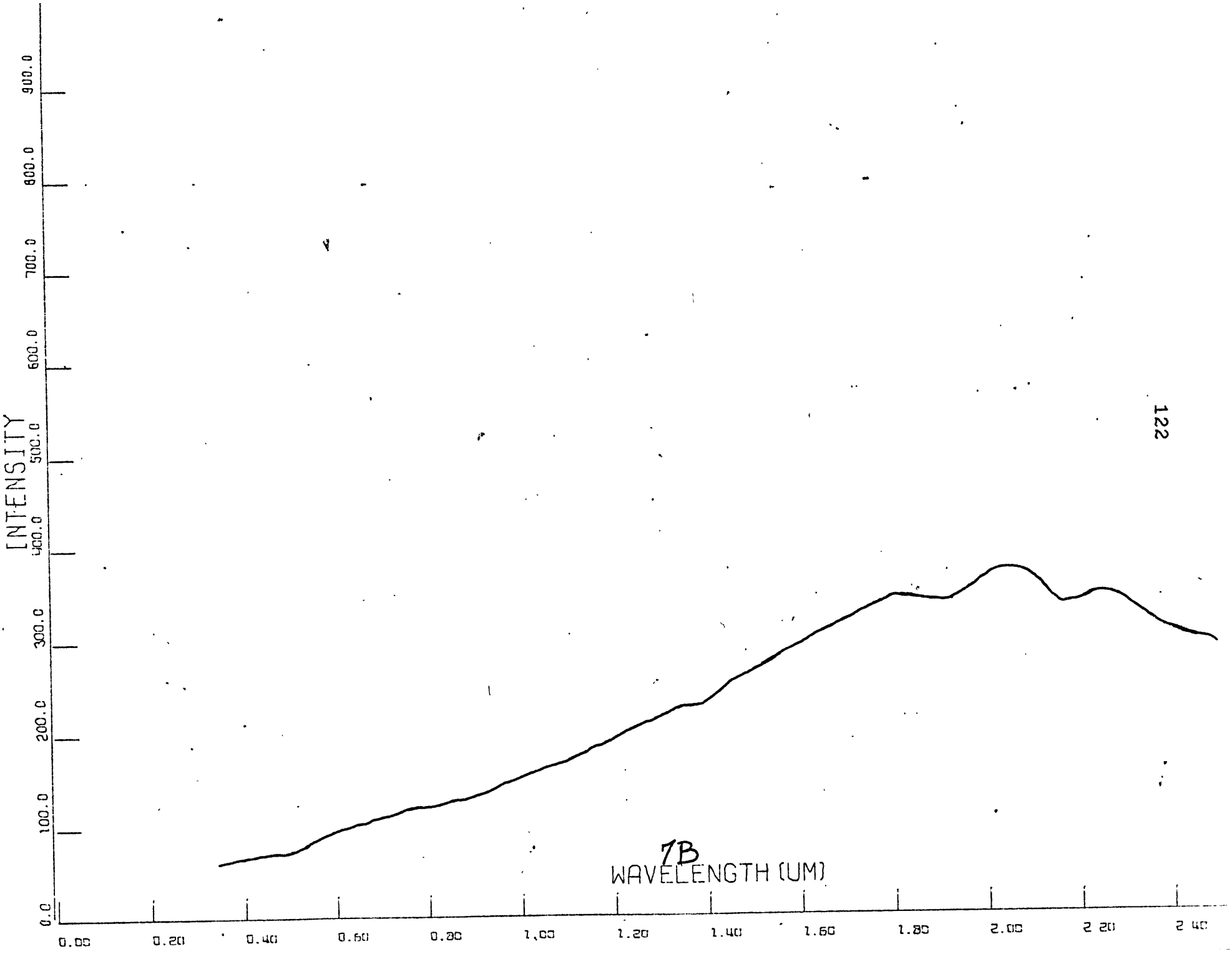
INTENSITY
900.0
800.0
700.0
600.0
500.0
400.0
300.0
200.0
100.0
0.0
0.00
0.20
0.40
0.60
0.80
1.00
1.20
1.40
1.60
1.80
2.00
2 20
2 40
WAVELENGTH (UM)
7B
122

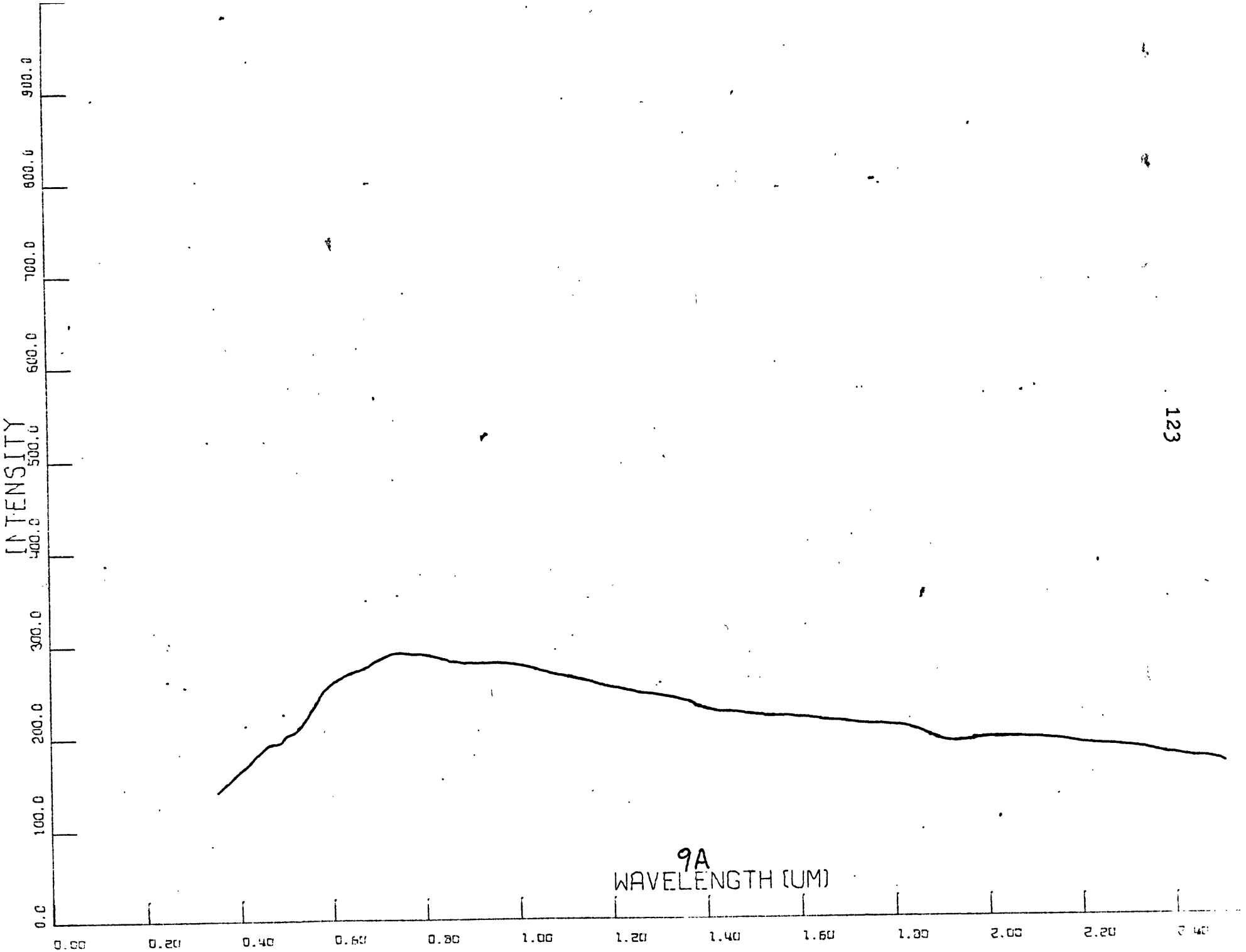
INTENSITY
900.0
800.0
700.0
600.0
500.0
400.0
300.0
200.0
100.0
0.0
0.00
0.20
0.40
0.60
0.80
1.00
1.20
1.40
1.60
1.80
2.00
2.20
WAVELENGTH (UM)

9A

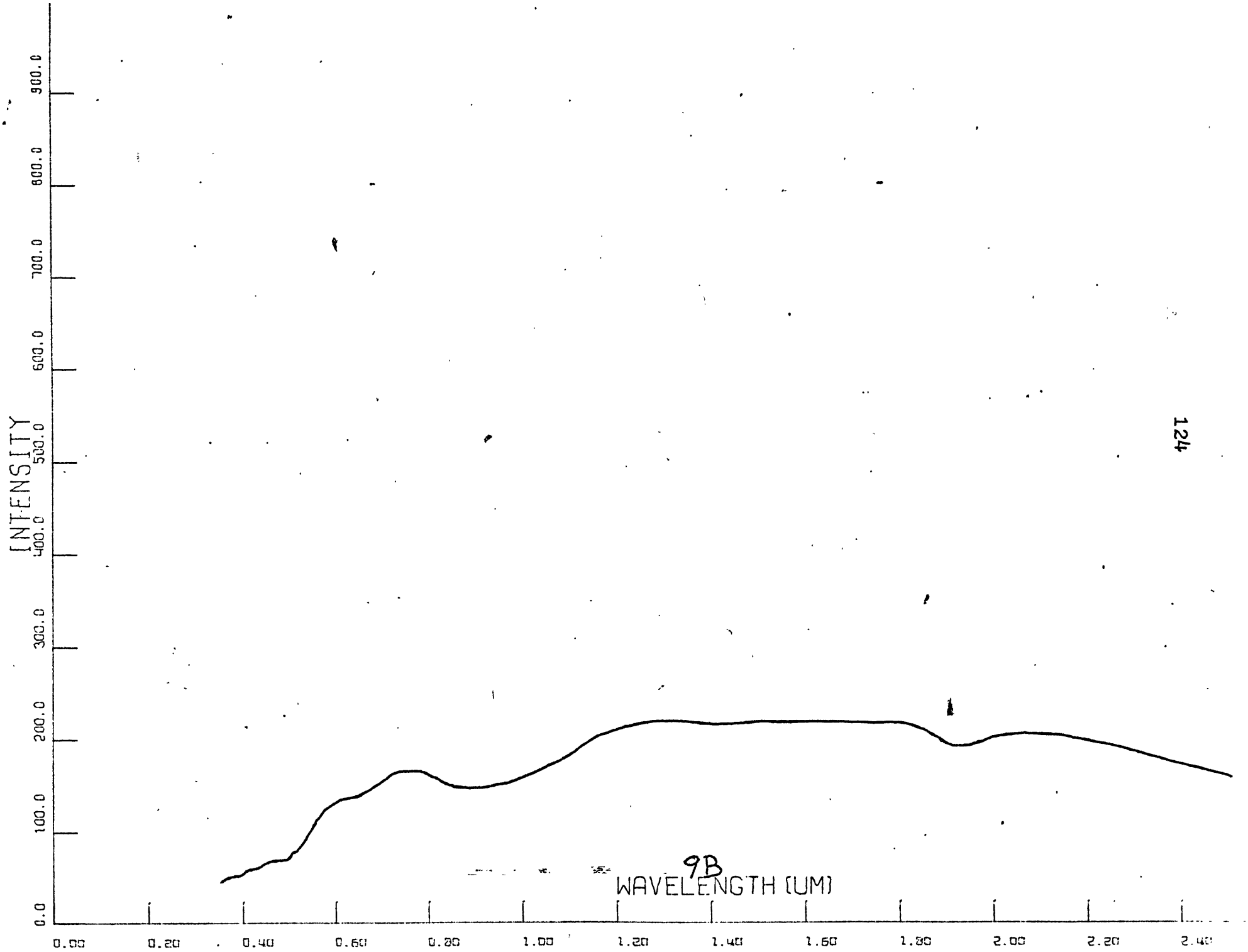
INTENSITY
900.0
800.0
700.0
600.0
500.0
400.0
300.0
200.0
100.0
0.0
0.00
0.20
0.40
0.60
0.80
1.00
1.20
1.40
1.60
1.80
2.00
2.20
2.40
WAVELENGTH (UM)
9B

CHRISTMAS DISTRICT

SAMPLE NUMBER	General Description
10 A	Relatively Unaltered Upper Paleozoic Limestone
10 B	Propylitic Altered Upper Paleozoic Limestone
11 A	Relatively Unaltered Quartz-Monzonite Porphyry
11 B	Propylitic Altered Quartz-Monzonite Porphyry
12 A	Relatively Unaltered Diorite(?) Porphyry
12 B	Propylitic Altered Diorite(?) Porphyry
13 A	Relatively Unaltered Cretaceous Andesite
13 B	Propylitic Altered Cretaceous Andesite

Note: For detailed descriptions refer to Figure: T-11, pages 80-81.

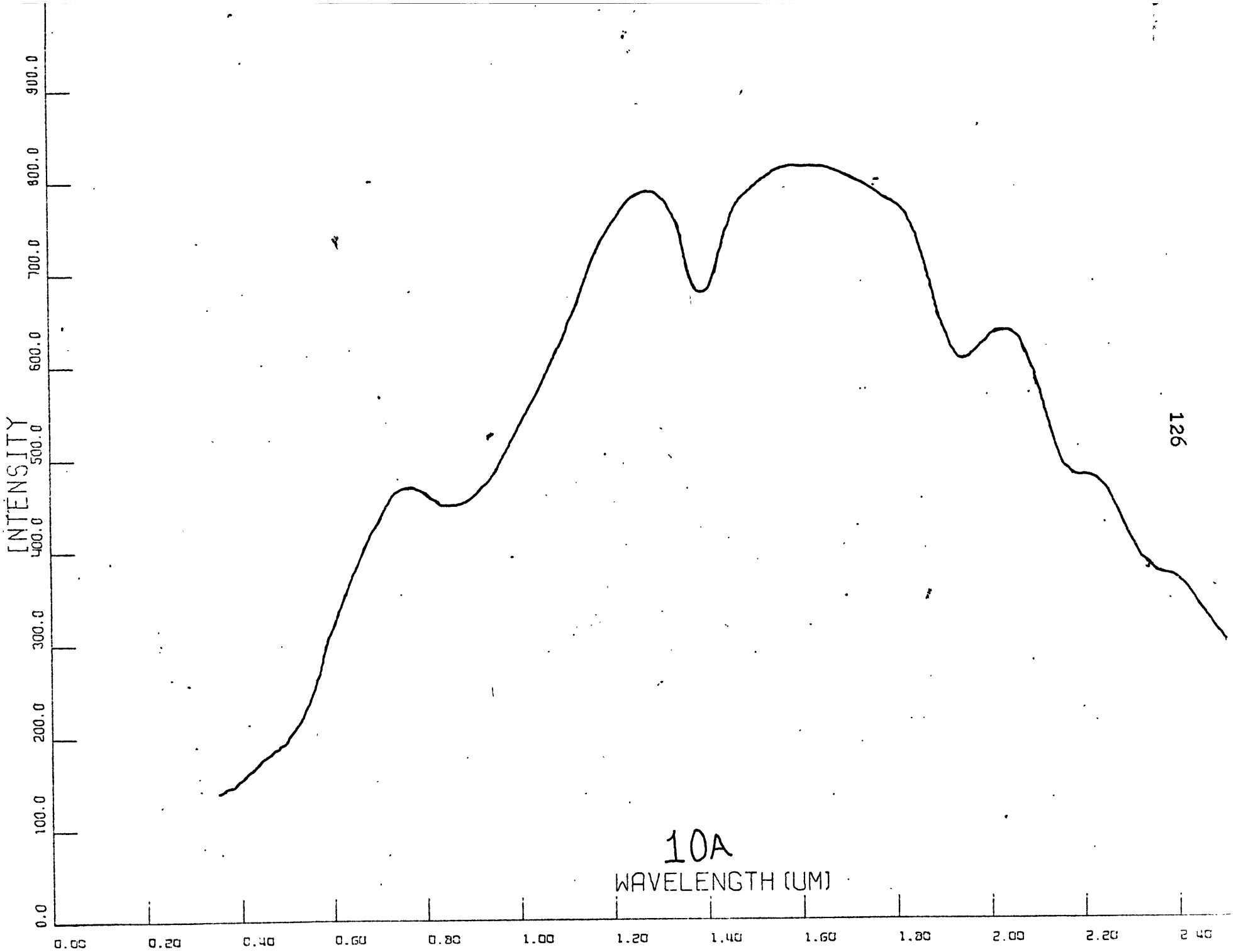
INTENSITY
0.0
100.0
200.0
300.0
400.0
500.0
600.0
700.0
800.0
900.0
0.00
0.20
0.40
0.60
0.80
1.00
1.20
1.40
1.60
1.80
2.00
2.20
2.40
WAVELENGTH (UM)
10A
126

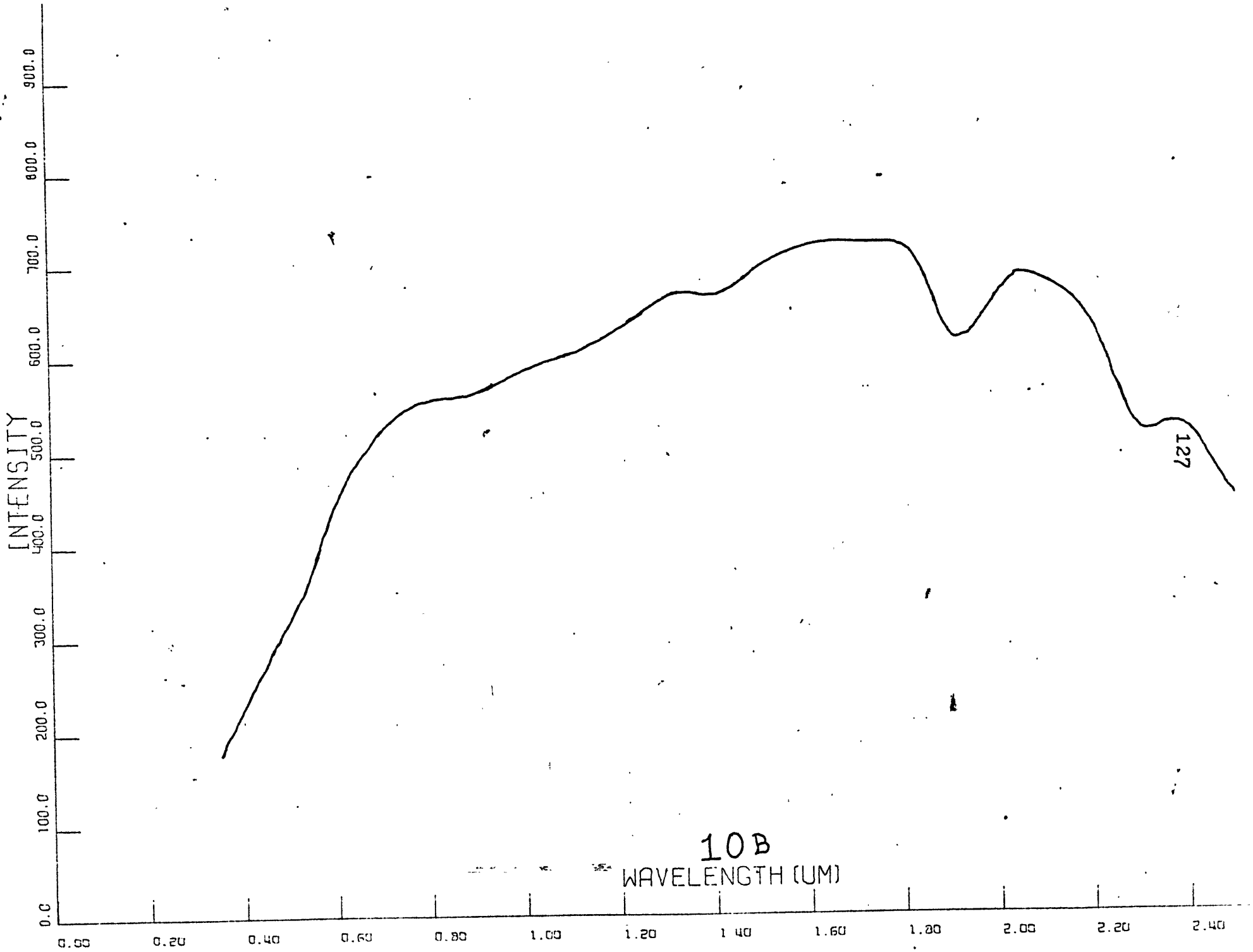
INTENSITY
900.0
800.0
700.0
600.0
500.0
400.0
300.0
200.0
100.0
0.0
0.00
0.20
0.40
0.60
0.80
1.00
1.20
1.40
1.60
1.80
2.00
2.20
2.40
WAVELENGTH (UM)
10B
127

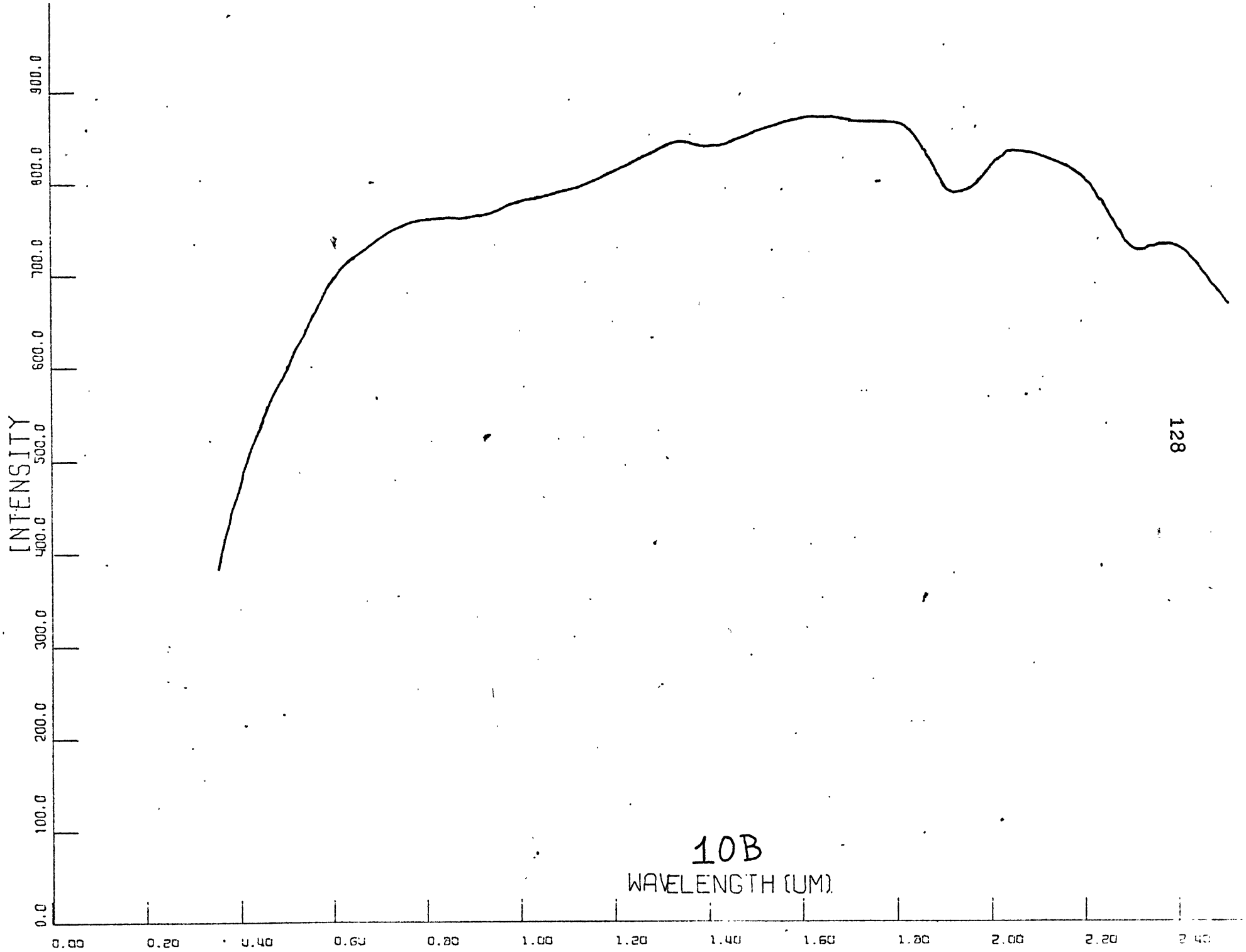
INTENSITY
900.0
800.0
700.0
600.0
500.0
400.0
300.0
200.0
100.0
0.0
0.00
0.20
0.40
0.60
0.80
1.00
1.20
1.40
1.60
1.80
2.00
2.20
2.40
WAVELENGTH (UM)
10B
128

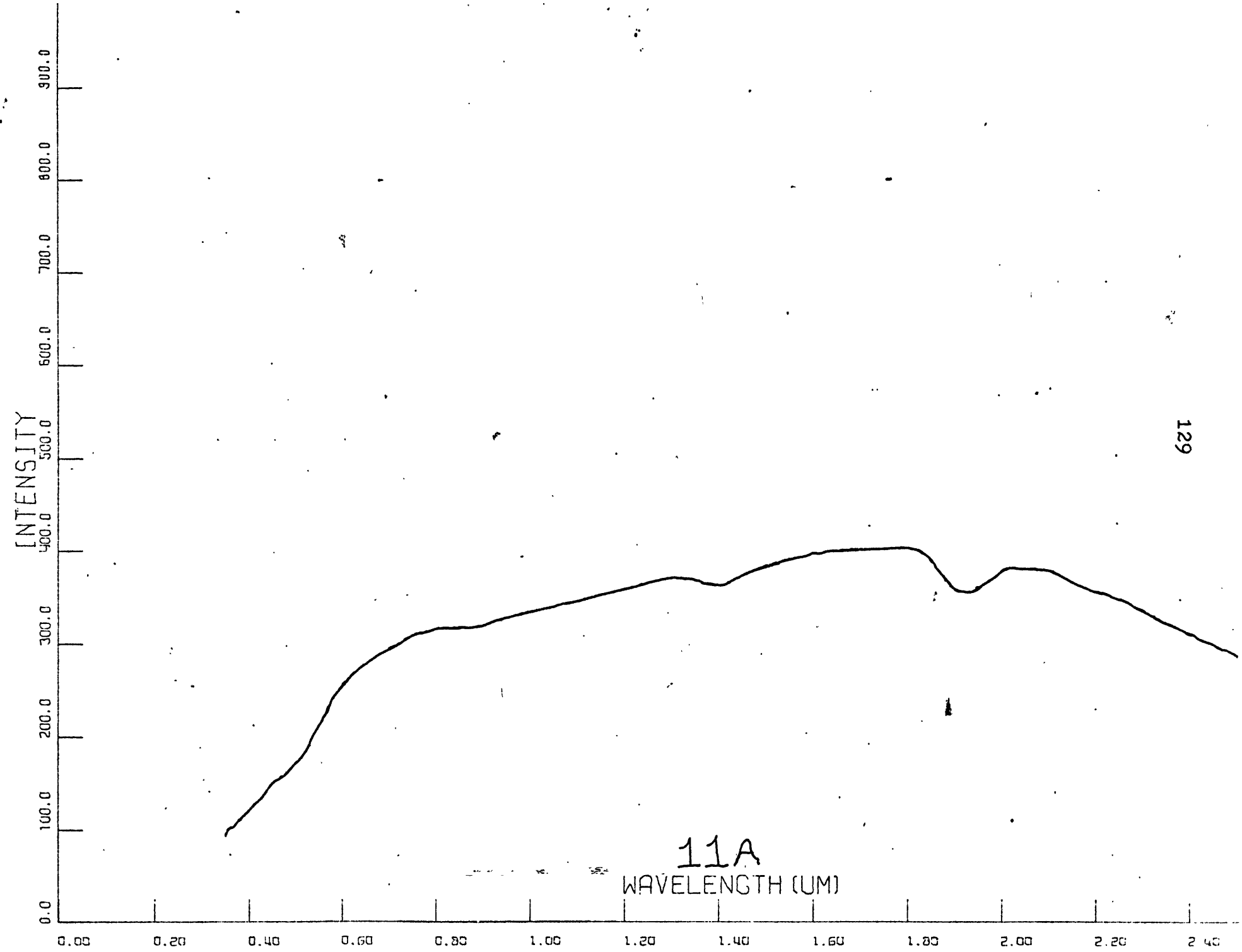
INTENSITY
0.0
100.0
200.0
300.0
400.0
500.0
600.0
700.0
800.0
900.0
0.00
0.20
0.40
0.60
0.80
1.00
1.20
1.40
1.60
1.80
2.00
2.20
2.40
WAVELENGTH (UM)
11A

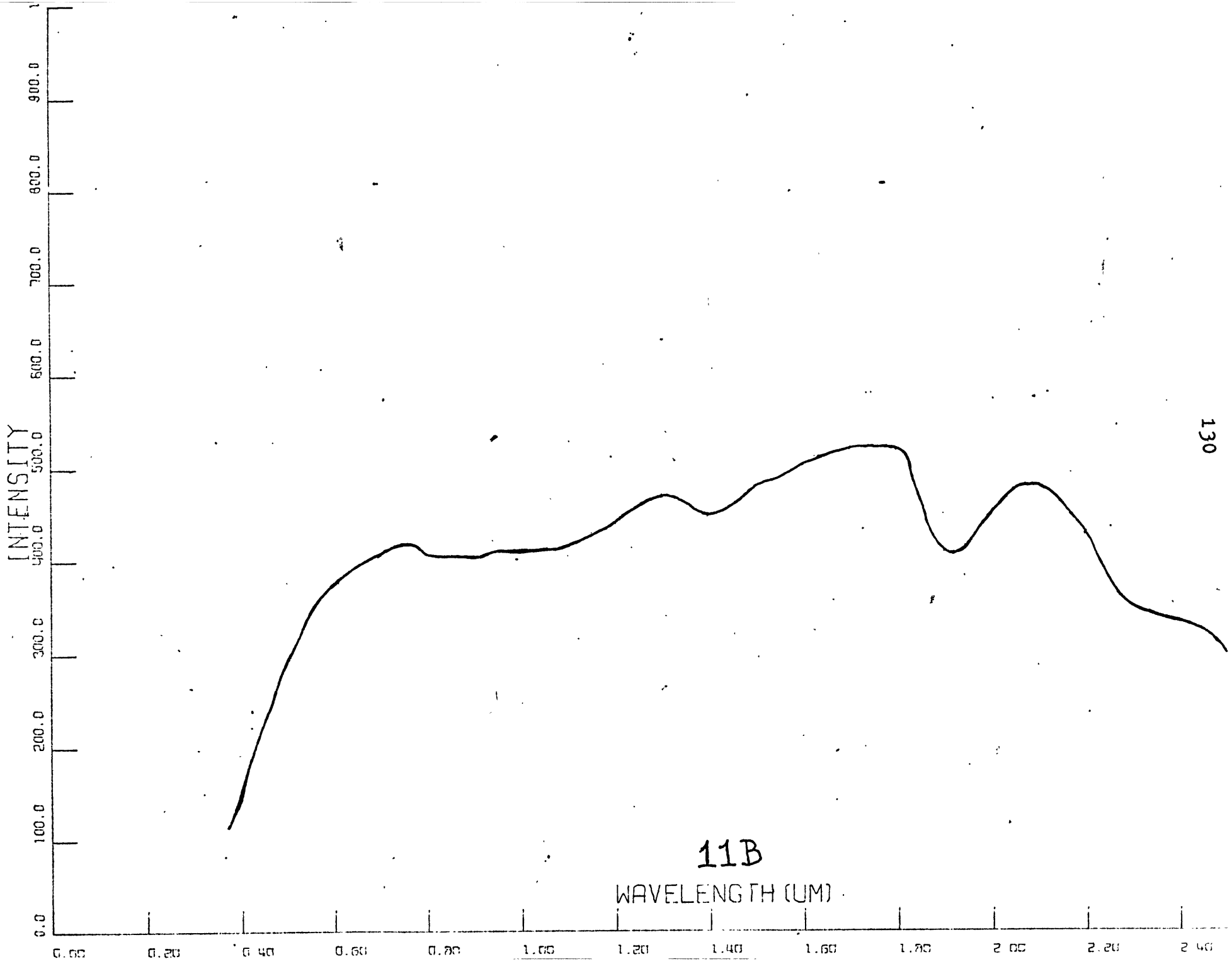
INTENSITY
0.0
100.0
200.0
300.0
400.0
500.0
600.0
700.0
800.0
900.0
0.00
0.20
0.40
0.60
0.80
1.00
1.20
1.40
1.60
1.80
2.00
2.20
2.40
WAVELENGTH (UM)
11B
130

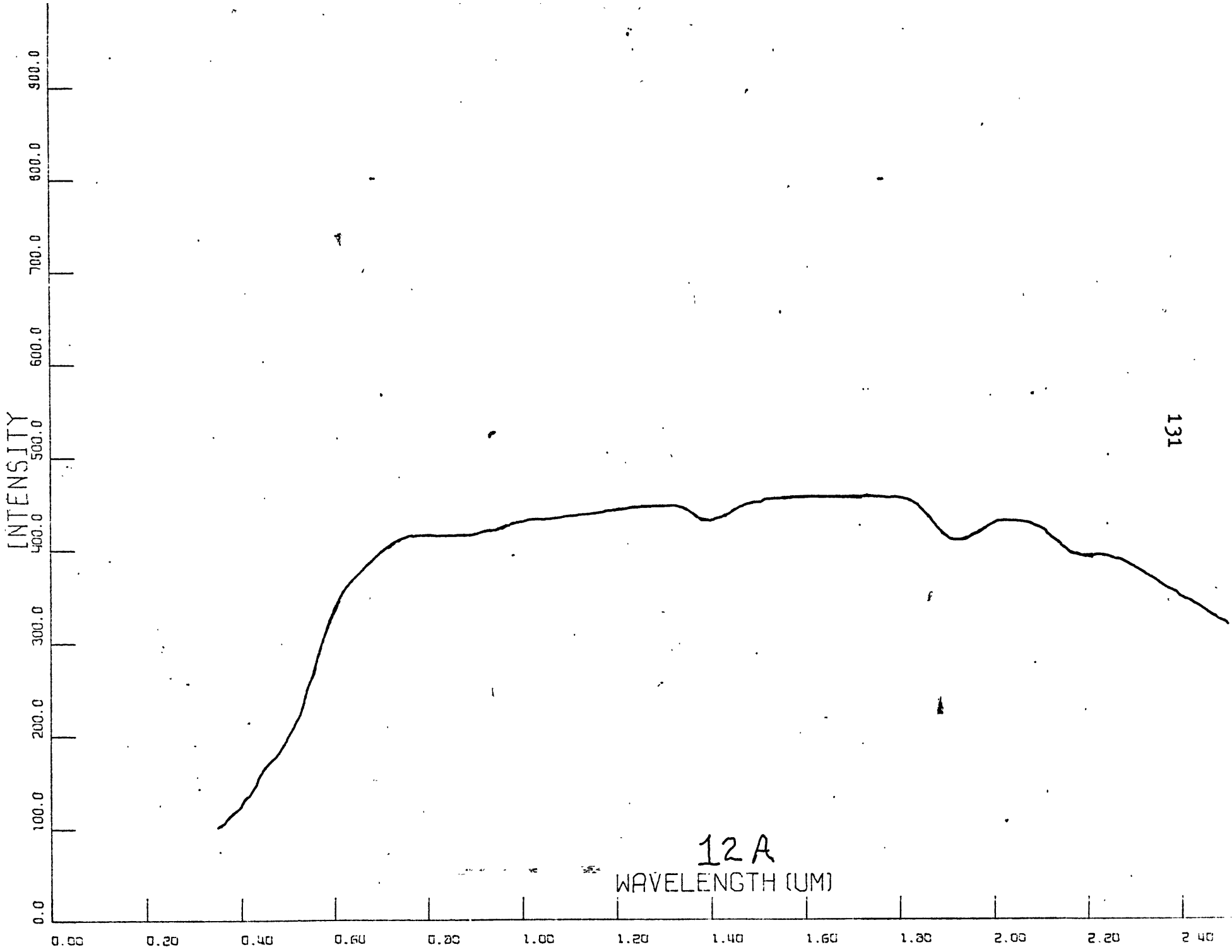
INTENSITY
0.0
100.0
200.0
300.0
400.0
500.0
600.0
700.0
800.0
900.0
0.00
0.20
0.40
0.60
0.80
1.00
1.20
1.40
1.60
1.80
2.00
2.20
2.40
WAVELENGTH (UM)
12A

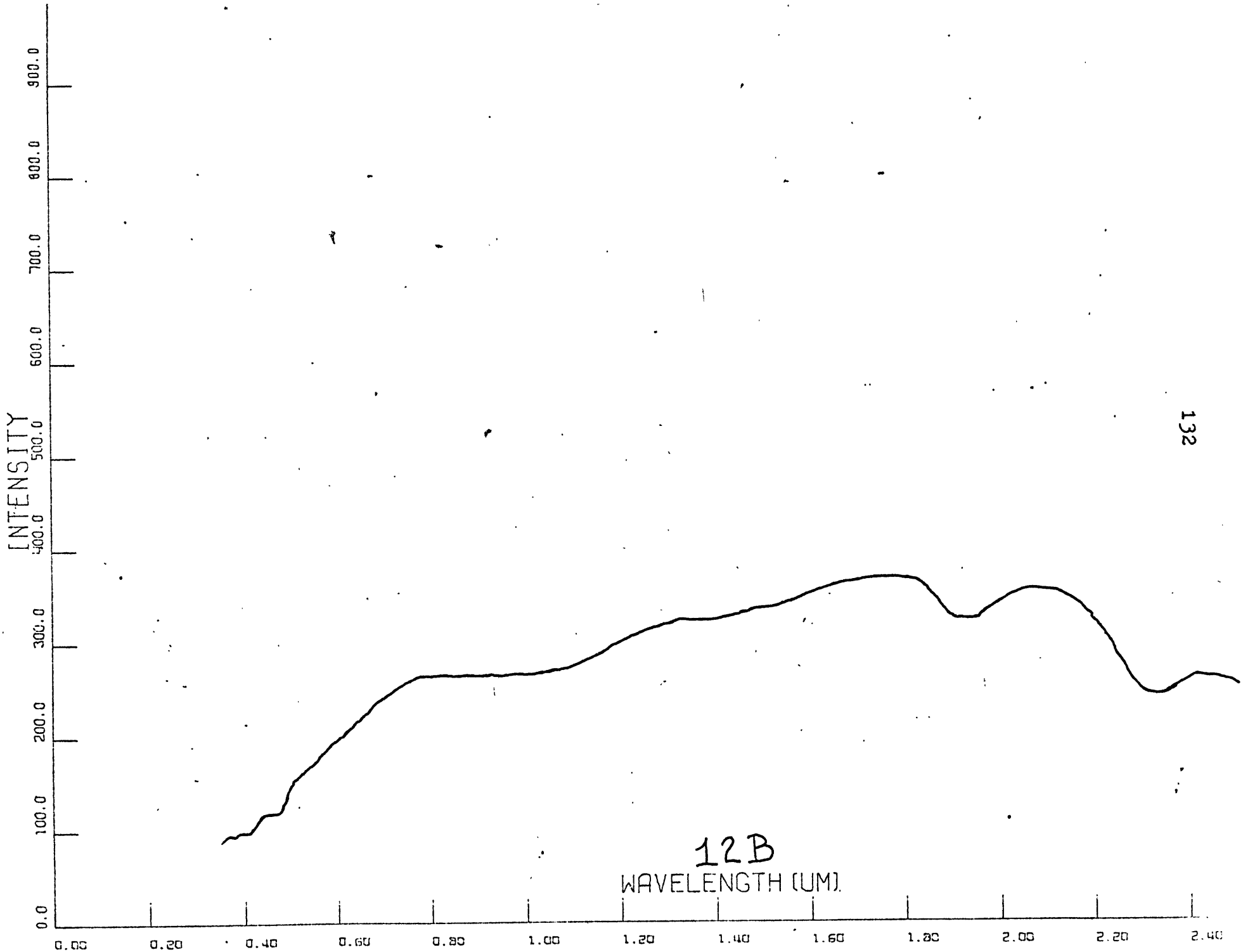
INTENSITY
0.0
100.0
200.0
300.0
400.0
500.0
600.0
700.0
800.0
900.0
0.00
0.20
0.40
0.60
0.80
1.00
1.20
1.40
1.60
1.80
2.00
2.20
2.40
WAVELENGTH (UM)

12B

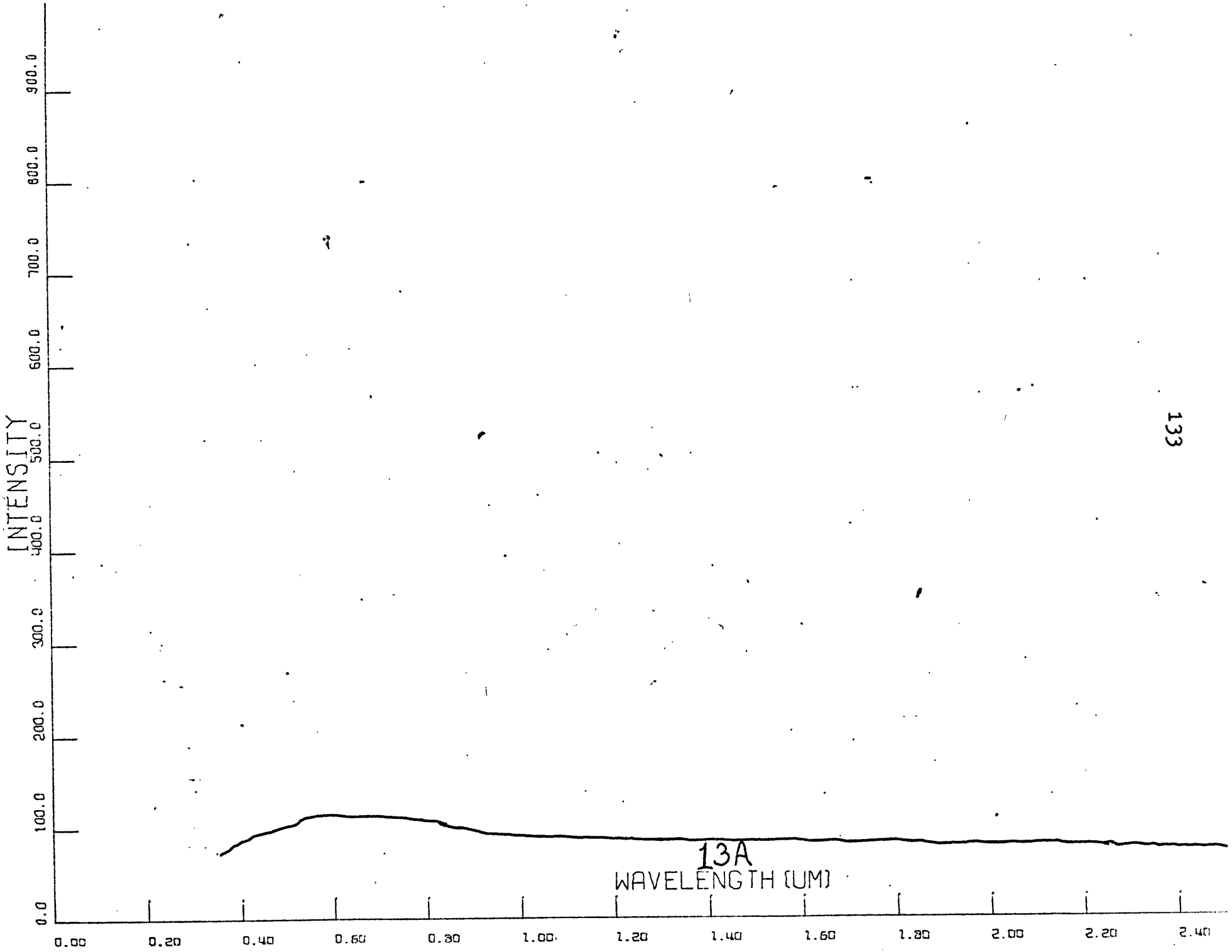
INTENSITY
900.0
800.0
700.0
600.0
500.0
400.0
300.0
200.0
100.0
0.0
0.00
0.20
0.40
0.60
0.80
1.00
1.20
1.40
1.60
1.80
2.00
2.20
2.40
WAVELENGTH (UM)

13A

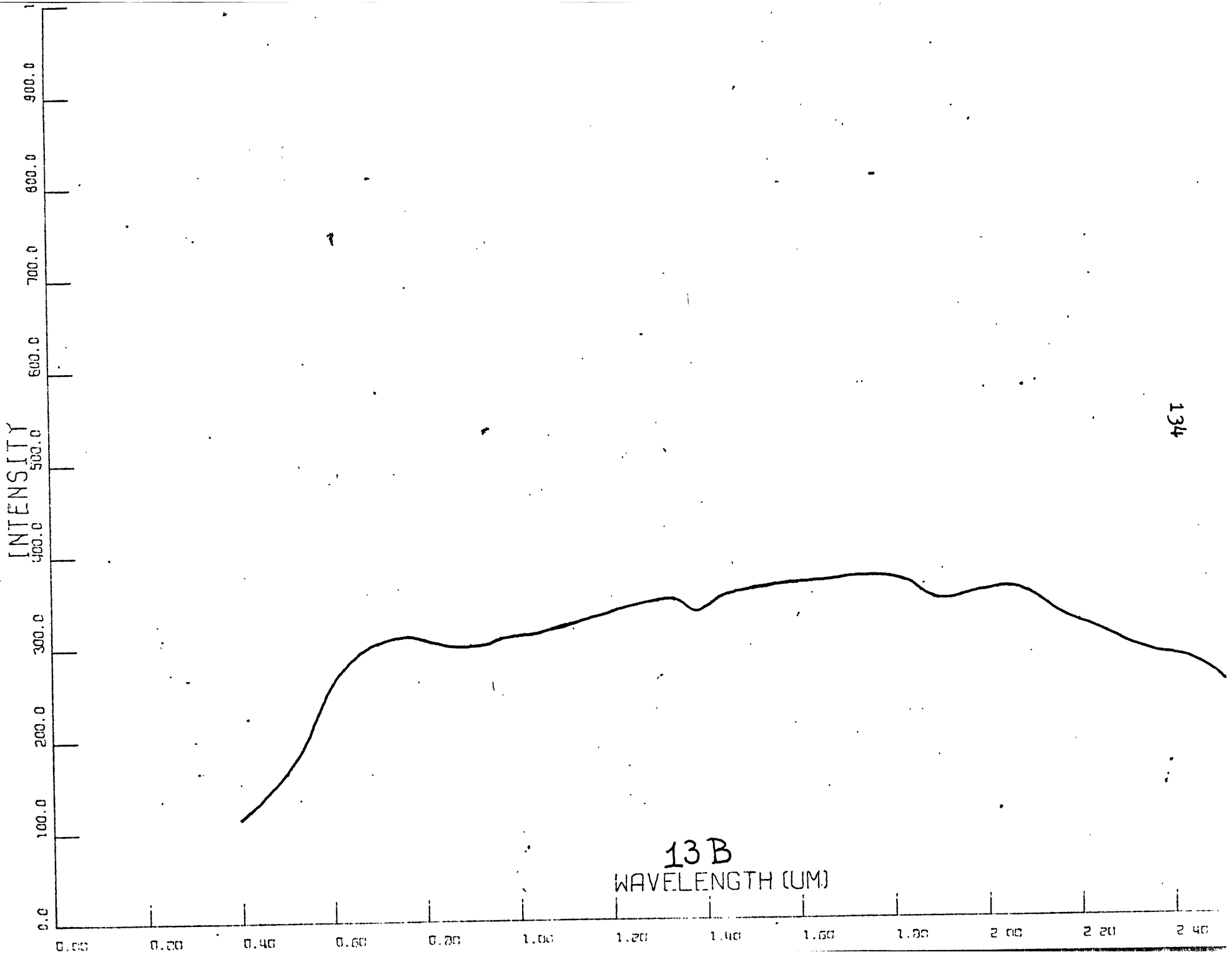
INTENSITY
0.0
100.0
200.0
300.0
400.0
500.0
600.0
700.0
800.0
900.0
0.00
0.20
0.40
0.60
0.80
1.00
1.20
1.40
1.60
1.80
2.00
2.20
2.40
WAVELENGTH (UM)

13 B

SILVER BELL DISTRICT

SAMPLE NUMBER	General Description
15 A	Relatively Unaltered Dacite(?) Porphyry
15 B	Propylitic Altered Dacite(?) Porphyry
16 A	Relatively Unaltered Latite(?)
16 B	Propylitic Altered Latite(?)
17 A	Relatively Unaltered Latite Porphyry
17 B	Propylitic Altered Latite Porphyry
18 A	Relatively Unaltered Dacite
18 B	Propylitic Altered Dacite

Note: For detailed descriptions refer to Figure: T-9, pages 74-75.

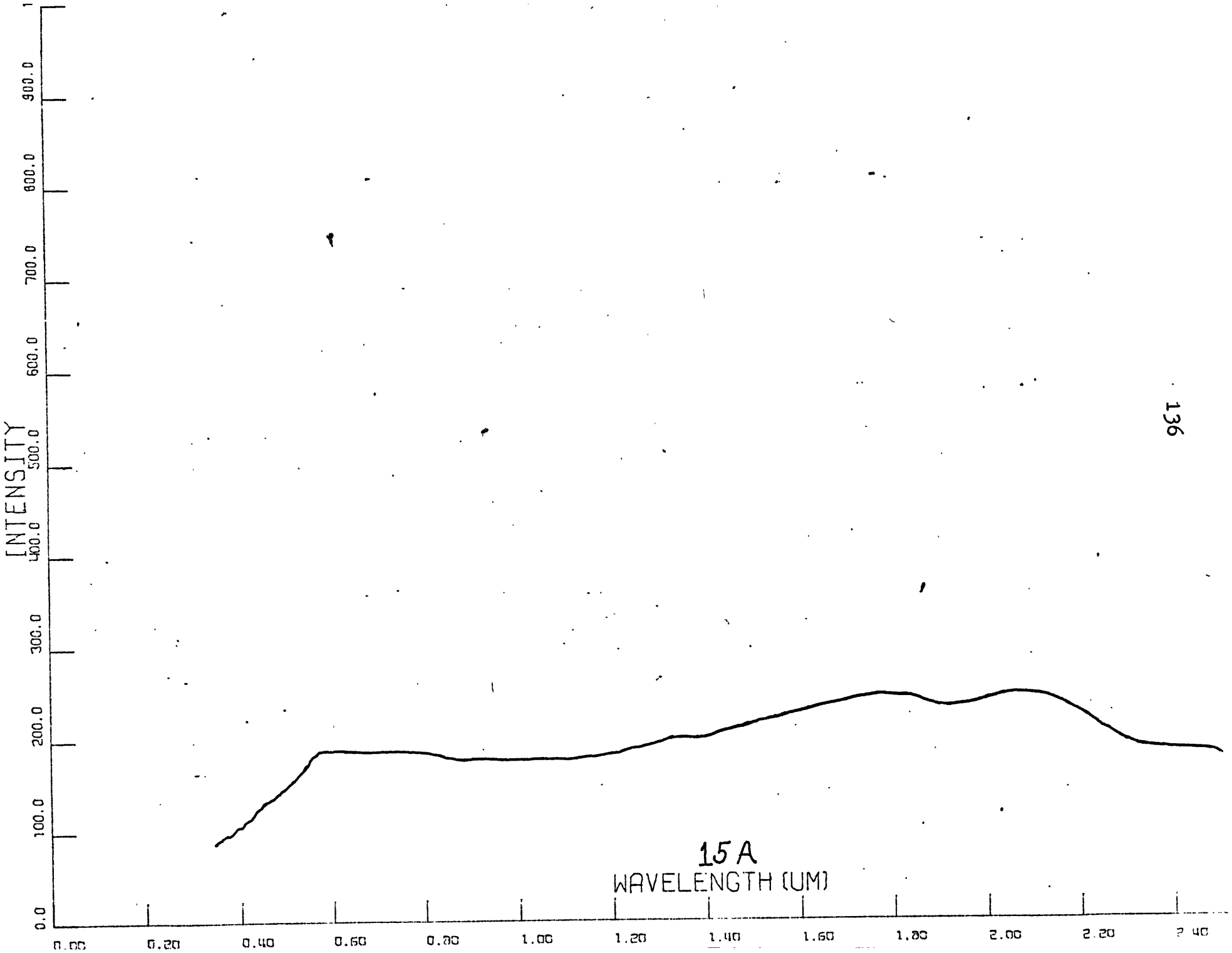
INTENSITY
0.0
100.0
200.0
300.0
400.0
500.0
600.0
700.0
800.0
900.0
1
0.00
0.20
0.40
0.60
0.80
1.00
1.20
1.40
1.60
1.80
2.00
2.20
2.40
15 A
WAVELENGTH (UM)

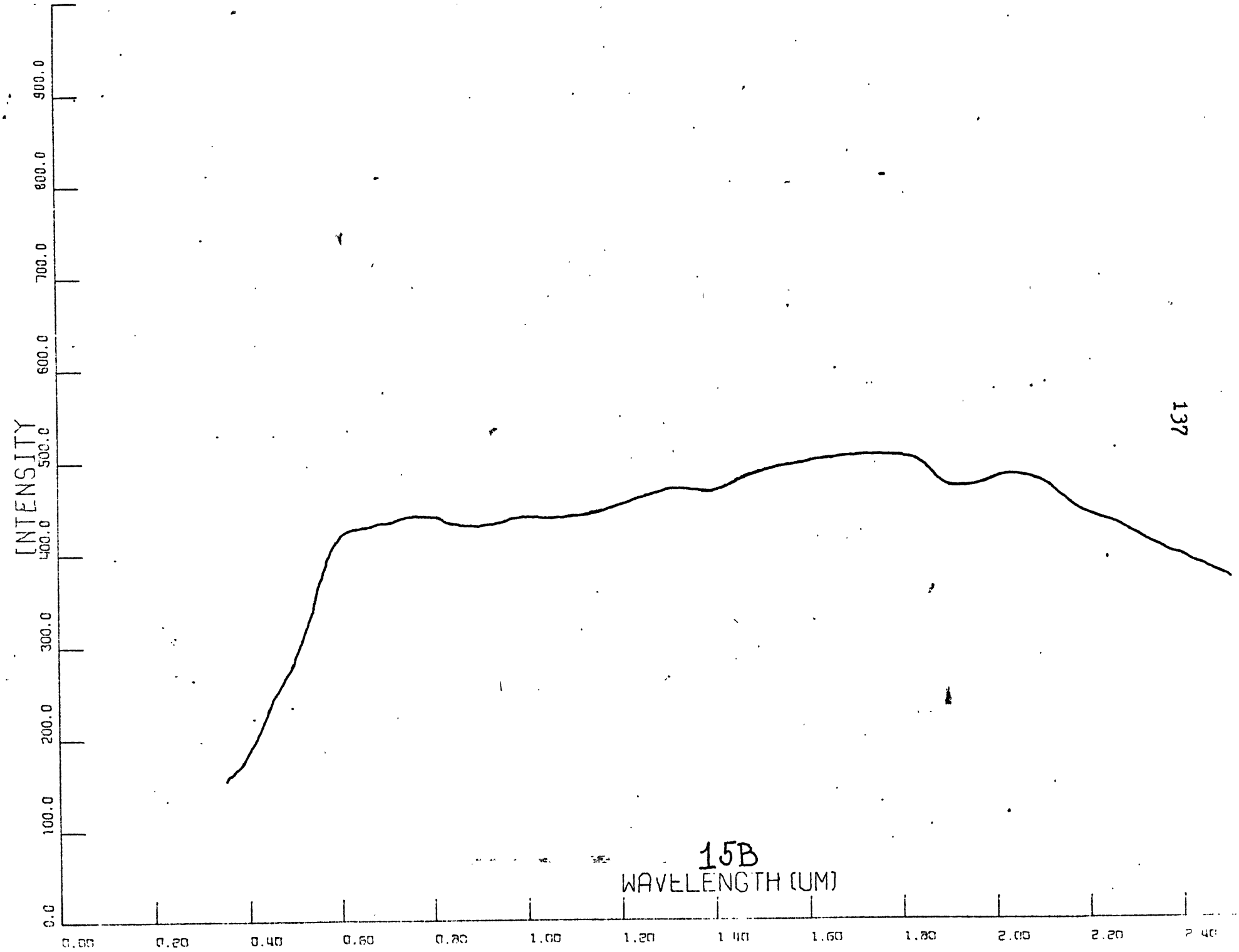
INTENSITY
0.0
100.0
200.0
300.0
400.0
500.0
600.0
700.0
800.0
900.0
0.00
0.20
0.40
0.60
0.80
1.00
1.20
1.40
1.60
1.80
2.00
2.20
2.40
WAVELENGTH (UM)

15B

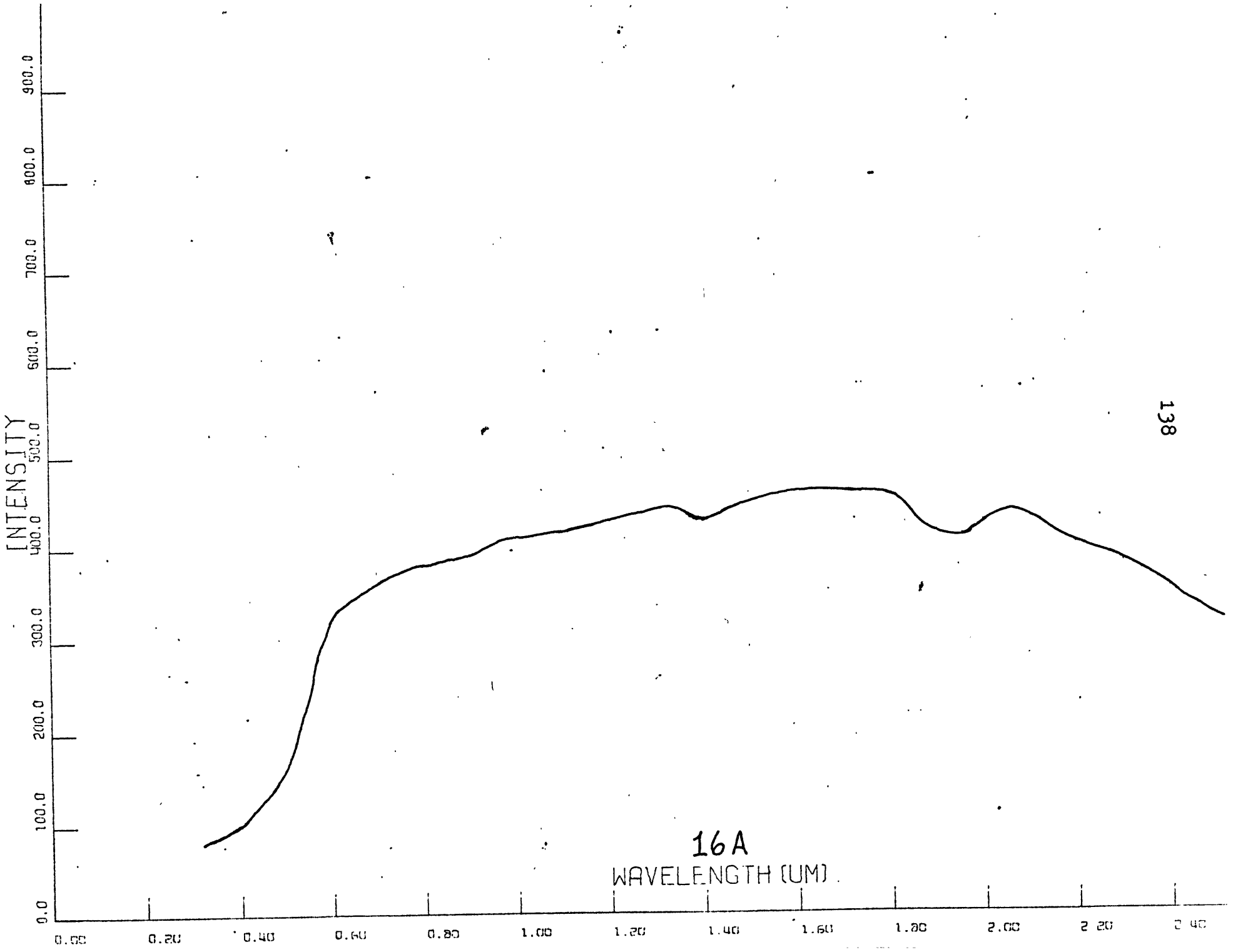
INTENSITY
0.0
100.0
200.0
300.0
400.0
500.0
600.0
700.0
800.0
900.0
0.00
0.20
0.40
0.60
0.80
1.00
1.20
1.40
1.60
1.80
2.00
2.20
2.40
16A
WAVELENGTH (UM)

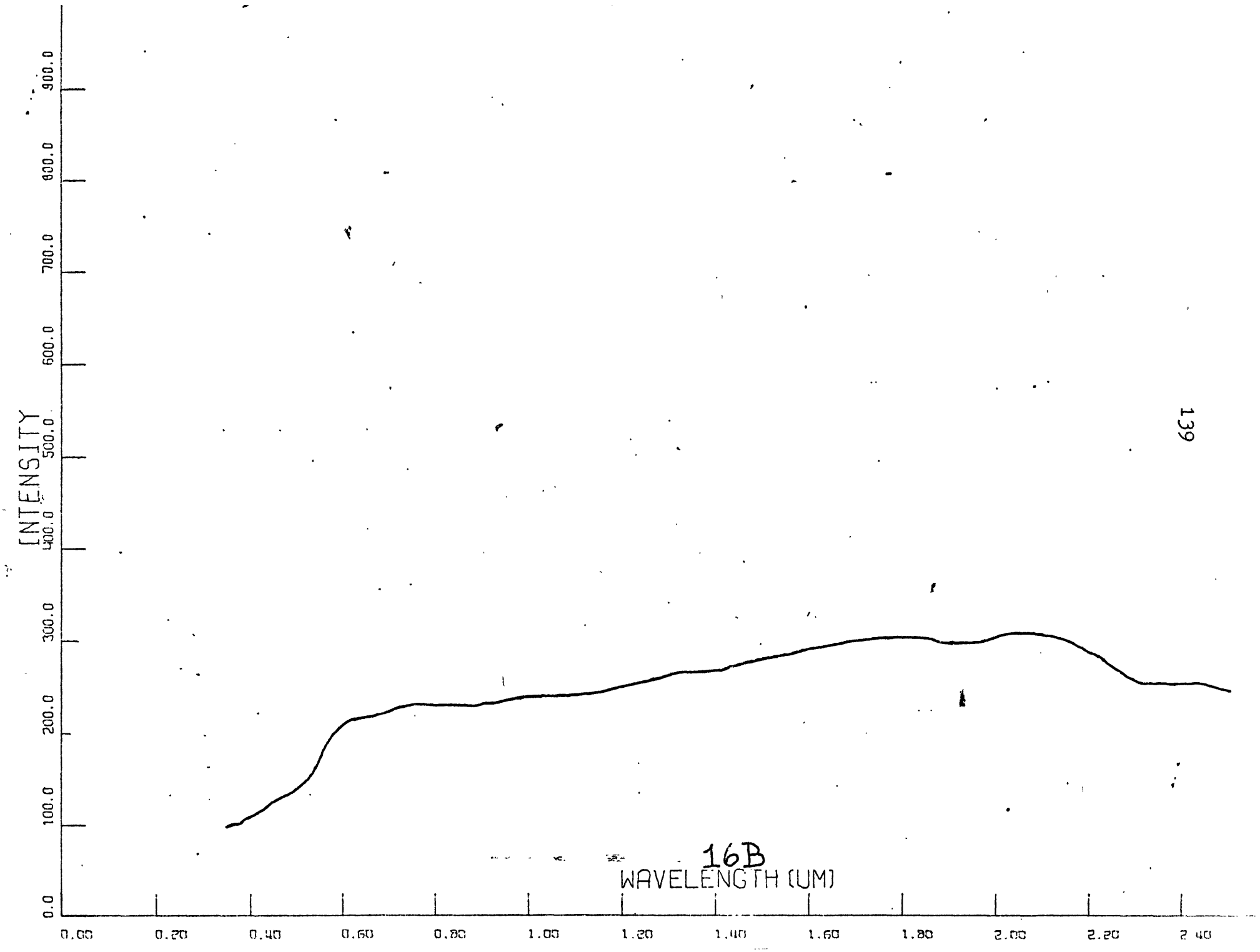
INTENSITY
0.0
100.0
200.0
300.0
400.0
500.0
600.0
700.0
800.0
900.0
0.00
0.20
0.40
0.60
0.80
1.00
1.20
1.40
1.60
1.80
2.00
2.20
2.40
WAVELENGTH (UM)
16B
139

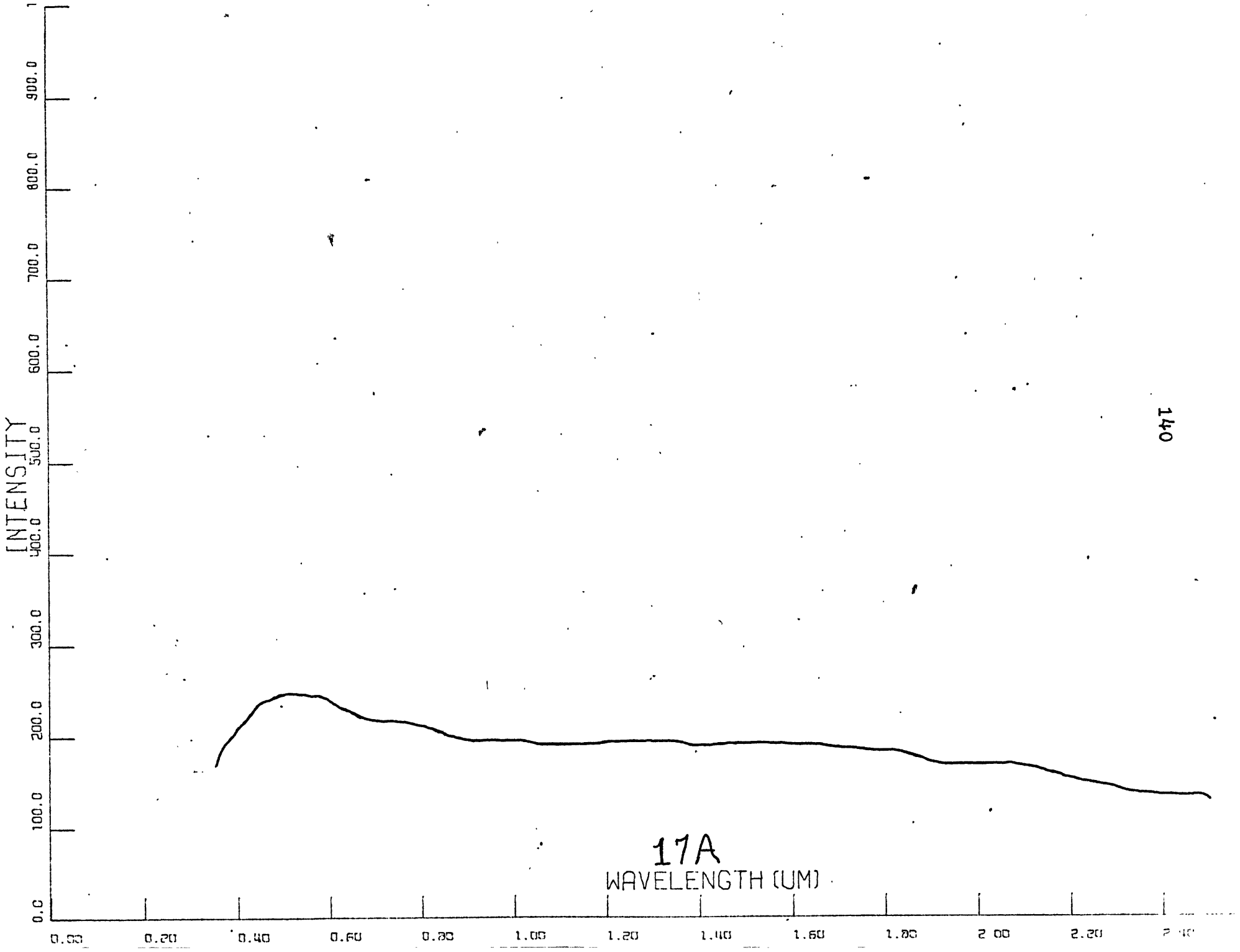
INTENSITY
0.0
100.0
200.0
300.0
400.0
500.0
600.0
700.0
800.0
900.0
1
0.00
0.20
0.40
0.60
0.80
1.00
1.20
1.40
1.60
1.80
2.00
2.20
17A
WAVELENGTH (UM)

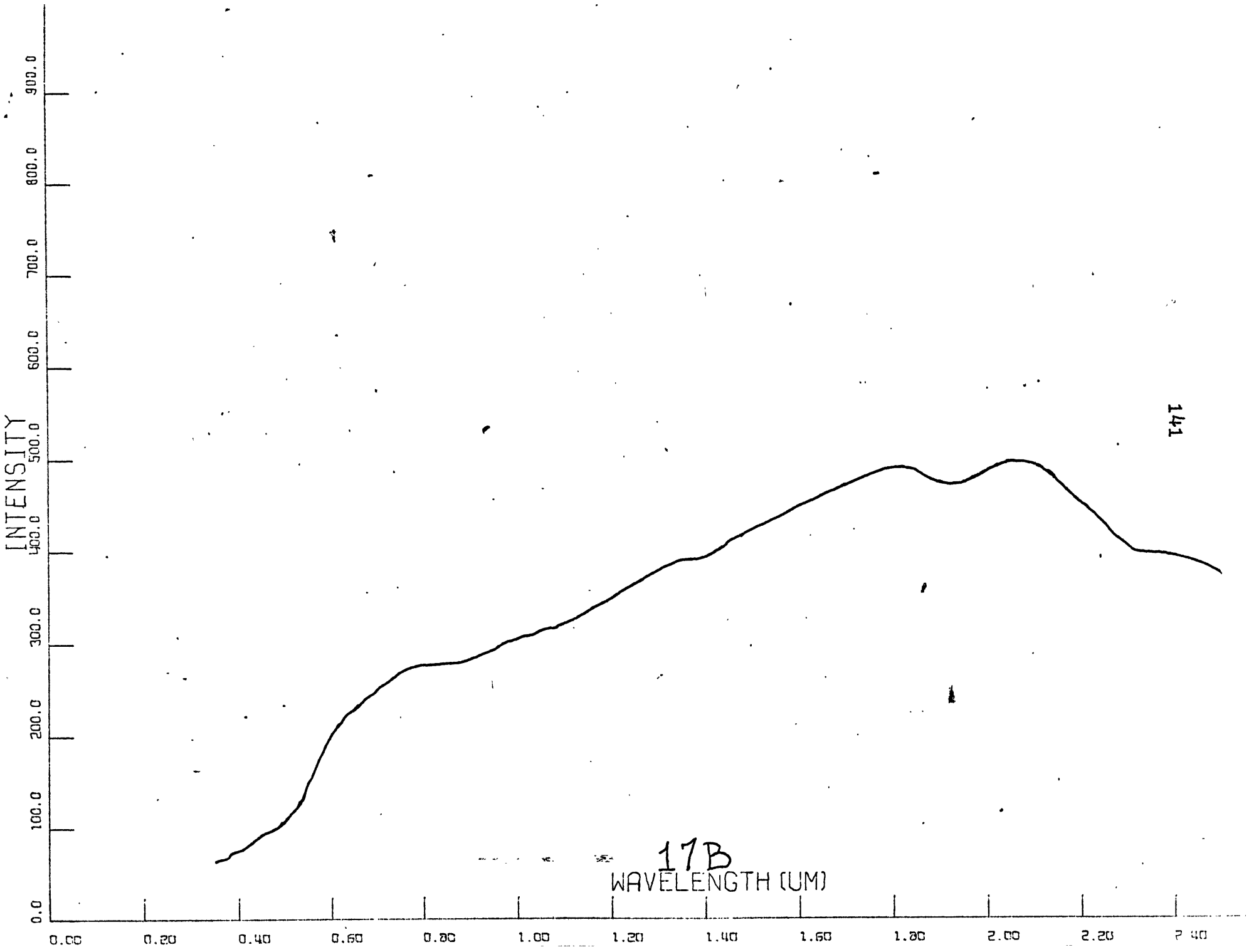
INTENSITY
0.0
100.0
200.0
300.0
400.0
500.0
600.0
700.0
800.0
900.0
0.00
0.20
0.40
0.60
0.80
1.00
1.20
1.40
1.60
1.80
2.00
2.20
2.40
WAVELENGTH (UM)
17B
141

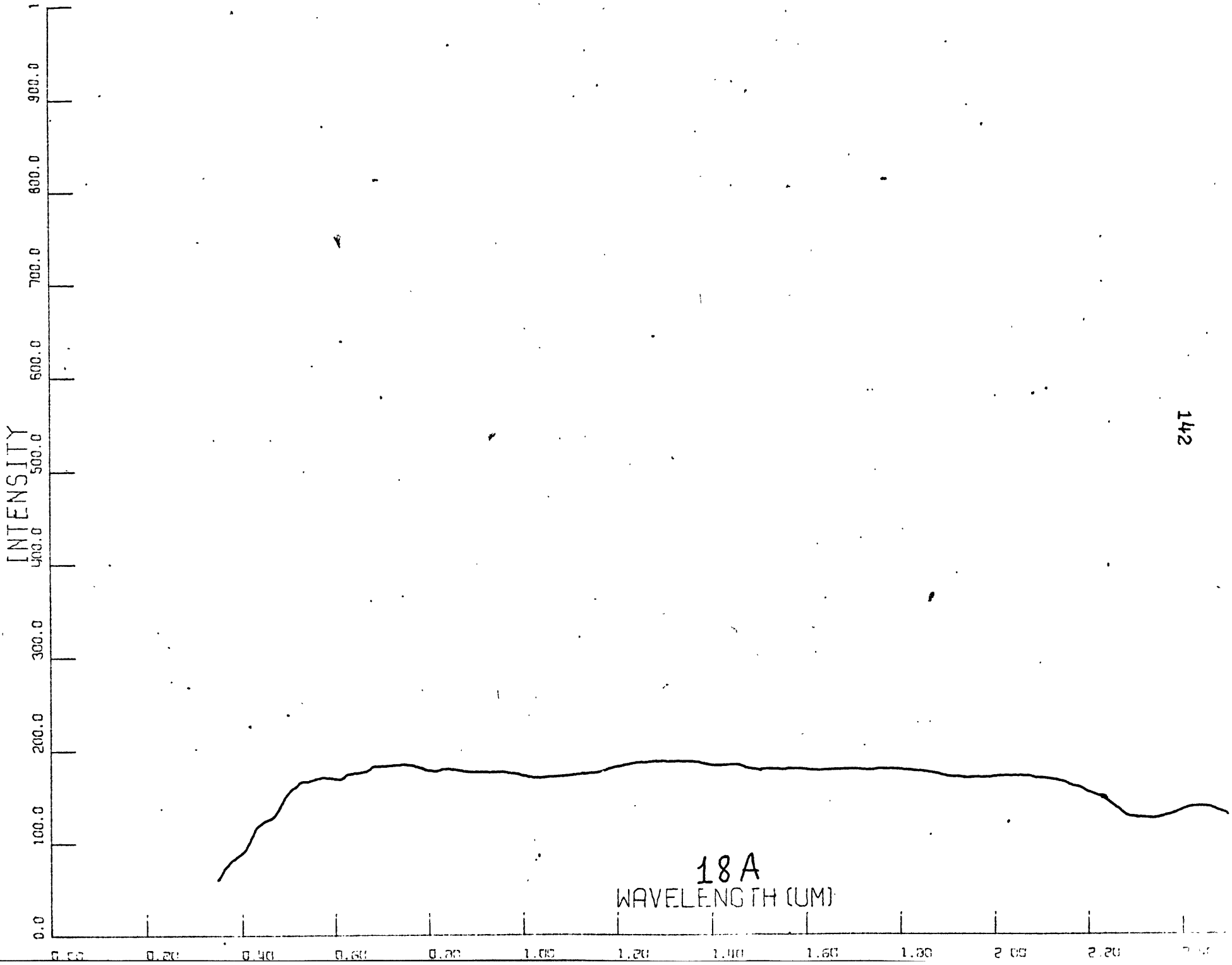

18A

WAVELENGTH (UM)

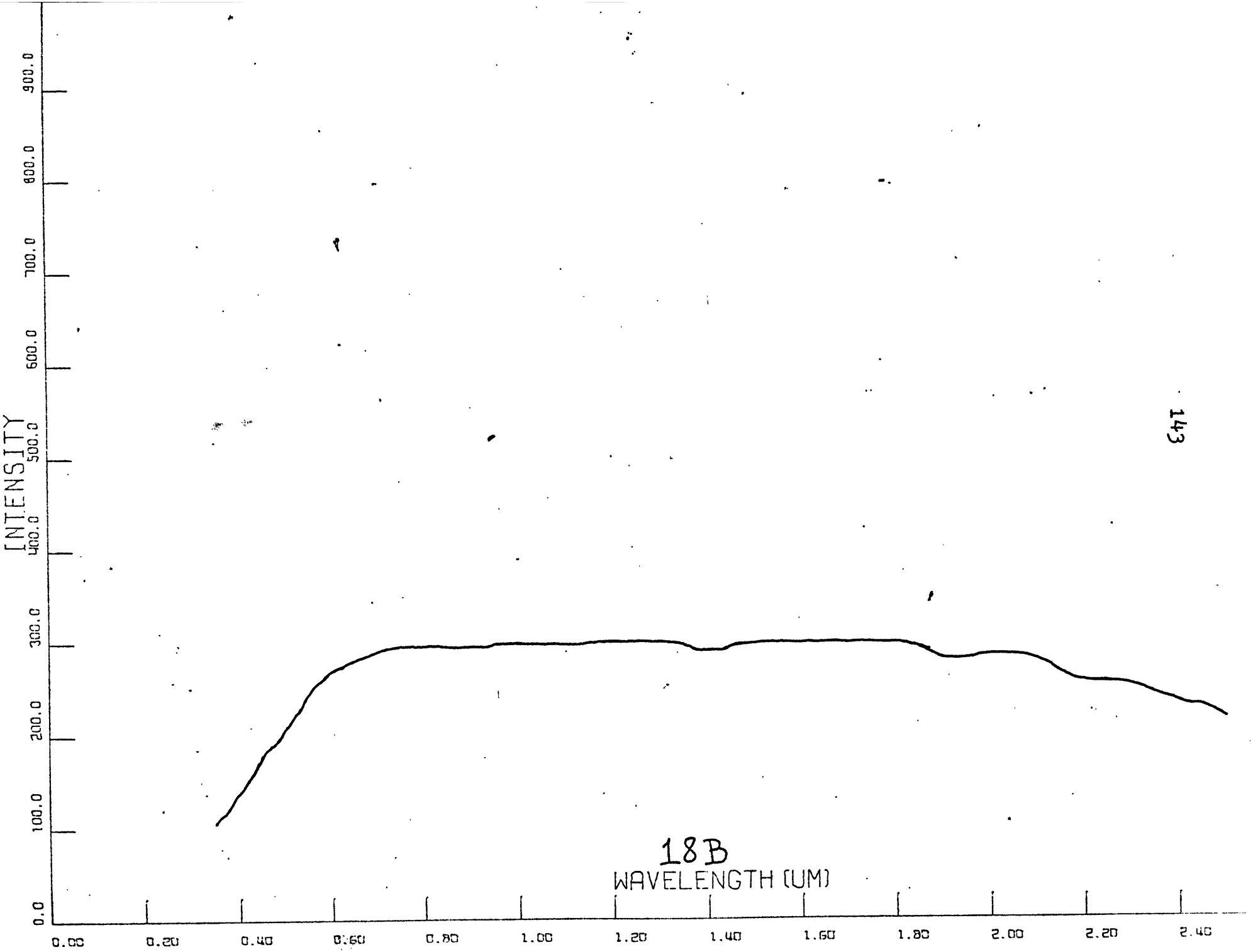
INTENSITY
0.0
100.0
200.0
300.0
400.0
500.0
600.0
700.0
800.0
900.0
0.00
0.20
0.40
0.60
0.80
1.00
1.20
1.40
1.60
1.80
2.00
2.20
2.40
18B
WAVELENGTH (UM)

REFERENCES

1) Adams, J.B. and A.L. Filice(1967), "Spectral Reflectance 0.4 to 2.0 Microns of Silicate Powders", Journal of Geophysical Research. Vol. 72, No.22. 5705-5715.

2) Billings, M.P., Structural Geology, 2nd. Edition, Prentice-Hall, Inc. Englewood Cliffs, N.J., 1954. 106-123.

3) Born, M. and E. Wolf, Principles of Optics, 4th. Edition, Pergamon Press, New York, 1970.

4) Burns, R.G., Mineralogical Applications of Crystal Field Theory, Cambridge University Press, London, 1970.

5) Castellan, G.W., Physical Chemistry, 2nd. Edition, Addison-Wesley Publishing Company, Reading, Mass. 1971. 417-658.

6) Compton, R.R., Manual of Field Geology, John Wiley and Sons, Inc., New York, 1962. 18-20,338.

7) Emerson, B.K., Geology of Massachusetts and Rhode Island, USGS Bulletin 597, 1917.

8) Fowles, G.R., Introduction to Modern Optics, Holt, Rinehart, and Winston, Inc., New York, 1968.

9) Gaffey, M.J., A Systematic Study of the Spectral Reflectivity Characteristics of the Meteorite Classes with Applications to the Interpretation of the Asteroid Spectra for Compositional Information, Phd Thesis, M.I.T. 1973. Chapters 2,3,4.

10) Holz, R.K.,(ed), The Surveillant Science - Remote Sensing of the Environment, Houghton-Mifflin Company, Boston, 1973. 2-65.

11) Huang, W.T., Petrology, McGraw-Hill Book Company, New York. 1962.

12) Hunt, G.R. and J.W. Salisbury,(1970),"Visible and Near-Infrared Spectra of Minerals and Rocks: I Silicate Minerals," Modern Geology, 283-300.

13) Hunt, G.R. and J.W. Salisbury,(1971),"Visible and Near-Infrared Spectra of Minerals and Rocks: II Carbonates", Modern Geology, Vol.2., 23-40.

14) Hunt, G.R., J.W. Salisbury, and C.J. Lenhoff.,"Visible and Near-Infrared Spectra of Minerals and Rocks: III Oxides and Hydroxides"; Modern Geology, Vol. 2, 1971. 195-205.

REFERENCES (continued)

15) Hunt, G.R., J.W. Salisbury, and C.J. Lenhoff, "Visible and Near-Infrared Spectra of Minerals and Rocks: IV Sulphides and Sulphates", Preprint submitted to Modern Geology. 1970.

16) Jenkins, F.A. and H.E. White, Fundamentals of Optics, McGraw-Hill Book Company, 3rd. Edition, New York, 1957.

17) Johannsen, A., A Descriptive Petrography of the Igneous Rocks, Vol.2., University of Chicago Press, 1931. 226,245.

18) Kunin, J.S., A Technique for Two-Dimensional Photoelectronic Astronomical Imaging with an Application to Lunar Spectral Reflectivity, S.M. Thesis, M.I.T., 1972.

19) Mason, B., and L.G. Berry, Elements of Mineralogy, W.H. Freeman and Company, San Francisco. 1968.

20) McCord, T.B. and J.B. Adams,(1973),"Progress in Remote Optical Analysis of Lunar Surface Composition", The Moon(in press).

21) McCord, T.B. and J. Bosel,(1973),"Silicon Vidicon Astronomy at MIT", Astronomical Observations with Television Type Sensors, (J.W. Glaspey and G.A. Walker, eds.). Vancouver: Institute of Astronomy,University of British Colombia.

22) McCord, T.B. and J.A. Westphal, "Two-Dimensional Silicon Vidicon Astronomical Photometer", Applied Optics,Vol.11., No.3, 1972. 522-526.

23) McCord, T.B., Color Differences on the Lunar Surface, Phd Thesis, California Insititute of Technology, 1968. 1-30.

24) Neuringer, L.J.,"Infrared Fundamentals and Techniques", Electrical Manufacturing. Conover-Mast Publication. 1960. 101-128.

25) Park, C.F. and R.A. MacDiarmid, Ore Deposits, 2nd. Edition, W.H. Freeman and Company, San Francisco, 1970.

26) Pieters, C.E., Wavelength Dependence of the Polarization of Light Reflected from a Particulate Surface in the Spectral Region of a Transition Metal Absorption Band, S.M. Thesis, M.I.T., 1972. 6-18, 41.

27) Pough, F.H., A Field Guide to Rocks and Minerals, Houghton-Mifflin Company, Boston, 1960.

28) Quagliano, J.V., Chemistry, 2nd. Edition, Prentice-Hall, Inc., Englewood Cliffs, N.J., 1963. 702-734.

REFERENCES (continued)

29) Sayer, S. Approximate Title:"Time Relationships and Age Relationships of the Blue Hill Granite - Pondville Conglomerate Contact(Using Neutron Activation, Neutron Probe, and Absolute Dating Techniques)", S.M. Thesis, M.I.T., 1973(in progress).

Titley, S.R., and C. Hicks, Geology of the Porphyry Copper Deposits, Southwestern North America, University of Arizona Press, Tucson, Arizona. 1966.

30) Creasey, S.C.,"Hydrothermal Alteration", 51-73.

31) Jerome, S.E.,"Some Features Pertinent in Exploration of Porphyry Copper Deposits",75-85.

32) Schwartz, M.,"The Nature of the Primary and Secondary Mineralization in Porphyry Copper Deposits", 41-49.

33) Stringham, B.,"Igneous Rock Types and Host Rocks Associated with Porphyry Copper Deposits", 35-40.